

# HEPATIC XENOBIOTIC RECEPTORS IN THE UBIQUITIN-PROTEASOME SYSTEM

by

**Jiong Yan**

Bachelor of Science, Xi'an Jiaotong University, 2009

Master of Science, Xi'an Jiaotong University, 2011

Submitted to the Graduate Faculty of  
School of Pharmacy in partial fulfillment  
of the requirements for the degree of  
Doctor of Philosophy

University of Pittsburgh

2018

UNIVERSITY OF PITTSBURGH  
SCHOOL OF PHARMACY

This dissertation was presented

by

Jiong Yan

It was defended on

Feb 27, 2018

and approved by

Donald B. DeFranco, PhD, Professor, Pharmacology and Chemical Biology

Paul A. Johnston, PhD, Associate Professor, Pharmaceutical Sciences

Xiaochao Ma, PhD, Associate Professor, Pharmaceutical Sciences

Yong Wan, PhD, Professor, Cell Biology

Dissertation Advisor: Wen Xie, MD, PhD, Professor, Pharmaceutical Sciences

Copyright © by Jiong Yan

2018

# **HEPATIC XENOBIOTIC RECEPTORS IN THE UBIQUITIN-PROTEASOME SYSTEM**

Jiong Yan, PhD

University of Pittsburgh, 2018

Constitutive androstane receptor (CAR) and aryl hydrocarbon receptor (AhR) are liver-enriched xenobiotic receptors that are essential in the regulation of drug-metabolizing enzymes (DMEs) and drug transporters. Emerging evidence has also implicated CAR and AhR in the energy metabolism, cell proliferation and immune response, in addition to their classical function of xenobiotic detoxification. The cellular effects mediated by these xenobiotic receptors can be achieved canonically by the transcriptional modulation via direct interaction with the genomic DNA. There are also indirect mechanisms via protein-protein interactions by which CAR and AhR can alter the transcriptome. The preliminary results together with previous studies by others have suggested an interplay between the xenobiotic receptors and ubiquitin-proteasome system (UPS). In this dissertation study, I studied the E3 ubiquitin ligase activity of CAR and AhR in the context of hepatic gluconeogenesis and hepatic stellate cell (HSC) activation, respectively. My results demonstrated that (1) CAR suppresses hepatic gluconeogenic gene expression through post-translational regulation of the subcellular localization and degradation of PPAR- $\gamma$  coactivator 1 $\alpha$  (PGC1 $\alpha$ ). Activated CAR translocates into the nucleus and serves as a substrate adaptor protein recruiting PGC1 $\alpha$  to the Cullin1 E3 ligase complex for ubiquitylation. The interaction between CAR and PGC1 $\alpha$  also leads to their sequestration within the promyelocytic leukemia protein-nuclear bodies (PML-NBs), where PGC1 $\alpha$  and CAR subsequently undergo proteasomal degradation, which is required for CAR-mediated inhibition of PGC1 $\alpha$ . (2) AhR negatively regulates HSC activation by disrupting the interaction of Smad3 with  $\beta$ -catenin and

impairing  $\beta$ -catenin-dependent stabilization of phosphorylated Smad2/3, which is independent of its E3 ubiquitin ligase activity. AhR is highly expressed in HSCs and activation of AhR prevents fibrogenesis and proliferation of HSCs. The expression of AhR in HSCs declines with the onset of HSC activation. Primary HSCs isolated from the AhR<sup>-/-</sup> mice exhibits accelerated spontaneous activation. Treatment with an AhR antagonist promotes, whereas the AhR agonists inhibit the activation of mouse and human HSCs, respectively. In vivo ablation of AhR in HSCs sensitizes mice to liver fibrosis. Overall, this dissertation elucidates a novel concept of xenobiotic receptors as the essential components in the UPS.

## TABLE OF CONTENTS

<b>PREFACE.....</b>	<b>XII</b>
<b>ABBREVIATIONS.....</b>	<b>I</b>
<b>1.0 INTRODUCTION.....</b>	<b>1</b>
<b>1.1 HYPOTHESIS AND SPECIFIC AIMS.....</b>	<b>2</b>
<b>1.2 DISSERTATION OUTLINE.....</b>	<b>4</b>
<b>2.0 XENOBIOTIC RECEPTORS AND HEPATIC METABOLISM .....</b>	<b>5</b>
<b>2.1 HOST DEFENSE MECHANISMS.....</b>	<b>5</b>
<b>2.2 DISCOVERY OF XENOBIOTIC RECEPTORS .....</b>	<b>7</b>
<b>2.3 XENOBIOTIC REGULATION BY PXR, CAR AND AHR.....</b>	<b>11</b>
<b>2.4 MODULATION OF XENOBIOTIC RECEPTORS: LIGAND-INDUCED NUCLEAR TRANSLOCATION .....</b>	<b>13</b>
<b>2.5 MODULATION OF XENOBIOTIC RECEPTORS: TRANSCRIPTIONAL REGULATION.....</b>	<b>18</b>
<b>2.6 MODULATION OF XENOBIOTIC RECEPTORS: POST- TRANSLATIONAL MODIFICATIONS (PTMS).....</b>	<b>20</b>
<b>2.7 ROLE OF UBIQUITIN PROTEOLYTIC SYSTEM IN XENOBIOTIC RECEPTORS.....</b>	<b>23</b>
<b>3.0 CAR AND HEPATIC GLUCONEOGENESIS .....</b>	<b>25</b>

3.1	RESEARCH BACKGROUND.....	25
3.2	MATERIALS AND METHODS.....	27
3.3	EXPERIMENTAL RESULTS .....	32
3.4	DISCUSSION AND CONCLUSION .....	53
4.0	AHR AND LIVER FIBROSIS.....	58
4.1	RESEARCH BACKGROUND.....	58
4.2	MATERIALS AND METHODS.....	60
4.3	EXPERIMENTAL RESULTS .....	67
4.4	DISCUSSION AND CONCLUSION .....	86
5.0	SUMMARY .....	90
5.1	NON-GENOMIC (NON-CANONICAL) FUNCTION OF XENOBIOTIC RECEPTORS.....	90
5.2	CAR IN THE REGULATION OF ENERGY METABOLISM.....	92
5.3	AHR IN THE HEPATIC TOXICITY AND HOMEOSTASIS.....	95
APPENDIX A .....		99
APPENDIX B .....		100
BIBLIOGRAPHY .....		102

## **LIST OF TABLES**

Table 1. Antibody information .....	99
Table 2. Real-time PCR primers sequences.....	100



## LIST OF FIGURES

Figure 1. Historical landmarks in the discovery of PXR, CAR and AhR .....	11
Figure 2. Paradigm of xenobiotic response by mouse PXR, CAR and AhR.....	13
Figure 3. Nuclear translocation of xenobiotic receptors .....	17
Figure 4. PGC1 $\alpha$ is a central transcriptional coactivator in hepatic gluconeogenesis .....	26
Figure 5. CAR suppresses gluconeogenic gene expression in primary mouse and human hepatocytes.....	34
Figure 6. CAR suppresses gluconeogenesis through inhibiting PGC1 $\alpha$ activity .....	35
Figure 7. CAR and PGC1 $\alpha$ are co-regulated during fasting and in diet-induced obesity.....	36
Figure 8. CAR decreases the DNA-binding of PGC1 $\alpha$ on the gluconeogenic genes .....	38
Figure 9. Activation of CAR leads to the redistribution of PGC1 $\alpha$ to PML-NBs.....	39
Figure 10. CAR promotes ubiquitylation-proteasomal degradation of PGC1 $\alpha$ .....	41
Figure 11. CAR's interaction with PGC1 $\alpha$ is essential for the ubiquitylation and degradation of PGC1 $\alpha$ .....	41
Figure 12. PML-NBs are required for CAR to induce PGC1 $\alpha$ degradation and suppress gluconeogenic gene expression in vitro.....	43
Figure 13. PML-NBs are required for CAR to induce PGC1 $\alpha$ degradation and suppress gluconeogenic gene expression in vivo .....	44

Figure 14. CAR interacts with the CUL1 E3 ligase components and forms a unique complex...	46
Figure 15. CAR recruits the CUL1 E3 ligase to promote the ubiquitylation of PGC1 $\alpha$ .....	47
Figure 16. CAR-mediated inhibition of PGC1 $\alpha$ requires active AF2 domain.....	50
Figure 17. CAR-mediated inhibition of PGC1 $\alpha$ is independent of DNA-binding .....	51
Figure 18. N-terminal PGC1 $\alpha$ fragment is resistant to the inhibition by CAR .....	52
Figure 19. Mechanism of CAR-mediated suppression of hepatic gluconeogenesis.....	53
Figure 20. Post-translational modifications of PGC1 $\alpha$ .....	55
Figure 21. Constitutive activation of AhR in the hepatocytes is sufficient to induce liver fibrosis .....	68
Figure 22. Non-toxic AhR ligand, ITE, ameliorates CCl <sub>4</sub> -induced liver fibrosis.....	69
Figure 23. AhR is highly expressed in HSCs and the expression of AhR declines with HSC activation.....	71
Figure 24. The expression of AhR inversely correlates with HSC activation .....	72
Figure 25. Pharmacological activation of AhR inhibits spontaneous HSC activation .....	73
Figure 26. Forced expression of AhR inhibits spontaneous HSC activation.....	74
Figure 27. Genetic ablation or pharmacological inhibition of AhR promotes HSC activation....	75
Figure 28. Ablation of AhR in HSCs, but not in hepatocytes or Kupffer cells, sensitizes mice to spontaneous liver fibrosis .....	77
Figure 29. Ablation of AhR in HSCs sensitizes mice to CCl <sub>4</sub> - and BDL-induced liver fibrosis .	78
Figure 30. AhR attenuates TGF $\beta$ -stimulated fibrogenesis .....	80
Figure 31. AhR disrupts the interaction of Smad3 and $\beta$ -catenin.....	82
Figure 32. AhR impairs $\beta$ -catenin-dependent stabilization of phosphorylated Smad2/3 .....	83
Figure 33. CRLs play a role in the AhR-exerted inhibition of fibrogenesis in the HSCs .....	85

Figure 34. AhR-mediated inhibition is independent of its E3 ligase activity .....	86
Figure 35. Molecular mechanism for AhR-mediated suppression of fibrogenesis in HSCs .....	89

## **PREFACE**

I would like to thank my advisor, Dr. Wen Xie, for his kindness and support in all these years: his willingness to take me as student, his trust and support to allow me to pursue my own research interest, his encouragement and incentives in the time of difficulties, his patience and understanding when the progress is slow, and his great mentorship to pave the road for my academic career.

It was also my great pleasure to know and work with so many people in the Xie lab in the past six years: Songrong Ren, Meishu Xu, Jie Gao, Mengxi Jiang, Chibueze Ihunnah, Peipei Lu, Yuhan Bi, Yang Xie, Xinran Cai, Anne Barbosa, Hungchun Tung, Yunqi An, Jinhan He, Xiongjie Shi, Nan Hu, Yuka Inaba, Wojciech Garbacz, Yueshui Zhao, Junjie Zhu, Pengfei Xu, Jibin Guan, Xiaojuan Chai, Lushan Yu, Bingfang Hu, Yan Guo, Zhihui Zheng, Zanmei Zhao, Dan Xu, Yongdong Niu, Li Gao, Ziteng Zhang, Ye Feng.

I also would like to thank my committee members, Dr. Donald B. DeFranco, Dr. Paul A. Johnston, Dr. Xiaochao Ma, and Dr. Yong Wan, for their insightful comments from various perspectives to help improve my research, the precious time and efforts they have committed.

My sincere gratitude also goes to the fellows in the Center of Pharmacogenetics, the staff, faculty, and students in the School of Pharmacy, in particular, I want to thank Maggie and Lori for their readiness for help whenever it was.

I also want to thank my beloved wife, my best friend and soul mate, with whom I shared joys and tears all over the years, my parents and in-laws for their endless support, and brothers and sisters in the Pittsburgh Chinese Church Oakland whose prayers held me up in the hard time.

Above all, this dissertation is dedicated to my heavenly father, who humbles me with all the trials, carries me through with patience, and comforts me with his faithfulness. Soli Deo Gloria.

## **ABBREVIATIONS**

AMP, Adenosine monophosphate; ATP, Adenosine triphosphate; AP-1, Activator protein 1; bHLH/PAS, basic helix-loop-helix/ Per-Arnt-Sim; cAMP, Cyclic AMP; DNA, Deoxyribonucleic acid; GMP, Guanosine monophosphate; IFN, Interferon; IL-1 $\beta$ , Interleukin-1 $\beta$ ; IL-6, Interleukin-6; IRF, Interferon regulatory factor; LPS, Lipopolysaccharide; NAD, Nicotinamide adenine dinucleotide; NF- $\kappa$ B, nuclear factor  $\kappa$ -light-chain-enhancer of activated B cells; PPAR, Peroxisome proliferator-activated receptor; RNA, Ribonucleic acid; Smad, Mothers against decapentaplegic homolog 3; TGF $\beta$ , Transforming growth factor  $\beta$ ; TNF $\alpha$ , Tumor necrosis factor  $\alpha$ .

## **1.0 INTRODUCTION**

Xenobiotic response is an essential biological process to defend organismal survival and physiological homeostasis. It is also the fundamental determinant for the efficacy of medications and drug-drug interactions. Xenobiotic detoxifying enzymes (Phase I and II) together with drug transporters (Phase III) compose the molecular machinery to metabolize the foreign compounds as well as endogenous steroids and/or non-steroids. Liver, as the major enteric organ for energy metabolism and xenobiotic disposition, is enriched of transcriptional factors that govern the transcription of glucose/lipid metabolic genes as well as xenobiotic responsive genes. Among these transcriptional factors, constitutive androstane receptor (CAR), pregnane X receptor (PXR), and aryl hydrocarbon receptor (AhR), are the three best established xenobiotic receptors that sense the exogenous chemicals and control the expression of distinct types of xenobiotic enzymes and drug transporters [1]. A growing body of evidence has also put the xenobiotic receptors in the physiological and pathophysiological context beyond the classical xenobiotic response, including endobiotic metabolism, cell proliferation, and immune responses. These newest findings propel further investigation of the novel functions of xenobiotic receptors and the underlying molecular mechanisms.

## 1.1 HYPOTHESIS AND SPECIFIC AIMS

CAR and AhR share several similarities in the molecular regulatory mechanism and biological activity, although they belong to the different transcription factor superfamilies. As the transcription factors in the nucleus, CAR and AhR normally exert their cellular function through direct binding to the specific DNA regions and promote or repress transcription. There are also indirect genomic mechanisms, through either epigenetic regulation or crosstalk with other transcriptional factors, that control the transcriptome alteration. More interestingly, preliminary experimental results and the studies by others have suggested that CAR and AhR have functional interaction with the ubiquitin-proteasome protein degradation system. The dissertation work was dedicating to the novel non-genomic activity of CAR and AhR in the proteolytic process and the pathophysiological relevance with the chronic liver diseases. The overall hypothesis is that the ligand-activated xenobiotic receptors CAR and AhR regulate hepatic glucose metabolism and liver fibrotic pathogenesis, respectively, through the non-genomic mechanisms that engage the ubiquitin-proteasome proteolysis system.

There are two specific aims for the dissertation study:

For the specific Aim 1, we have investigated the role of CAR in the hepatic gluconeogenesis. Previous work in our lab and other groups has shown that activation of CAR by its ligand 1,4-Bis- [2-(3,5-dichloropyridyloxy)]benzene (TCPOBOP) suppresses hepatic gluconeogenesis and ameliorates hyperglycemia in genetic and diet-induced obese mice. However, the molecular pathway that underlies the CAR-mediated suppression of gluconeogenesis is not fully understood. In this specific study, we have found that CAR couples with the Cullin1 (CUL1) ubiquitin ligase to promote the ubiquitylation of the key gluconeogenic regulator PGC1 $\alpha$ . This event is associated with protein degradation in the PML-NBs. We have



characterized the molecular orchestration of the CAR-associated CUL1 ubiquitin ligase by mutagenic analysis and demonstrated that CAR is the adaptor protein of PGC1 $\alpha$  to the CUL1 scaffold complex. We have further determined the requirement of the CAR-associated CUL1 ubiquitin ligase in suppressing the gluconeogenic gene expression using the dominant negative CUL1 and the cullin neddylation inhibitor MLN4924. We have also proven the necessity of the PML-NBs for CAR to inhibit the gluconeogenic process using in vitro overexpression and knockdown approaches and in vivo glucose metabolic analysis in the PML null mice. Further mutagenic approaches have also been employed to assess the molecular structural determinants of CAR in carrying out the ubiquitylation and degradation of PGC1 $\alpha$ .

For the specific Aim 2, we have investigated the role of AhR in the hepatic stellate cell (HSC) activation and liver fibrosis. The background of the study is that there is a paradoxical role of AhR in the liver fibrosis based on the existing evidence. Both activation and genetic ablation of AhR promote liver fibrosis. In this specific study, we have shown that AhR has a cell-type specific role in the liver fibrosis. The in vitro analysis has proven that activation of AhR by its ligand suppresses the activation of HSCs, a key event for the development of liver fibrosis. In vivo study using carbon tetrachloride (CCl<sub>4</sub>) and bile duct ligation (BDL)-induced liver fibrosis models in the conditional AhR knockout mice has established the inhibitory effect of AhR in the HSCs. For the mechanistic study, the preliminary results suggested that AhR suppresses the activation of hepatic stellate cells via TGF $\beta$ -Smad pathway. Molecular biological analysis was performed to identify the structural determinants that mediate the inhibitory effect by AhR in the HSCs.

## 1.2 DISSERTATION OUTLINE

The contents of the dissertation include:

**Chapter I. Introduction** (this chapter) is a concise description of the dissertation, including research background, overall research hypothesis, and specific aims with general research approaches.

**Chapter II. Xenobiotic Receptors and Hepatic Metabolism** is a literature review of the xenobiotic response by PXR, CAR and AhR, historical overview for the discovery of xenobiotic receptors, and molecular mechanisms that regulate the xenobiotic receptors.

**Chapter III. CAR and Hepatic Gluconeogenesis** is a complete research report for the specific Aim 1 that describes the study background, methodology, experimental results, and discussion and conclusion.

**Chapter IV. AhR and Liver Fibrosis** is a complete research report for the specific Aim 2 describes the study background, methodology, experimental results, and discussion and conclusion.

**Chapter V. Summary** is a conclusive overview for the interplay between xenobiotic receptors and the ubiquitin-proteasome system (UPS), the role of CAR in the energy metabolism, and the role of AhR in the hepatic toxicity and homeostasis.

## **2.0 XENOBIOTIC RECEPTORS AND HEPATIC METABOLISM**

### **2.1 HOST DEFENSE MECHANISMS**

Humans, like many vertebrates, are created and evolved with a sophisticated system that protects the host against the infections of microorganisms and the toxicity of environmental chemicals. The frontier protection by the natural barriers, including skin, mucous membranes, and respiratory/gastrointestinal/genitourinary tracts, significantly reduce the risk of infection and poisoning [2]. The protection can be achieved with unique physical structures, acidic pH, and secretion of immunological reactive and enzymatic proteins. Once entered in the blood circulation, bacteria and viruses can be recognized and engulfed by the phagocytic cells, such as neutrophils and macrophages. These cells promote the clearance of microbes by releasing phagocytic lysosomal contents and oxidative products. Macrophages also trigger nonspecific acute phase response through the production of cytokines (IL-1 $\beta$ , IL-6, TNF $\alpha$ , and IFNs) that cause inflammation, and chemokines that recruit lymphocytes to the infection site. Production of antibodies by the lymphocytes further facilitates the recognition and elimination of exogenous microbes [3].

Microbial sensing by the mammalian macrophages and other cells is executed by the pattern recognition receptors (PRRs) of the innate immune system [4, 5]. Different classes of PRR families have been discovered, including Toll-like receptors (TLRs), C-type lectin receptors

(CLRs), retinoic acid-inducible gene (RIG)-I-like receptors (RLRs), NOD-like receptors (NLRs), and cyclic GMP-AMP (cGAMP) synthase (cGAS)-stimulator of interferon genes (STING). The microbial conserved structures so-called pathogen-associated molecular patterns (PAMPs) (e.g. LPS, lipoprotein, RNA, or DNA) are recognized by a specific receptor, either a cell membrane-bound receptor (TLRs or CLRs) or a cytoplasmic receptor (RLRs, NLRs, or cGAS-STING). Activation of the sensors induces the inflammatory responses through transcriptional regulation by many transcriptional factors (e.g. AP-1, NF- $\kappa$ B, and IRFs) [4]. The inflammatory response is also regulated through the caspase-dependent cleavage of pro-cytokines underlying the activation of inflammasomes [6, 7]. The PAMP-sensing pathways are also responsible for the inflammation and autoimmunity induced by the damage-associated molecular patterns (DAMPs) (e.g. high mobility group box-1/HMGB1) that are released by the damaged tissues.

Whereas the large molecules of biological origins are sensed by the innate immune system, the sensing and biotransformation of the environmental toxins and medicinal drugs are generally elicited by a group of transcriptional factors, named the xenobiotic receptors [8]. The xenobiotic receptors PXR and CAR belong to the nuclear receptor superfamily. Many clinical drugs and natural compounds have been reported to be the activators of PXR and CAR, through either direct agonism or indirect mechanisms involving signaling transductions [9, 10]. As the Type 1 nuclear receptors, PXR and CAR are sequestered in the cytoplasm with chaperone proteins without activation. Once stimulated by the activators, PXR and CAR translocate into the nucleus and form a heterodimer with retinoid X receptor (RXR), another nuclear receptor, on the specific promoter regions of the drug-metabolizing enzyme (DME) and transporter genes. A similar activation mechanism is also employed for the xenobiotic receptor AhR, although it belongs to a different protein superfamily, the bHLH/PAS transcription factors [11]. Many

environmental pollutants, such as polycyclic aromatic hydrocarbons (PAHs), have been reported as AhR ligands [12]. Upon binding with ligands, AhR enters the nucleus where it heterodimerizes with AhR nuclear translocator (ARNT) on the xenobiotic response elements (XREs) to regulate the transcription of multiple genes, including DMEs and transporters.

## **2.2 DISCOVERY OF XENOBIOTIC RECEPTORS**

The molecular mechanisms by which environmental contaminants or drugs regulate DME and transporter expression have been elusive until the discovery and characterization of the xenobiotic receptors in the 90s (Figure 1). The nuclear receptor PXR was independently cloned in the laboratories of Steven Kliewer then at the Glaxo Wellcome and Ronald Evans at the Salk Institute in 1998 [13, 14]. The Kliewer lab discovered the mouse PXR from a gene fragment in the Washington University Mouse Expressed-Sequence Tag (EST) Database by Gene Trapper solution hybridization cloning technology using a mouse liver cDNA library [13]. PXR was named based on its activation by the pregnanes 21-carbon steroids. The Evans lab cloned the human PXR as a homolog of the *Xenopus* Benzoate X receptors (BXR) from a human genomic library/liver cDNA library hybridized with a full-length cDNA encoding the *Xenopus* BXR, which was originally discovered in a screen for maternally expressed nuclear hormone receptors and cloned from a *Xenopus* egg cDNA library [14, 15]. The human PXR was originally named by the Evans lab as steroid and xenobiotic receptor (SXR) due to its activation by multiple natural and synthetic steroids as well as xenobiotics [14].

The discovery of PXR benefited from earlier work published by Phil Guzelian's laboratory at the University of Colorado who suggested that there are "cellular factor" and

defined “DNA element” which are responsible for the drug responsive regulation of the human and rodent CYP3A genes in hepatocytes [16, 17]. The consensus glucocorticoid-responsive “DNA element” identified by DNase I footprint turned out to be the PXR response element on the CYP3A gene promoter, which is occupied by the “cellular factor” PXR. Therefore, CYP3A is considered a prototypical target gene of PXR. The in vivo role of PXR as a xenobiotic sensor has been firmly established through the creation and characterization of PXR knockout mice, in which the CYP3A induction in response to prototypic inducers, such as pregnenolone-16 $\alpha$ -carbonitrile (PCN) and dexamethasone was completely abolished [18, 19]. The identification of PXR as a xenobiotic sensor also provides a molecular basis for the species specificity of CYP3A induction [16]. Human and mouse PXR have high homology (95% at the amino acid level) in the DNA-binding domain (DBD), so they can share PXR binding sites found on the promoters of the human or rodent CYP3A genes. In contrast, the homology in the ligand-binding domain (LBD) is significantly lower (73% at the amino acid level), which may have explained the ligand specificity between these two receptors. This notion was supported by the X-ray crystal structure analysis of the PXR LBD [20]. The spherical ligand-binding pocket of PXR was estimated to be at least twice as large as those of the other steroid hormone- or retinoid receptors. In addition, the ligand-binding pocket of PXR was extremely hydrophobic and flexible. These structural features may have accounted for the promiscuity of this receptor in recognizing a wide range of xenobiotics. Using both transfection and transgenic approaches, it has been functionally demonstrated that the species origin of the PXR receptor, rather than the promoter structure of CYP3A genes, dictates the species-specific pattern of CYP3A inducibility [18]. These findings also led to the creation of the so-called “humanized” PXR transgenic mice, in which the mouse PXR in the liver was genetically replaced by its human counterpart PXR. The humanized mice

exhibit the human profile of drug response, such as their responsiveness to the human-specific inducer rifampicin and a lack of response to the rodent-specific inducer PCN [18]. Since the propensity of drugs to induce CYP3A and many other DMEs is implicated in drug metabolism, drug-drug interactions, and drug toxicity, the humanized mice represent a major step toward creating humanized toxicological models that may aid in the development of safer drugs and nutraceuticals.

The xenobiotic receptor identity of CAR, a human orphan nuclear receptor cloned in David Moore's lab in 1994 whose physiological function was then unknown [21], was revealed shortly after the discovery of PXR in 1998. CAR was initially identified as MB67 from the human cDNA library using a degenerate oligonucleotide directed to the P-box sequence of the thyroid hormone receptor (TR)/retinoid acid receptor (RAR)/orphan receptor subgroup. The receptor was shown to activate a direct repeat spaced by five nucleotides (DR-5) type of retinoid acid response element (RARE) in a ligand-independent manner, which can be further augmented by the addition of the heterodimerization partner RXR [21]. The mouse CAR was cloned using the human CAR (MB67) cDNA probe in 1997 [22]. The identity of CAR as a xenobiotic receptor was first hinted by the ability of selective androstane metabolites to inhibit its constitutive activity [23]. The constitutive activity and the structural mechanism of agonism and antagonism of CAR were eventually revealed by three crystal structures reported almost at the same time [24-26]. The role of CAR in the positive xenobiotic regulation was suggested when CAR was shown to activate the phenobarbital response element (PBRE) found on the promoters of phenobarbital (PB)-inducible CYP2B genes that were independently reported by several labs [27-29]. Masahiko Negishi's laboratory at the National Institute of Environmental Health Sciences (NIEHS) was the first to purify CAR from mouse hepatocytes as a protein bound to the

PB-responsive enhancer module (PBREM) of the Cyp2b10 gene, the mouse homolog of CYP2B, where it heterodimerizes with RXR [24-26, 30]. CYP2B is therefore a prototypical target gene of CAR. The *in vivo* xenobiotic function of CAR was firmly established through the creation and characterization of CAR knockout mice. Disruption of the mouse CAR locus by homologous recombination resulted in the loss of PB and TCPOBOP activation of Cyp2b10 gene [31].

AhR is best known for its ability to mediate the induction of CYP1A1 by the halogenated aromatic hydrocarbons (HAHs), such as 2,3,7,8-tetrachlorodibenzo-p-dioxin (TCDD) [32]. Similar with the discovery of PXR, the identification of AhR was based on the early characterization of the consensus XREs in the enhancer region of the rat cytochrome P450-c [33-35], which is bound and regulated by an unknown soluble protein. ARNT was first identified as one of the XRE-binding proteins [36], before the cloning of mouse AhR in 1992 by two independent groups, the Christopher Bradfield's lab then at Northwestern University and the Yoshiaki Fujii-Kuriyama's lab in Japan [37, 38]. The human AhR was cloned from the HepG2 cDNA library shortly after the discovery of murine AhR in the Bradfield lab [39]. The paradigm for the AhR-ARNT heterodimer to induce CYP1A1 expression is well accepted. However, the molecular details for the protein-DNA interaction and transcriptional regulation were only revealed very recently by the crystal structure of the AHR-ARNT transcription factor complex bound to the XRE [40, 41]. The toxicological relevance of AhR was well established using the AhR knockout mice. At least three independent mouse strains were generated to study the function of AhR *in vivo* [42-44]. Biological importance of AhR was also gradually appreciated using the AhR-null mice, suggesting a much broader scope of AhR in the physiological and pathophysiological settings [45-49].



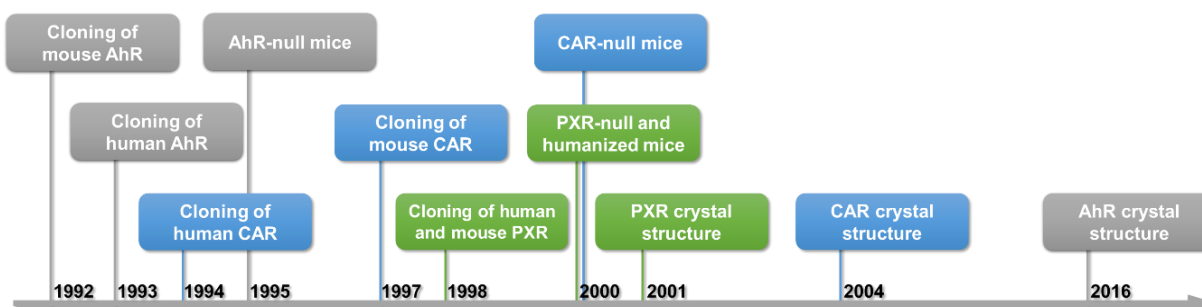


**Figure 1. Historical landmarks in the discovery of PXR, CAR and AhR**

### **2.3 XENOBIOTIC REGULATION BY PXR, CAR AND AHR**

Accumulation of xenobiotic chemicals, such as carcinogens, environmental pollutants, and therapeutic drugs, often causes damage to organismal tissues. Thus, the scrutiny and detoxification of these compounds are essentially important to maintain the physiological homeostasis. The DMEs and transporters encoded by the xenobiotic responsive genes are the major executors of the detoxification of xenobiotics. As depicted in Figure 2, the elimination of these exogenous toxic chemicals involves the biotransformation by the Phase 1 hydroxylating enzymes (cytochrome P450s, CYPs) that reduce the hydrophobicity and the Phase 2 conjugating enzymes (e.g. UDP-glucuronosyltransferases, UGTs; glutathione S-transferase, GST; sulfotransferase, SULTs; N-acetyltransferase, NATs; and natural product methyltransferases, NPMTs) that further reduce the toxicity of xenobiotic compounds. The detoxified chemicals can be excreted through efflux transporters, such as organic anion transporting polypeptides (OATPs), P-glycoproteins, and multidrug resistance-associated proteins (Mrps), to the bile and urine. Specifically, some classical Phase 1, 2, and 3 target genes for mouse PXR and CAR are

Cyp2b10 and Cyp3a11, Sult2a1 and Sult1e1, and Mrp2/3, respectively, whereas AhR is responsible for the TCDD-induced Cyp1a/b, Ugt1a1, and Abcg2.

Earlier studies focusing on the individual DME and drug transporter genes have characterized the essential promoter regions, regulatory mechanisms, and crosstalk of multiple xenobiotic receptors in the liver [8]. For example, PXR and CAR have been well established in the reciprocal regulation of CYP3A and CYP2B genes. In fact, the expression and promoter-based reporter activity of these classical target genes are frequently used as readouts for the screening of xenobiotic receptor modulators. PXR- and CAR-controlled DME genes are somewhat overlapped due to their affinity to the similar DNA elements, with CYP2B, CYP2C and CYP3A being the most outstanding examples [8, 50]. AhR, on the other hand, mediates the highly inducible expression of CYP1 enzymes. It was estimated that CYP2B6 and CYP2C enzymes are responsible for the metabolism of approximately 25% and 20% of all xenobiotics, respectively [51], whereas CYP3A4 alone metabolizes more than half of the clinical drugs [52]. CYP1A1 is a cancer-related susceptibility gene that mediates the DNA mutations caused by carcinogens [53]. Not only in the liver, the xenobiotic receptors and their target genes also play an vital role in the blood-brain barrier [54]. In addition, the target genes for these xenobiotic receptors are not limited to DME and drug transporter genes. High throughput profiling approaches (e.g. microarray, RNA-seq, ChIP-seq) have identified numerous target genes of xenobiotic receptors, other than the DME and drug transporter genes, in the genome [55-59]. Overall, the xenobiotic receptor-mediated expression of DMEs and drug transporters is an important determinant for the efficacy and adverse effects of clinically used drugs.

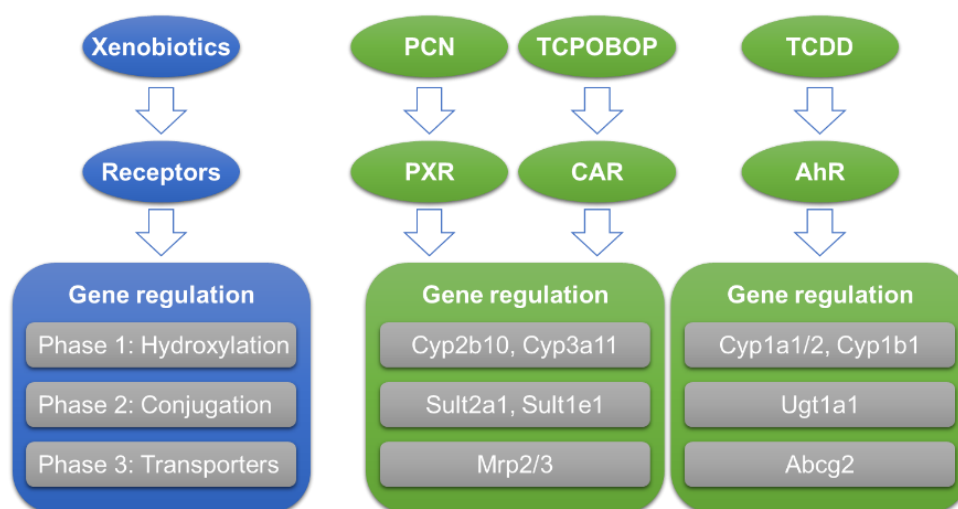


**Figure 2. Paradigm of xenobiotic response by mouse PXR, CAR and AhR**

Xenobiotics are sensed by the xenobiotic receptors. Once activated by the xenobiotic ligands, the receptors enter the nucleus and up-regulate the genes of DMEs and transporters that participate in the conversion and excretion of xenobiotic compounds. The prototypical PXR ligand PCN and CAR ligand TCPOBOP regulate similar downstream target genes, such as Cyp2b10, in the mouse liver. The prototypical AhR ligand TCDD induces genes, such as Cyp1a1, in the liver.

## 2.4 MODULATION OF XENOBIOTIC RECEPTORS: LIGAND-INDUCED NUCLEAR TRANSLOCATION

The xenobiotic response is often very fast. For instance, the induction of Cyp2b10 in liver peaks within one hour upon acute treatment of TCPOBOP in mice [60]. Such rapid response is largely benefited from massive translocation of the xenobiotic receptors from the cytoplasm into the nucleus [61]. Like many other steroid hormone receptors, the xenobiotic receptors are associated with heat shock proteins (HSPs) and immunophilin chaperones as a cytoplasmic retention complex [62]. PXR, CAR and AhR were all found associated with HSP90 [63-65] (Figure 3). Specifically, PXR and CAR interacts with the tetratricopeptide repeat protein (TRP), designated as cytoplasmic CAR retention protein (CCRP) [64, 66], whereas AhR is bound with the TRP named Hepatitis B Virus X-Associated Protein 2 (XAP2) [67-69]. Some evidence

strongly suggests the cytoplasmic retention is presumably an adaptive mechanism that accumulates xenobiotic receptors in the cytoplasmic reservoir for the quick response to cellular stress. First, HSP90 and the associated microtubule network is required for the PB-induced CAR activation [70]. Second, genetic deletion of CCRP attenuates TCPOBOP-induced Cyp2b10 [71], and likewise, XAP2 ablation attenuates TCDD-induced Cyp1b1 and Ahrr [72]. Third, the accumulation of CAR in the cytoplasm is not derived from nuclear exclusion, because CCRP does not affect the nuclear content of CAR [66]. Fourth, the CAR-HSP70/90-CCRP complex is coordinatively regulated by the degradation of CCRP in response to thermal stress [73].

In the past two decades, Masahiko Negishi's laboratory and others have identified several key proteins participating in the PB-induced nuclear translocation of CAR. The protein phosphatase 2A (PP2A) is recruited to the cytoplasmic retention complex of CAR in response to PB, the CAR activator [63]. The fact that okadaic acid, a PP2A inhibitor, diminishes PB-mediated induction of CYP2B expression in primary rat hepatocytes suggests that PP2A is involved in the activation of CAR [74]. In fact, phosphorylation plays an important role in regulating nuclear translocation of CAR. Human CAR threonine 38 (corresponding to mouse CAR threonine 48) is a conserved Protein Kinase C (PKC) target site that is found in many nuclear receptors [75]. Mutational analysis showed that T38A which lacks phosphorylation mimics the effect of PB treatment while T38D which resembles phosphorylated CAR is majorly retained in the cytoplasm [76]. This indicates that phosphorylation at threonine 38 is a repressive signal for nuclear translocation of CAR, although further study is needed to elucidate the upstream events of PKC. Hepatic growth factors negatively regulate PB-mediated induction of CYP2B through activation of MEK-ERK signaling. Phosphorylated ERK sequesters the phosphorylated CAR in the cytoplasm via the C-terminal leucine-rich peptide on CAR, named

xenochemical response signal (XRS) [77, 78]. The PP2A core enzyme is recruited to the phosphorylated CAR by the receptor for activated C kinase 1 (RACK1) and exerts its phosphatase activity [79]. RACK1 preferentially binds to the phosphorylated threonine 38. The binding of RACK1 and recruitment of PP2A can be repressed by a “dormant” homodimer of phosphorylated CAR that buries the PP2A/RACK1 binding site within the dimer interface [80]. RACK1 is negatively regulated by Src kinase, one of downstream pathways of epidermal growth factor receptor (EGFR). Phosphorylation of RACK1 by Src prevents its interaction with CAR. PB, demonstrated as an antagonist of EGFR, competes with EGF binding to EGFR, therefore abrogating the blockade of RACK1 by activated EGFR cascades [79]. Collectively, the two signaling branches downstream of EGFR, MEK/ERK and Src/RACK1, integrates at the cytoplasmic CAR to inhibit its nuclear translocation.

The mitogen-activated protein kinase (MAPK) p38-mediated phosphorylation of threonine 38 in the nucleus is required for the transcriptional activity of CAR and the exclusion from the nucleus [81, 82]. In addition to the phosphorylation of CAR on threonine 38, the phosphorylation of serine 202 is also involved in CAR nuclear translocation [83]. Moreover, one of the protein phosphatase 1 catalytic subunits, PPP1R16A, was reported to interact with CAR and prevents nuclear translocation of CAR, which is also dependent on its phosphatase activity [84]. AMP-activated protein kinase (AMPK) has also been implicated in PB-induced CAR activation [85-87]. PB seems to increase the AMP/ATP ratio or down-regulate miR-122, to activate AMPK [88, 89]. It remains unknown if CAR is a direct substrate for AMPK or some indirect mechanisms exist. Pharmacological activation of AMPK can down-regulate HSP70 and EGFR while activate PP2A, suggesting AMPK may trigger CAR nuclear translocation through regulation of the suppressive proteins [90-92]. The molecular mechanism of nuclear

translocation of CAR can be also applied to PXR, based on that (1) PXR exists in the cytoplasmic retention complex with HSP90 and CCRP [64], and (2) PKC and MEK modulators regulate CYP3A4, the classical PXR target gene, in the same manner as with CAR [93, 94]. Yet the mechanism that controls the nuclear translocation of PXR may be distinct from CAR. The  $\text{Ca}^{2+}$ /Calmodulin-Dependent Protein Kinase II (CaMKII) and protein phosphatase 1 (PP1) counteract at the human PXR threonine 290 to regulate the nuclear translocation of PXR, which resembles the “PKC-versus-PP2A” mechanism for the CAR [95].

Similarly, the nuclear translocation of AhR is majorly regulated by the HSP90 and XAP2-containing cytoplasmic retention complex. Forced expression of HSP90 abrogates the AhR-mediated transactivation, indicating its inhibitory role for the AhR activity [96]. In contrast, overexpression of XAP2 enhances AhR-mediated transcription, likely due to its dual function as a component of cytoplasmic retention complex and a ligand-dependent transcriptional coactivator of AhR in the nucleus [67-69]. Also in the multiprotein complex of AhR are the carboxyl terminus of hsc70-interacting protein (CHIP) that controls the overall cytoplasmic pool of AhR [97], the co-chaperone protein p23 that regulates ligand-independent response and protects AhR from degradation [98, 99], and the phosphodiesterase type 2A (PDE2A) that inhibits the relay of cAMP signal to AhR [100]. c-Src, the protein tyrosine kinase, was found to be associated with the AhR cytoplasmic complex as well [101]. Unlike the canonical xenobiotic response, TCDD-induced release of c-Src triggers a phosphorylation cascade.

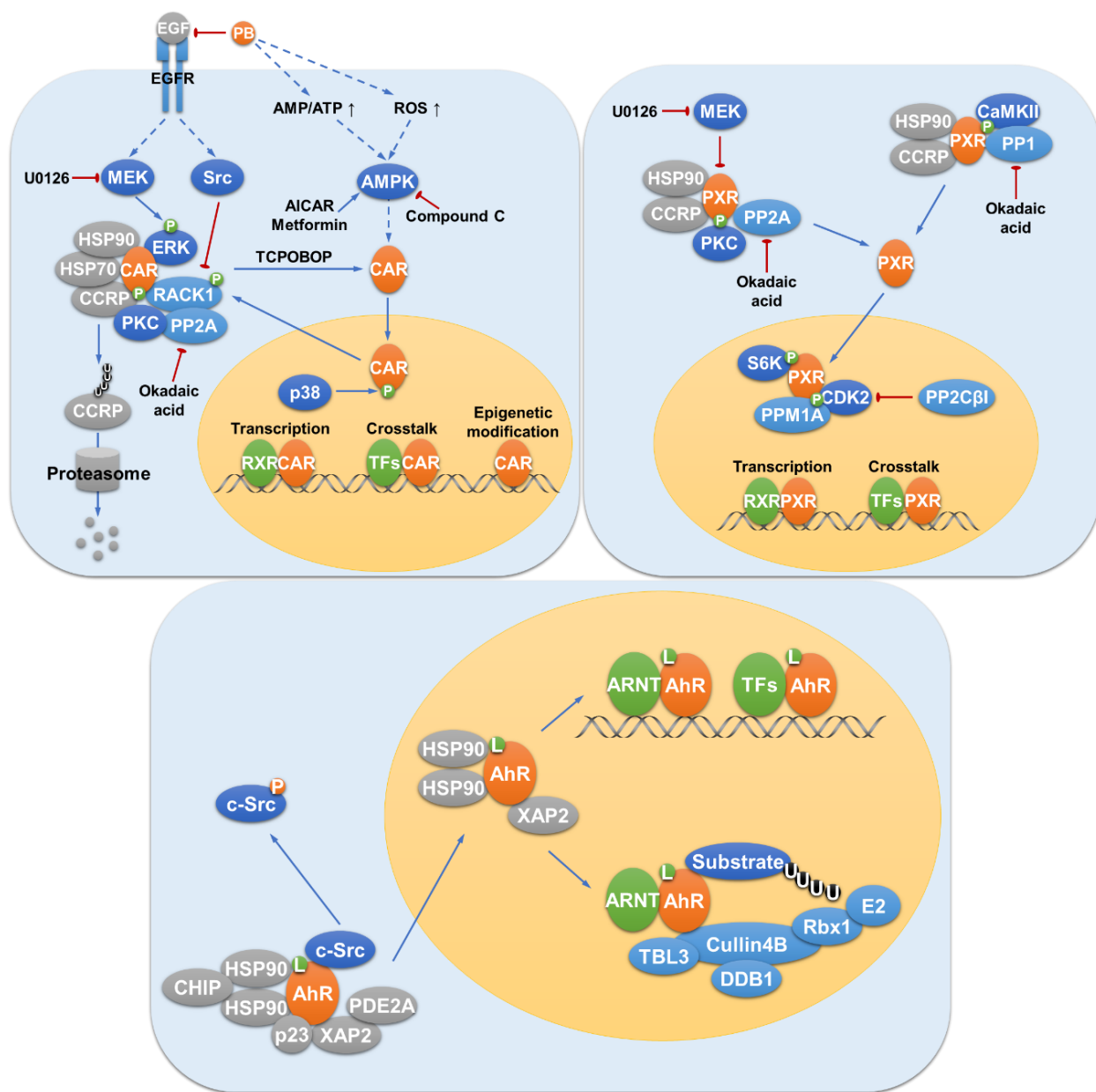


**Figure 3. Nuclear translocation of xenobiotic receptors**

Activation of xenobiotic receptors involve the nuclear translocation from the cytoplasmic retention complexes. The disruption of the retention complex containing protein chaperones precedes the nuclear entry. The nuclear translocation of CAR and PXR are also regulated by multiple phosphorylation events. In the nucleus, the xenobiotic receptors exert transcriptional activity by direct binding to DNA or indirectly through crosstalk with other transcriptional factors (TFs). AhR also possesses ubiquitin E3 ligase activity by integrating the CUL4B complex.

## **2.5 MODULATION OF XENOBIOTIC RECEPTORS: TRANSCRIPTIONAL REGULATION**

While immediate response resulted from nuclear translocation and activation of xenobiotic receptors quickly defends the intracellular homeostasis against external xenobiotic insults, long term protection, and inevitably the adverse effects, can be augmented by transcriptional up-regulation of xenobiotic receptor genes themselves. Many chemicals from drugs, herbal medicine as well as environmental exposure have been shown to increase PXR and CAR messenger RNA (mRNA) level [9]. AhR is likely the upstream transcriptional factor that mediates up-regulation of CAR, and possibly PXR, as supported by experimental evidence [102]. In addition, the bile acid sensor, farnesoid X receptor (FXR), may also mediate the xenobiotic regulation of PXR and CAR [103]. In contrast to xenobiotic-induced expression which is mostly marginal, the expression of PXR and CAR is more responsive to hormonal regulation. Glucocorticoids (e.g. dexamethasone) efficiently induce PXR, CAR, and their binding partner RXR expression, and subsequently the target genes (e.g. CYP2B6 and CYP3A4) in human primary hepatocytes at a nanomolar concentration [104-106]. A distal glucocorticoid response element (GRE) was found on the CAR promoter, indicating CAR is a direct target gene of glucocorticoid receptor (GR) [107]. On the other hand, inflammatory cytokines, such as IL-1 $\beta$  and IL-6, down-regulate the expression of PXR and CAR, possibly through antagonizing the effect of GR [108, 109]. Glucocorticoids are also capable of inducing AhR expression [110]. Thyroid hormones, through the activation of TR, are able to induce CAR expression at a physiological concentration as well [111]. Inversely, activated CAR affects serum thyroid hormone concentration and influences thyroid-follicular cell proliferation [112]. All-trans



retinoic acid (ATRA), a metabolite of vitamin A, is also found to up-regulate CAR expression through RAR [113], whereas PXR has contributed to the ATRA catabolism [114].

As described above, it is suggested that endogenous hormones and endobiotic metabolites are very important for the maintenance of basal expression of PXR and CAR. Several studies also showed that PXR and CAR expression is highly inducible during feeding-fasting switch. Fasting-dependent induction of CAR is majorly mediated by hepatocyte nuclear factor 4 $\alpha$  (HNF4 $\alpha$ ) and PPAR $\alpha$  [115, 116]. While fasted WT mice exhibit higher CAR mRNA level compared to fed mice, this fasting response is almost completely attenuated in either HNF4 $\alpha$  knockout or PPAR $\alpha$  knockout mice. HNF4 $\alpha$  and PPAR $\alpha$  responsive element were defined on the promoter of CAR, indicating HNF4 $\alpha$  and PPAR $\alpha$  directly bind to the promoter of CAR and induce gene expression. Moreover, PGC1 $\alpha$  co-activates HNF4 $\alpha$  and PPAR $\alpha$  on the CAR promoter and co-activates CAR on the Cyp2b10 promoter, which may contribute to the amplification of CAR downstream genes [116]. Similarly, PGC1 $\alpha$  also regulates the fasting-induced PXR expression as well as its target genes [117].

The research with regards to the transcription and function of PXR and CAR mainly focus on the liver, because they are highly enriched in the liver tissue. AhR is ubiquitously expressed in multiple tissues, and the basal expression and inducibility of AhR gene in response to cellular environmental cues are cell- and tissue-specific [118]. Epigenetic modification on the AhR promoter region may explain the distinct inducibilities in different cell types [119, 120]. The analysis of human AhR promoter in the HepG2 cells revealed potential binding sites for several transcriptional factors, such as AP1 and SP1 [121]. The accessibility of the promoter region to these basic transcriptional factors (e.g. SP1) due to different epigenetic signatures may have determined the basal expression and inducibility for the AhR gene [120, 122]. In addition,

cell type-specific regulation of AhR gene could also be attributed to the presence of specific transcriptional factors in the context of genome [123]. For example, transforming growth factor  $\beta$  (TGF $\beta$ ) suppresses AhR promoter activity in a Smad-dependent manner [123]. In agreement with this observation, in the pancreatic cancer cell lines, the basal expression and transcriptional activity of AhR coincides with the loss-of-function of Smad4, which is a tumor suppressor in pancreatic cancer-associated neoplasia [124-126]. In contrast, AhR is up-regulated in the immune cells by TGF $\beta$  plus IL-6, possibly due to the predominant role of NF- $\kappa$ B that positively regulates the expression of AhR [127, 128].

Post-transcriptional regulation via microRNA (miR) is another mechanism that controls the abundance of xenobiotic receptor mRNAs. miR-137 and miR-148a negatively regulates CAR and PXR mRNA, respectively [129, 130], whereas miR-124 is found to bind with the 3'-UTR of AhR mRNA [131]. The fate of mature AhR mRNA is under the control of a RNA binding protein Musashi-2 (MSI2) in the hematopoietic stem cells [132]. Overexpression of MSI2 attenuates the AhR pathway by binding to 3'-UTR of AhR mRNA, which mimics the effect of AhR antagonism [133]. Lastly, the expression of xenobiotic receptors and at least some of their downstream target genes fluctuate in accordance with the diurnal rhythm, indicating that physiological circadian system also has impact on the xenobiotic response [134, 135].

## **2.6 MODULATION OF XENOBIOTIC RECEPTORS: POST-TRANSLATIONAL MODIFICATIONS (PTMS)**

Protein PTMs, such as phosphorylation and ubiquitylation, are critical processes that control the transduction of cell signaling, stability of proteins, and genomic accessibility. It has been

described above the essential role of the consensus PKC phosphorylation site in regulating the nuclear translocation of CAR and PXR [75]. While the PKC-dependent phosphorylation of CAR and PXR is inhibitory for the xenobiotic response, PKC kinase activity is required for the XRE-binding of AhR/ARNT and CYP1A1 induction [136-139]. However, the specific target site for PKC on the AhR protein is still unknown. Another consensus phosphorylation site across the nuclear receptors is threonine 57 on the human PXR [140]. This phosphorylation, at least partially by S6K, reduces DNA-binding of PXR by changing the sub-nuclear distribution of PXR. Human PXR is also phosphorylated at serine 350 by the cyclin-dependent kinase 2 (CDK2) [141]. This phosphorylation attenuates the gene induction of CYP3A4, which links the cell cycle to the xenobiotic response. On the other hand, the  $Mg^{2+}/Mn^{2+}$ -dependent phosphatase 1A (PPM1A) and protein phosphatase 2C $\beta$ 1 (PP2C $\beta$ 1) seem to antagonize the inhibitory phosphorylation thus augmenting PXR's activity [142, 143]. PXR is also reported to be phosphorylated at many other amino acid residues with altered transcriptional activity [144]. Moreover, cAMP-dependent protein kinase (PKA) also modulates the phosphorylation status of PXR and is inhibitory for the CYP3A4 expression in a species-dependent manner [145]. Likewise, cAMP signaling is also able to abolish the PB-induced CYP2B and TCDD-induced CYP1A1 [146, 147]. Whether these xenobiotic receptors are direct targets of PKA needs to be further determined. Yet in the case of AhR, cAMP stimulation leads to the formation of a XRE-binding AhR complex that excludes ARNT, indicating there is probably some proteins underlying PKA signaling interacting with AhR in response to cAMP [147].

Acetylation of PXR is another PTM that regulates the activity of PXR [148]. It was shown that acetylation at the Lysine 109, inhibits DNA binding and heterodimerization with RXR $\alpha$ , and down-regulates PXR's transcriptional activity [149]. Furthermore, the deacetylase

p300 and SIRT1 seem to positively regulate PXR's transcriptional activity by manipulating the acetylation status. The acetylation of CAR and AhR remains unclear. Yet conversely, AhR can affect global acetylation of the proteome by transcriptional up-regulation of TCDD-inducible poly(ADP-ribose) polymerase (TiPARP) [150]. TiPARP is an enzyme that consumes  $\text{NAD}^+$  which is the coenzyme for multiple acetylases, such as sirtuin 1 (SirT1), SirT3, and SirT6 [150-152]. Indeed, the loss of  $\text{NAD}^+$  and acetylase activity through the TiPARP elevation has been implicated in the TCDD-induced toxicity and the inhibitory effect of TCDD on the gluconeogenesis [150-152]. In addition, TiPARP, as an ADP-ribosyltransferase, can also directly regulate the enzymatic activity of phosphoenolpyruvate carboxykinase (PEPCK), the rate-limiting enzyme in the hepatic gluconeogenesis, and the lipogenic nuclear receptors, liver X receptor  $\alpha$  (LXR $\alpha$ ) and LXR $\beta$  [153, 154]. More interestingly, AhR itself is a direct target of TiPARP for ADP-ribosylation [155]. This PTM serves as a negative feedback mechanism to restrain the activity of AhR, as ADP-ribosylation of AhR suppresses its transactivation activity [155, 156]. Supporting this, it was reported that the loss of TiPARP increases sensitivity to dioxin-induced steatohepatitis and lethality [157].

SUMOylation is a critical PTM for the anti-inflammatory response exerted by the nuclear receptors, such as PPAR $\gamma$  and LXR $\alpha/\beta$  [158-160]. Similarly, the anti-inflammatory activity of PXR is relied on its SUMOylation [161-163]. SUMOylation is also a PTM for the AhR signaling pathway. AhR, ARNT, and AhR repressor (AhRR) are all found to be modified by SUMOylation [164-166]. It was shown that SUMOylation of AhR potentially prevents its degradation through the ubiquitylation-proteasome pathway. Overall, the PTMs of xenobiotic receptors add another layer of network to regulating the xenobiotic response.

## **2.7     ROLE OF UBIQUITIN PROTEOLYTIC SYSTEM IN XENOBIOTIC RECEPTORS**

Theoretically, all proteins can end up with degradation. The half-life of a protein is determined by the ubiquitylation-mediated degradation through either proteasome or autophagy [167]. The ubiquitylation modification is carried out by three types of enzymes: the E1 ubiquitin-activating enzymes, the E2 ubiquitin-conjugating enzymes, and the E3 ubiquitin ligases [168, 169]. While the E1 and E2 enzymes are relatively conserved and quantitatively limited, the E3 ligases are diverse. E3 ligases target select protein substrates thereby determine the substrate specificity. Three types of E3 ligases have been categorized based on the distinct catalytic mechanisms: the Cullin-really interesting new gene (RING) E3 ligases (CRLs), the homologous to E6AP carboxyl terminus (HECT) E3 ligases, and the RING-between-RING (RBR) E3 ligases [168]. The CRL is the largest E3 ligase family and is best characterized by virtue of their essential roles in the development and diseases [169]. The CRLs are modular E3 ligases that are assembled based on different cullin scaffold proteins with corresponding substrate adaptor proteins and E2-binding proteins [170]. There are eight different cullins (CUL1, 2, 3, 4A, 4B, 5, 7, and 9) identified in the human cells.

The xenobiotic receptors are all protein substrates for the UPS. AhR was found to be rapidly eliminated after activation by the ligand [171, 172]. Proteasome inhibitors block the degradation of AhR and ligand-independently induce AhR target genes. More interestingly, AhR itself is a ubiquitin E3 ligase for the estrogen receptor (ER) and androgen receptor (AR) in breast cancer cells and prostate cancer cells, respectively [173]. This transcription-independent enzymatic activity is also observed for the degradation of  $\beta$ -catenin in the intestine [174]. The AhR-containing E3 ligase is a typical CRL that is consists CUL4B as the scaffold and AhR as

the substrate adaptor (Figure 3). A recent study has demonstrated that the E3 ligase activity is enhanced when the transcriptional activity is impeded [175], suggesting the transactivation and E3 activity are relatively exclusive. PXR also undergoes ubiquitylation and its stability is controlled by various E3 ligases [176-179], while the ubiquitylation of CAR is less understood. In summary, the ubiquitylation-mediated proteolysis plays an important role in the xenobiotic response. The xenobiotic receptors also seem to play a role in the UPS vice versa. Therefore, its interplay with the UPS is investigated by this dissertation study.

### **3.0 CAR AND HEPATIC GLUCONEOGENESIS**

#### **3.1 RESEARCH BACKGROUND**

CAR was initially recognized as a xenobiotic receptor that senses foreign chemicals and transcriptionally regulates the expression of DMEs and transporters in the liver [180]. More recent studies suggested that CAR can also restore glucose homeostasis under diabetic conditions. We and others showed that activation of CAR suppressed hepatic gluconeogenic gene expression and glucose production, and ameliorated hyperglycemia in genetic (ob/ob) and diet-induced obese mice [181, 182], as well as in a mouse model of gestational diabetes [183]. A potential metabolic benefit of CAR activation in human glucose metabolism has been suggested by several clinical reports showing that administration of phenobarbital, a prototypical CAR activator, decreased plasma glucose levels and improved insulin sensitivity in diabetic patients [184-186].

Although the role of CAR in the crosstalk between xenobiotic metabolism and glucose homeostasis has been recognized, few studies have probed into the underlying molecular mechanisms. It has been suggested that CAR may prevent the recruitment of the Forkhead box protein O1 (FoxO1) to the gluconeogenic gene promoters [187], or interfere with the HNF4 $\alpha$ -mediated gluconeogenesis by competing for the DR1 binding motif and its coactivators [188]. However, due to the limited evidence and mostly in vitro nature of the previous studies, the

molecular pathway that underlies the CAR-mediated suppression of gluconeogenesis in physiological context remained to be identified.

Hepatic gluconeogenesis is a biochemical process that de novo biosynthesizes glucose from non-carbohydrate carbon substrates, including amino acids, glycerol, pyruvate and lactate. The rate of gluconeogenesis is considered limited by the transcription of the gluconeogenic genes PECK and G6Pase. PGC1 $\alpha$  is an inducible transcriptional coactivator that plays a tissue specific role in regulating energy metabolism [189]. For the hepatic gluconeogenesis, PGC1 $\alpha$  is a versatile coactivator that synergizes the transcriptional activity of the key gluconeogenic transcriptional factors, such as FoxO1, HNF4 $\alpha$ , and GR [190-192] (Figure 4). During fasting, cAMP signaling, driven by glucagon, induces the hepatic expression of PGC1 $\alpha$  by activating the transcription factor cAMP response element binding protein (CREB) [190]. Insulin, on the other hand, suppresses the expression of PGC1 $\alpha$  when prandial glucose level is elevated [193]. The hepatic expression of PGC1 $\alpha$  is robustly increased in obese mice to a level comparable to the fasting state, contributing to the hyperglycemia and obesity-related pre-diabetic symptoms [194].

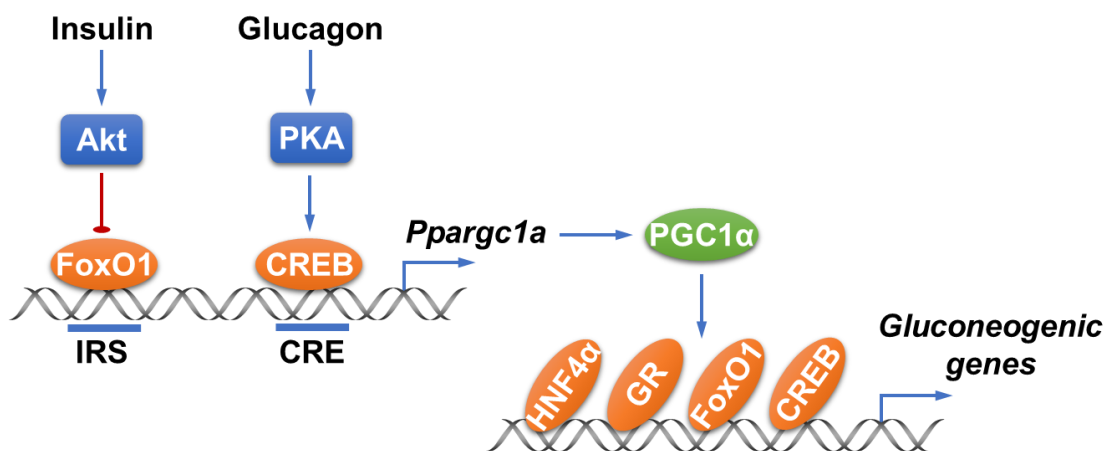


**Figure 4. PGC1 $\alpha$  is a central transcriptional coactivator in hepatic gluconeogenesis**



The PML-NBs are macromolecular nuclear structures distributed in discrete nuclear foci [195]. Dynamic orchestrations of PML-NBs constantly sequester and release transcriptional factors/coactivators and mediate their post-translational modifications in response to cellular stresses. PML-NBs have been implicated in the regulation of diverse cellular functions, including the induction of apoptosis and cellular senescence, inhibition of proliferation, maintenance of genomic stability and antiviral responses [195]. Recent evidence suggests that PML also participates in glucose and lipid metabolism. PML regulates fatty acid oxidation, which is essential for hematopoietic stem cells maintenance and cancer cell survival [196, 197]. PML ablation in mice leads to accelerated fatty acid metabolism, abnormal glucose metabolism, and insulin resistance [198].

In the present work, we discovered a post-translational mechanism by which CAR suppresses the gluconeogenic activity of PGC1 $\alpha$ . Upon ligand activation, CAR translocates from cytoplasm into the nucleus where it recruits PGC1 $\alpha$  to the CUL1 E3 ligase complex for ubiquitylation. The interaction between CAR and PGC1 $\alpha$  also triggers the sequestration of both proteins into PML-NBs, which is required for the degradation of PGC1 $\alpha$  and suppression of gluconeogenesis both in vitro and in vivo. Interestingly, CAR can inhibit the gluconeogenic activity of PGC1 $\alpha$  independent of its traditional transcription-regulatory activity.

### 3.2 MATERIALS AND METHODS

**Animals.** C57BL/6J mice were purchased from Jackson Laboratory (Bar Harbor, ME). PML<sup>-/-</sup> mice were purchased from the National Cancer Institute Mouse Repository [199]. CAR<sup>-/-</sup> mice

were previously described [31]. For the fasting-refeeding experiment, mice were subjected to overnight fasting (16 h), followed by 12 h re-feeding before sacrifice. For the high-fat diet (HFD) feeding, mice were fed with HFD (TD.06414) from Harlan (Madison, WI). When necessary, mice were i.p. injected with TCPOBOP in DMSO (0.25 mg/kg) once per week. Intraperitoneal glucose tolerance test (IPGTT) were performed after overnight fasting. The mice were intraperitoneally injected with 2 mg/kg glucose and blood glucose were measured at the time point of 0, 15, 30, 60, 90, and 120 min, respectively. All mice were housed in a pathogen-free animal facility under a standard 12h light-dark cycle with free access to food and water. The use of mice in this study complied with all relevant federal guidelines and institutional policies.

**Plasmids, cell transfection and reporter assay.** pCMX-HA-CAR (WT, D8, D30, CBM, CC/AA, and L346F), pCMX-Flag-PGC1 $\alpha$ , pCMX-PPAR $\alpha$ , pCMX-HA-PPAR $\gamma$ , pCMX-FXR, pCMX-LXR, pCMX-HNF4 $\alpha$ , pCMX-HA/Flag-Cullin1 (WT, Cul1NT, CullNT\_Mut), pCMX-HA/Flag-Skp1 (WT, Mut), pCMX-Flag-Rbx1, Gal4-PGC1 $\alpha$  (1-400) and pCMX-PML/Myc-PML were cloned using standard molecular cloning techniques. pcDNA-Flag-PGC1 $\alpha$  [200] (plasmid #1026), Gal4-PGC1 $\alpha$  [201] (Plasmid #8892), and pcDNA3-DN-CUL1-FLAG [202] (Plasmid #15818) were purchased from Addgene (Cambridge, MA). The G6pase-luciferase reporter plasmid [203] was a gift from Dr. Richard M. O'Brien (Department of Molecular Physiology and Biophysics, Vanderbilt University Medical School). pcDNA-CAR (CC/AA) [188] was a gift from Dr. Jongsook Kim Kemper (Department of Molecular and Integrative Physiology, University of Illinois at Urbana-Champaign). HEK293T, HepG2 and Hepa1-6 cells were obtained from ATCC (Manassas, VA). Transient transfections were performed with the TransIT®-LT1 Transfection Reagent (Mirus, WI). Cells were harvested and measured for

luciferase and  $\beta$ -gal activities 24 h after transfection. Transfection efficiency was normalized against  $\beta$ -gal activity derived from the co-transfected pCMX- $\beta$ -gal plasmid.

**Adenovirus, lentivirus and stable cell line.** Flag-tagged mouse CAR adenovirus (Ad-Flag-CAR) was generated by using the AdEasy Adenoviral Vector System from Life Technologies (Grand Island, NY). HA-tagged PGC1 $\alpha$  adenovirus (Ad-HA-PGC1 $\alpha$ ) were made using shuttle vector pAd-Track HA-PGC1 $\alpha$  [204] (Plasmid #14427) from Addgene. Ad-PGC1 $\alpha$  RNAi and scrambled RNAi adenoviruses [205] were gifts from Dr. Marc R. Montminy (Salk Institute for Biological Sciences). The sequences for scrambled RNAi and PGC1 $\alpha$  RNAi are 5'-GGCATTACAGTATCGATCAGA-3' and 5'-GGTGGATTGAAGTGGTGTAGA-3', respectively. Mouse PML RNAi lentivirus was generated using pLKO.1-mPML RNAi vector from Open Biosystems (Pittsburgh, PA). pLKO.1-non-specific RNAi vector, packaging vector psPAX2 and envelope vector pMD2.G were from Addgene. PML RNAi knockdown Hepa 1-6 cells were selected by puromycin (5-10  $\mu$ g/ml) for 2 weeks after the lentiviral infection.

**Western blotting and coimmunoprecipitation (coIP).** For Western blot analysis, cells were lysed in ice-cold RIPA buffer containing a protease inhibitor cocktail from Roche (Indianapolis, IN). Primary antibodies used include anti-HA (C29F4) and anti-HNF4 $\alpha$  (C11F12) from Cell Signaling (Danvers, MA), anti-Flag (M2) and anti-Myc (M4439) from Sigma (St. Louis, MO), anti-PML (clone 36.1-104) from Millipore (Billerica, MA), and anti-PGC1 $\alpha$  (H300) and anti-CAR (M-150) from Santa Cruz Biotechnology (Santa Cruz, CA). For coIP, cells were lysed in IP buffer (150 mM NaCl, 50 mM Tris-HCl at pH 7.5 and 1% NP-40) supplemented with a protease-inhibitor cocktail. The lysates were pre-cleared by incubation with protein G magnetic beads and

incubated with primary antibody overnight at 4°C, followed by incubation with protein G magnetic beads for 1h at room temperature. Protein G beads were then washed five times with ice-cold IP buffer, eluted with protein loading buffer, and analyzed by Western blotting.

**Chromatin immunoprecipitation (ChIP) assay.** Primary mouse hepatocytes were infected with Ad-HA-PGC1 $\alpha$  and/or Ad-Flag-CAR (MOI=5) for 48 h and fixed in 1% formaldehyde for 15 min in room temperature. Nuclear extracts were sonicated and aliquot of sheared chromatin (equivalent of 2x10<sup>5</sup> cells) was immunoprecipitated with anti-HA, anti-HNF4 $\alpha$ , or normal rabbit IgG. Immunoprecipitated chromatin was de-crosslinked, ethanol precipitated, and quantified by quantitative real-time PCR. Recoveries were calculated as the percentage of input.

For the mouse G6pase promoter, we used the following primers:

G6pase\_-300 bp\_F: 5'-GCTGTTTTTGTGTGCCTGTT-3',

G6pase\_-300 bp\_R: 5'-TGCTATCAGTCTGTGCCTTG-3';

G6pase\_-3000 bp\_F: 5'-CAGTGCTCCCAGAGTTCCTC-3',

G6pase\_-3000 bp\_R: 5'-TGAGGAGCAGGGCTGTCTGT-3'.

For the mouse Pepck promoter, we used the following primers:

Pepck\_-300 bp\_F: 5'-GGCCTCCCAACATTCATTAAC-3',

Pepck\_-300 bp\_R: 5'-CGCCCTCCTTGCTTTAAATA-3';

Pepck\_-3000 bp\_F: 5'-TCCAGCATACACAGAGGATCA-3',

Pepck\_-3000 bp\_R: 5'-TGCAGTCCAGCTAATGCAAC-3'.

**In vitro ubiquitylation assay.** The in vitro ubiquitylation assay was performed based on a previously described protocol [206]. The CAR associated E3 complex was purified from the

293T cells transfected with HA-Flag-CAR and HA-Cullin1/Skp1/Rbx1 with the anti-Flag M2 affinity gel from Sigma. The recombinant Flag-PGC1 $\alpha$  was purified from the 293T cells transfected with Flag-PGC1 $\alpha$  with the anti-Flag M2 affinity gel. For the in vitro ubiquitylation reaction, the purified E3 complex and PGC1 $\alpha$  were incubated in the presence of ATP, ubiquitin, and E1/E2 (UbcH5a and UbcH3) from a Ubiquitylation Assay Kit from Enzo Life Sciences (Farmingdale, NY). The reactions were terminated by adding Western blotting loading buffer and the products were resolved on SDS-PAGE.

**Mouse primary hepatocyte isolation and culture.** Mouse primary hepatocytes were isolated from 8-12 weeks old male WT, CAR<sup>-/-</sup>, or PML<sup>-/-</sup> mice. Briefly, the liver was first perfused with Hank's buffered salt solution containing 0.5 mM EGTA, 0.1 M Hepes at 5 ml/min for 5-10 min and then perfused with L-15 medium containing 1.8 mM CaCl<sub>2</sub>, 0.1 M Hepes, 20  $\mu$ g/ml liberase TM (Roche). After perfusion, the dissociated hepatocytes were filtered through 50- $\mu$ m pore mesh and collected by centrifugation at 400 rpm for 4 min at 4°C. Hepatocytes were seeded onto type 1 collagen-coated dishes or slides in William E medium containing 5% FBS, 1  $\mu$ M dexamethasone, 100 nM insulin. The hepatocytes were maintained with medium (HepatoZYME-SFM supplemented with 100 nM dexamethasone, 100 nM insulin, 0.2% BSA) the following day. For forskolin treatment, primary hepatocytes were changed to maintenance medium without hormones for 6 h before treating with forskolin (10  $\mu$ M) and/or TCPOBOP (500 nM) for mRNA analysis, or in 1 ml gluconeogenic medium (glucose free DMEM, 20 mM sodium lactate, 2 mM sodium pyruvate, 0.5% BSA) for hepatic glucose production assay. Medium glucose concentration was measured using a glucose (GO) assay kit (GAGO20-1KT) from Sigma.

**Immunofluorescence and confocal microscopy.** Primary mouse hepatocytes or cell lines were grown on slides and treated when necessary. Cells were fixed in 4% paraformaldehyde for 15 min in room temperature followed by blocking with PBS containing 5% donkey serum and 0.3% Triton X-100 for 30 min. Slides were incubated in diluted primary antibody overnight at 4 °C followed by incubation with fluorochrome-conjugated secondary antibody for 2 h at room temperature in the dark. Slides were mounted and scanned using confocal microscopy to obtain images.

**Quantitative real-time PCR.** Total RNA was isolated using the TRIZOL reagent from Invitrogen (Carlsbad, CA). Reverse transcription was performed with random hexamer primers and Superscript RT III enzyme from Invitrogen. SYBR Green-based real-time PCR was performed with the ABI 7300 Real-Time PCR System. Data was normalized against internal control Cyclophilin A.

**Statistical analysis.** All results were presented as means  $\pm$  SD. Statistical significance between groups was determined using an unpaired two-tailed Student t test, with P values of less than 0.05 considered statistically significantly.

### **3.3 EXPERIMENTAL RESULTS**

**CAR suppresses gluconeogenic gene expression through inhibiting the PGC1 $\alpha$  activity.** Activation of CAR has been shown to suppress hepatic gluconeogenesis and ameliorate hyperglycemia in animal models and human patients [181, 182, 184-186]. In primary mouse

hepatocytes, forskolin (FSK) treatment increased the expression of G6pase and Pepck mainly via the CREB-mediated induction of PGC1 $\alpha$  [207]. We showed that treatment with TCPOBOP suppressed the FSK-responsive induction of G6pase and Pepck without affecting the expression of PGC1 $\alpha$  (

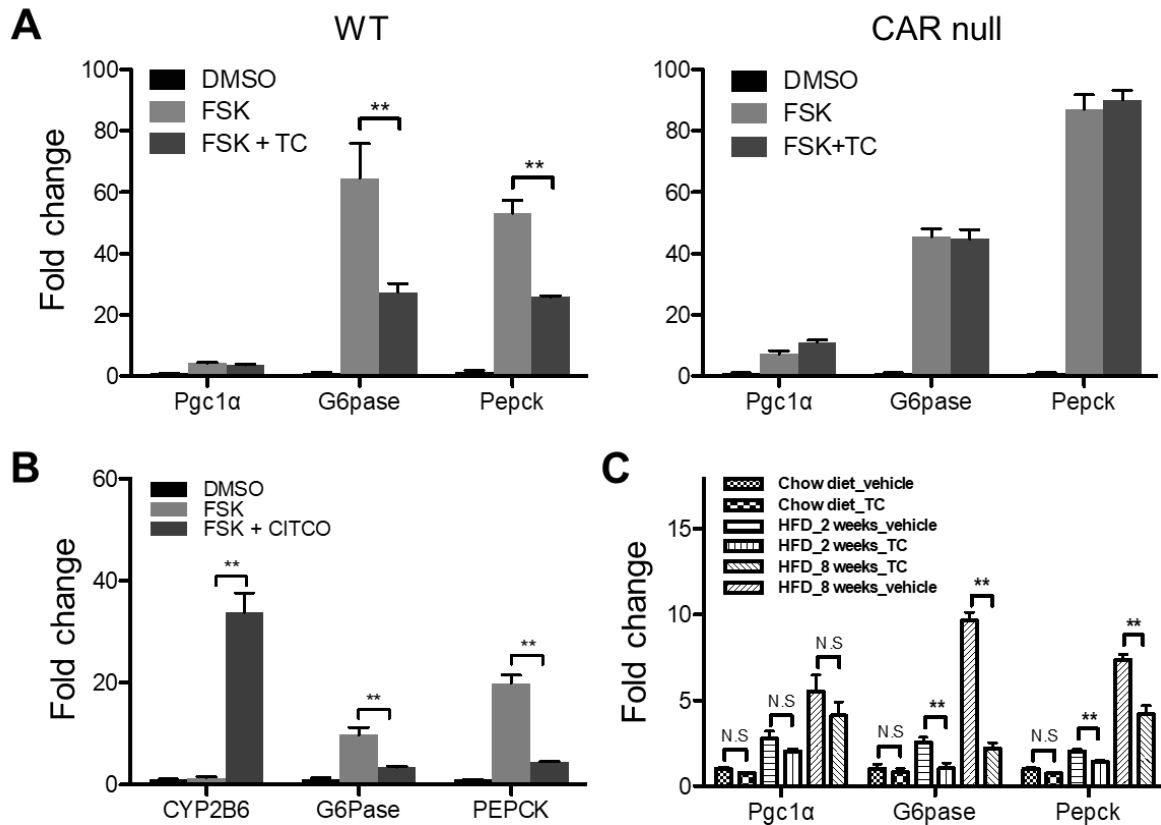


**Figure 5. CAR suppresses gluconeogenic gene expression in primary mouse and human hepatocytes** (A, left panel), and this effect was abolished in hepatocytes isolated from the CAR<sup>-/-</sup> mice (

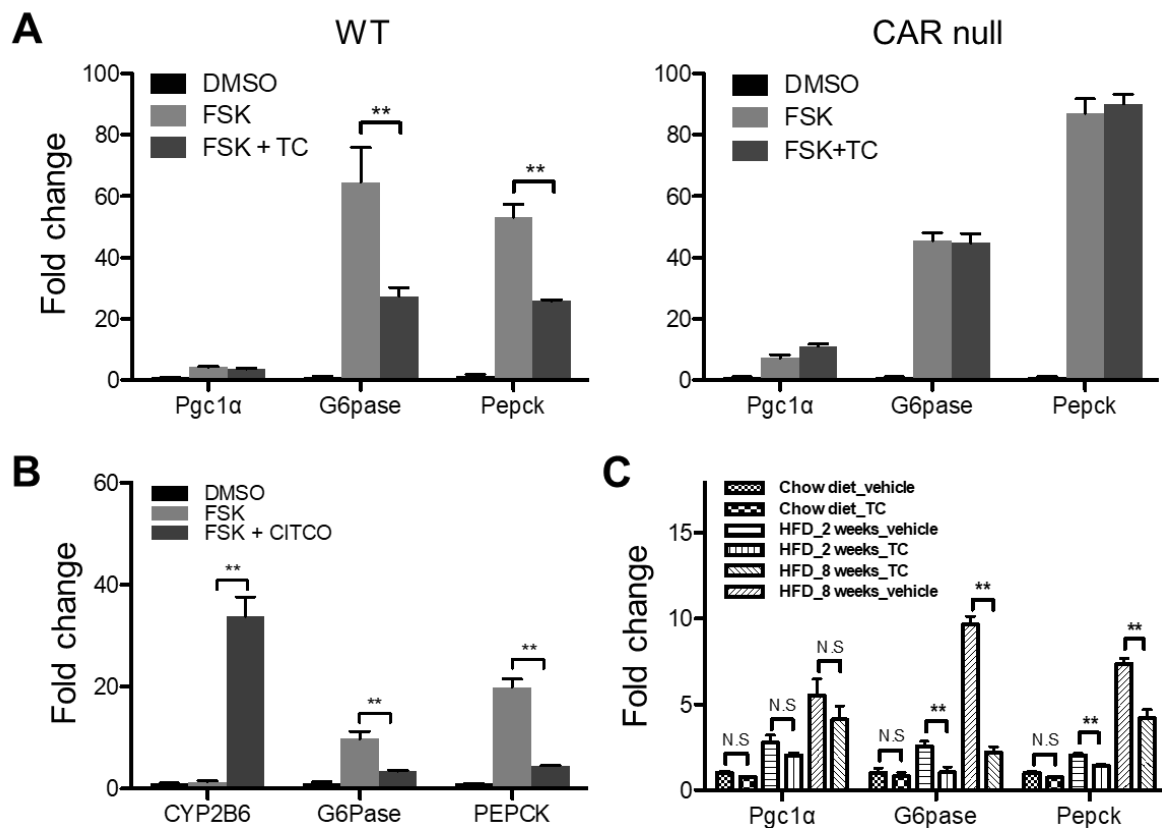


**Figure 5. CAR suppresses gluconeogenic gene expression in primary mouse and human hepatocytes** (A, right panel). The inhibition of FSK-responsive induction of G6Pase and PEPCK was also observed in primary human hepatocytes treated with CITCO, a human CAR specific agonist (



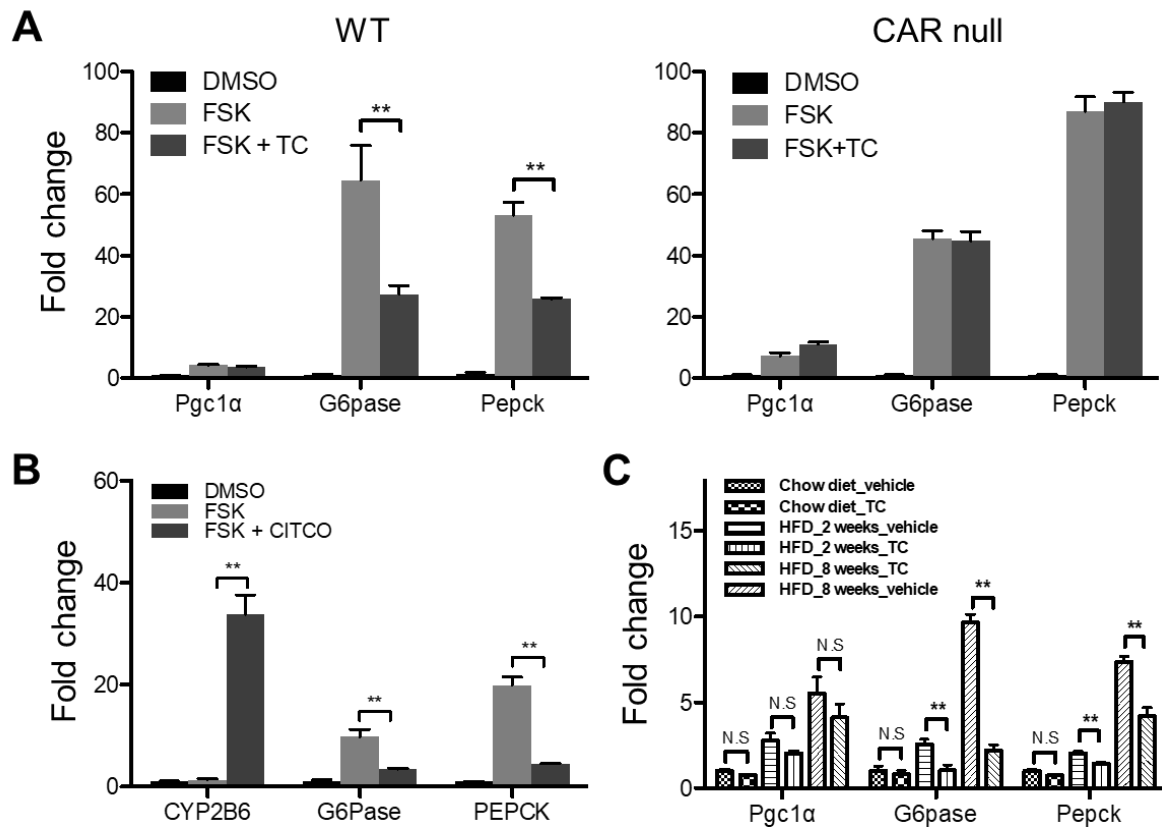


**Figure 5. CAR suppresses gluconeogenic gene expression in primary mouse and human hepatocytes**  
 B). In searching for the mechanism by which CAR inhibits gluconeogenesis, we noticed the inhibitory effect of the CAR agonist TCPOBOP on hepatic gluconeogenic gene expression was most dramatic in high-fat diet (HFD)-fed mice (

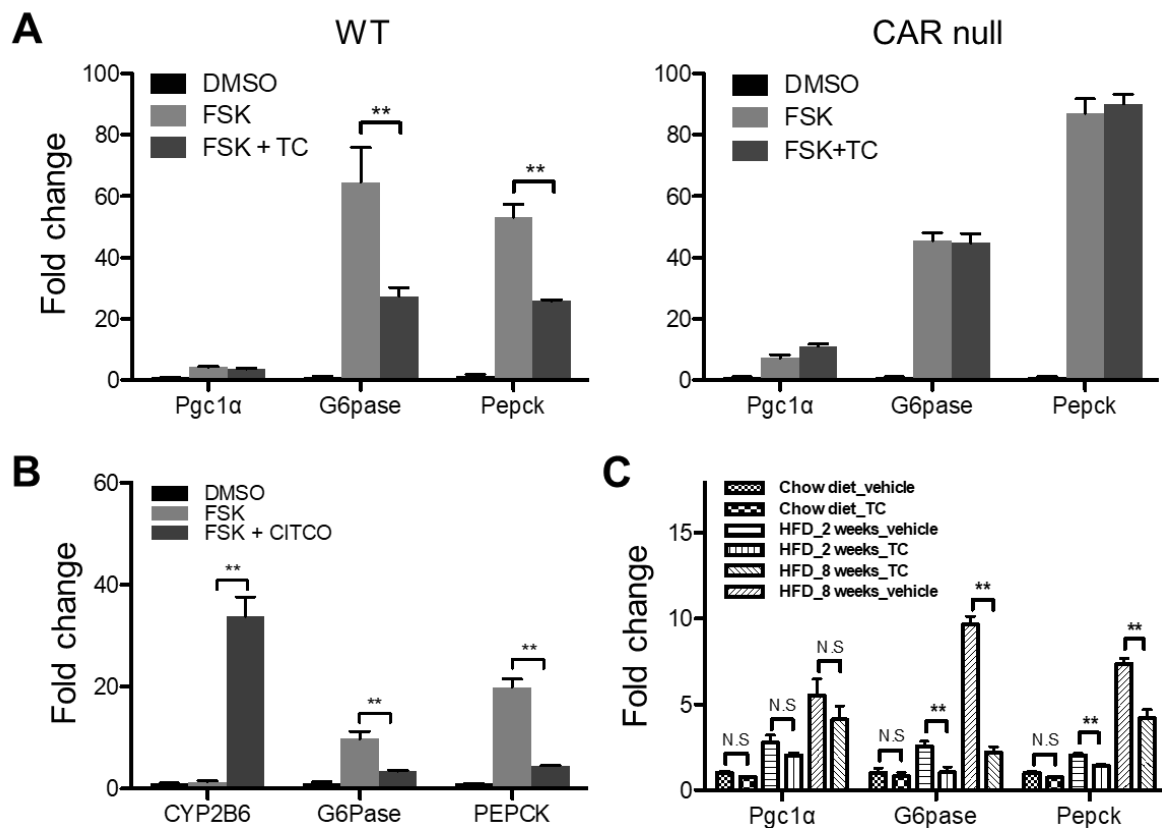


**Figure 5. CAR suppresses gluconeogenic gene expression in primary mouse and human hepatocytes** C), suggesting that CAR might have targeted a HFD inducible factor in the liver. One such candidate factor is PGC1 $\alpha$ , whose expression is markedly elevated in diabetic conditions (

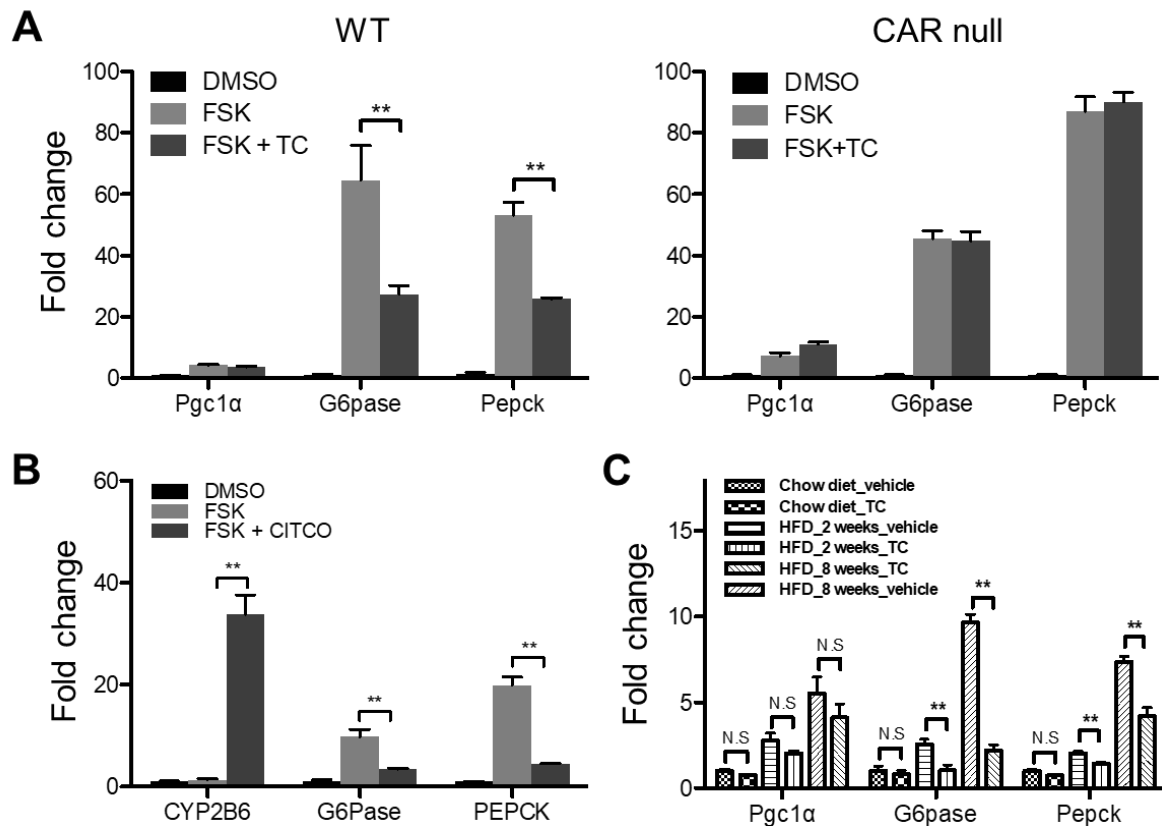


**Figure 5. CAR suppresses gluconeogenic gene expression in primary mouse and human hepatocytes** C) [192, 194].

To directly evaluate the effect of CAR on PGC1α activity, we found that CAR efficiently suppressed the PGC1α responsive activation of the G6pase-luciferase reporter gene (**Error! Reference source not found.A**). The inhibition was obvious in the absence of an exogenously added ligand and was enhanced by the addition of TCPOBOP. The inhibitory effect of TCPOBOP was PGC1α dependent, because the inhibition of both gluconeogenic gene expression and glucose production was attenuated by PGC1α knockdown (**Error! Reference source not found.B-C**). To directly test whether CAR activation inhibited PGC1α, we overexpressed PGC1α in primary mouse hepatocytes using adenovirus. Overexpression of PGC1α was sufficient to induce the expression of G6pase and Pepck as expected, which was attenuated in cells co-infected with the CAR expressing adenovirus and treated with TCPOBOP

(**Error! Reference source not found.**D). At the functional level, CAR activation inhibited PGC1 $\alpha$ -induced glucose production in primary mouse hepatocytes (**Error! Reference source not found.**E).

In the loss-of-function model, we showed the chow diet-fed CAR<sup>-/-</sup> mice had elevated basal expression and compromised fasting responsive induction of G6pase and Pepck (Figure 7A). In addition, the hepatic expression of CAR fluctuated in response to fasting, re-feeding and HFD feeding, mirroring the pattern of PGC1 $\alpha$  (Figure 7B), suggesting CAR may be co-regulated with PGC1 $\alpha$  and suppresses its activity to fine-tune hepatic glucose homeostasis.

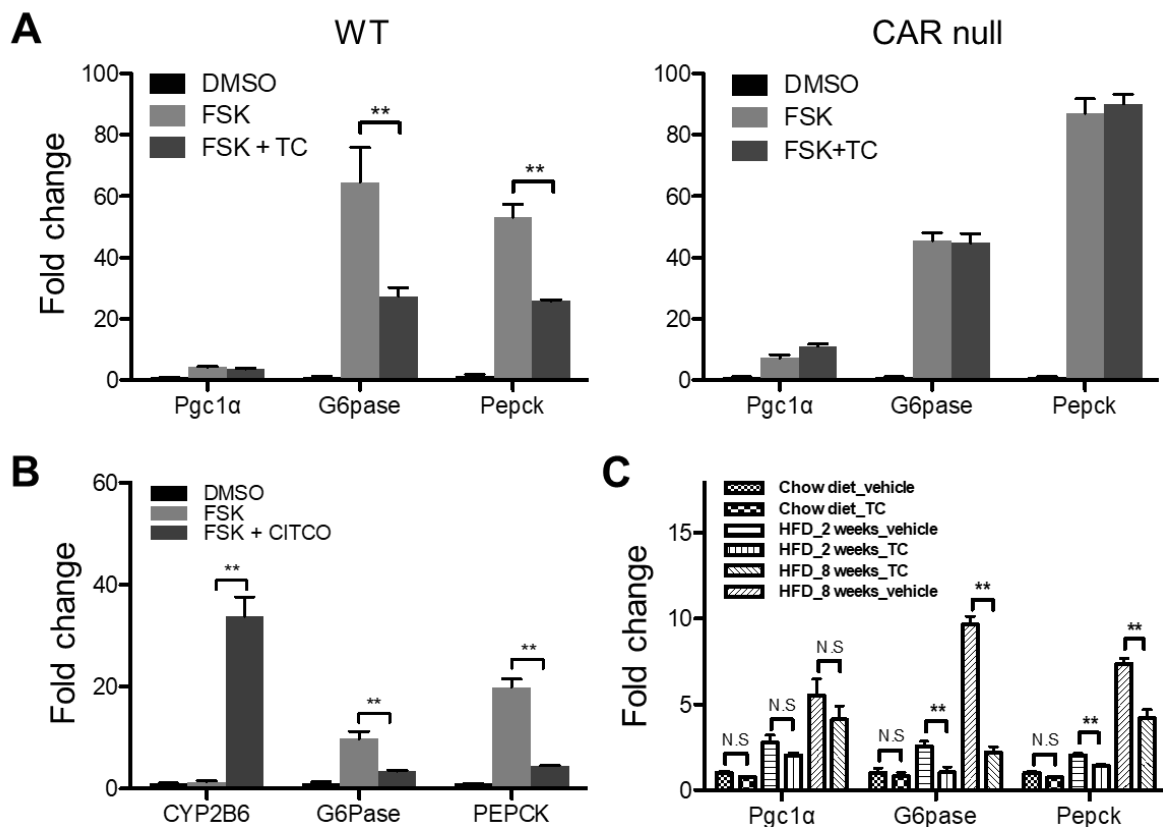


**Figure 5. CAR suppresses gluconeogenic gene expression in primary mouse and human hepatocytes**  
 (A) Mouse primary hepatocytes isolated from WT (left panel) or CAR null (right panel) mice were treated with TCPOBOP (TC) (500 nM) or DMSO for 12 h before treatment of Forskolin (FSK, 10  $\mu$ M) for 2 h. The gene expression was measured by real-time PCR. (B) Human primary hepatocytes were treated with CITCO (1  $\mu$ M) for 12 h, followed by FSK (10  $\mu$ M) treatment for 2 h. The gene expression was measured by real-time PCR. (C) Wild type C57BL/6J mice were fed with chow diet or HFD for

indicated amounts of time. The hepatic gene expression was measured by real-time-PCR ( $n \geq 4$  per group). \*,  $p < 0.05$ ; \*\*,  $p < 0.01$ ; N.S., not significant.

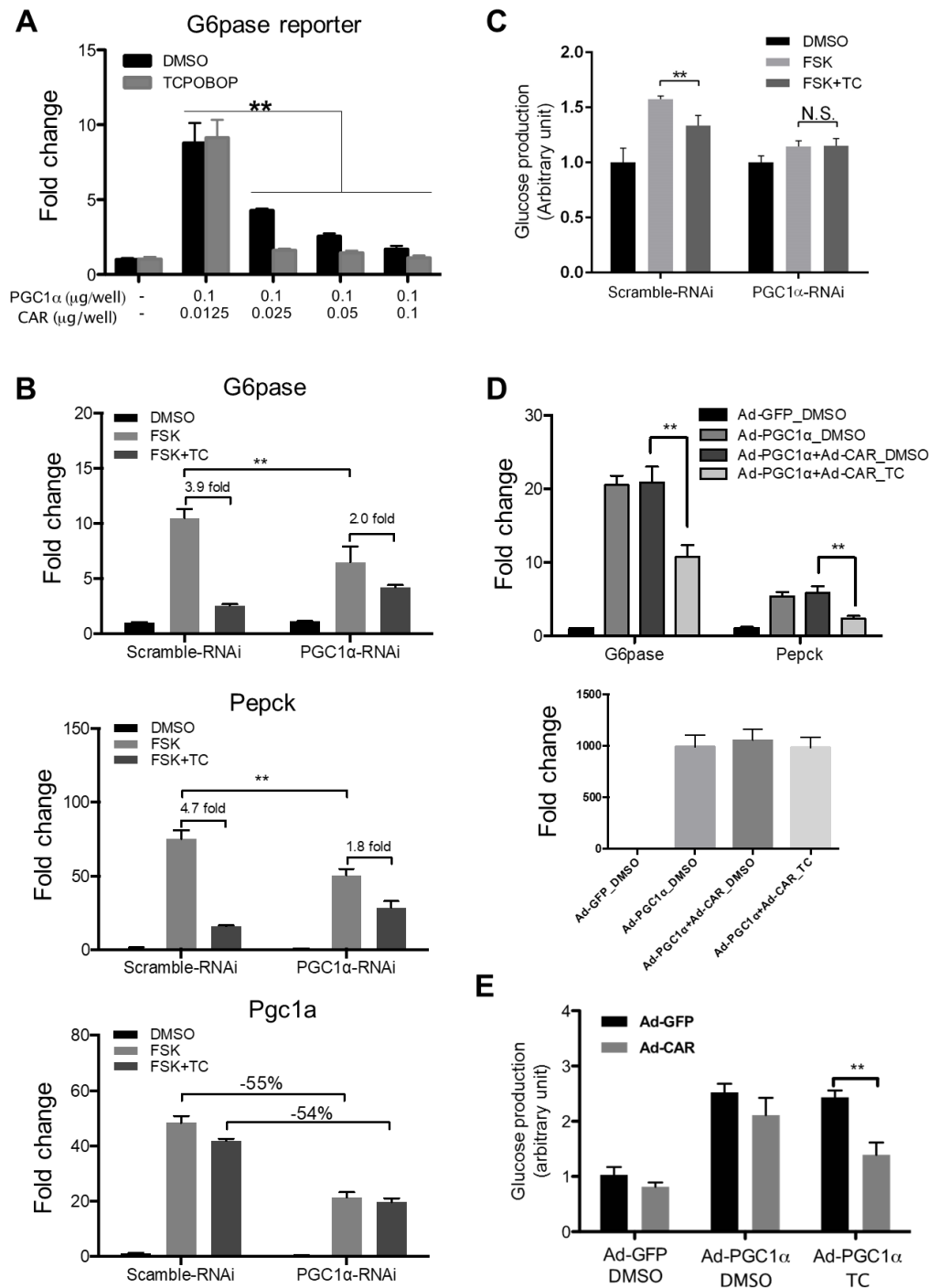


**Figure 6. CAR suppresses gluconeogenesis through inhibiting PGC1α activity**

(A) Co-transfection of CAR inhibited the PGC1α responsive activation of the G6pase luciferase reporter in 293T cells. (B) Primary hepatocyte from WT mice infected with Ad-scramble RNAi or Ad-PGC1α

RNAi for 48 h were treated with TC (500 nM) or DMSO for 12 h before treatment of FSK (10  $\mu$ M) for 2 h. The gene expression was measured by real-time PCR. (C) Primary mouse hepatocytes were pretreated with TCPOBOP (500 nM) overnight in the maintenance medium. Glucose production was measured after incubation with FSK (10  $\mu$ M) with or without TCPOBOP (500 nM) in the glucose-free medium for 4 h (n=3 with triplicates). (D and E) Primary hepatocytes from CAR null were infected with Ad-GFP, Ad-CAR or Ad-PGC1 $\alpha$ , and treated with or without TC (500 nM) for 12 h before measuring the mRNA expression of G6pase and Pepck (D, left panel) and Pgc1a (D, right panel) and glucose production (E). \*\*, p<0.01; N.S., not significant.

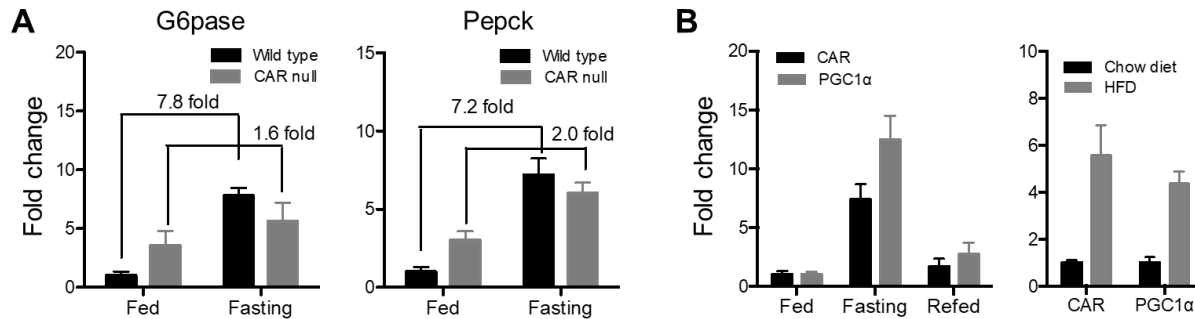


**Figure 7. CAR and PGC1 $\alpha$  are co-regulated during fasting and in diet-induced obesity**  
 (A) Hepatic expression of G6pase and Pepck in fed, overnight fasted (16 h), and re-fed (12 h) WT and CAR null mice. n=5 per group. (B) Expression of CAR and PGC1 $\alpha$  in mouse liver during the fasting-re-fed transition (left panel, n=4 per group), and upon a 12-week high-fat diet (HFD) feeding (right panel, n=5 per group).

**CAR reduces the recruitment of PGC1 $\alpha$  to the gluconeogenic gene promoters and causes redistribution of PGC1 $\alpha$  to PML-NBs.** We then used chromatin immunoprecipitation (ChIP) assay to determine whether CAR activation reduced the recruitment of PGC1 $\alpha$  to the promoters of gluconeogenic genes. Indeed, treatment of primary mouse hepatocytes with TCPOBOP suppressed the recruitment of PGC1 $\alpha$  to the proximal promoter regions of G6pase (-250 bp) and Pepck (-300 bp) genes that harbor the HNF4 $\alpha$  and FoxO1 binding sites without affecting the non-specific binding of PGC1 $\alpha$  to the distal promoter regions (Figure 8A). The inhibition appeared to be PGC1 $\alpha$  specific, because the recruitment of HNF4 $\alpha$  to the G6pase and Pepck gene promoters was not affected in the same cells (Figure 8B).

A direct interaction between CAR and PGC1 $\alpha$  had been reported [116, 208], which was verified by our coIP experiment (**Error! Reference source not found.A**). However, a simple “coactivator quenching” model in which CAR competes with other transcriptional factors for the binding of PGC1 $\alpha$  was unlikely the underlying mechanism, because among a panel of nuclear receptors known to interact with and coactivated by PGC1 $\alpha$ , only CAR showed inhibition of the PGC1 $\alpha$  activity (**Error! Reference source not found.B**). Instead, we found CAR activation induced a dramatic redistribution of nuclear PGC1 $\alpha$ . Treatment of primary mouse hepatocytes with TCPOBOP triggered the translocation of CAR from cytoplasm to nucleus to concentrate at the spot-like subnuclear loci, which turned out to be PML-NBs, a multi-protein subnuclear structures, as confirmed by their colocalization with the PML protein [209] (**Error! Reference source not found.C-D**). A similar pattern of CAR-responsive redistribution of PGC1 $\alpha$  and CAR to the PML-NBs was observed in the human hepatoma HepG2 cells co-transfected with CAR and PGC1 $\alpha$  (**Error! Reference source not found.E-F**). The interaction between CAR and PGC1 $\alpha$  was required for their targeting to the PML-NBs, because transfection of CAR or PGC1 $\alpha$  alone resulted in an even distribution of both proteins in the nucleus (**Error! Reference source not found.E-F**). PML is the essential component of the PML-NBs, in which PML multimerizes to function as a critical scaffold for the assembly of the entire complex [210]. We then hypothesized that redistribution of CAR and PGC1 $\alpha$  may have been mediated through the interaction between the CAR-PGC1 $\alpha$  complex and PML. Indeed, coIP assay showed that transfection of PGC1 $\alpha$  or CAR alone in 293T cells resulted in little interaction with PML, whereas co-expression of both proteins significantly enhanced their association with PML (**Error! Reference source not found.G**), which was consistent with the immunofluorescence

results (**Error! Reference source not found.**E-F). These results suggested that the formation of CAR-PGC1 $\alpha$  complex was a prerequisite for their interaction with PML.

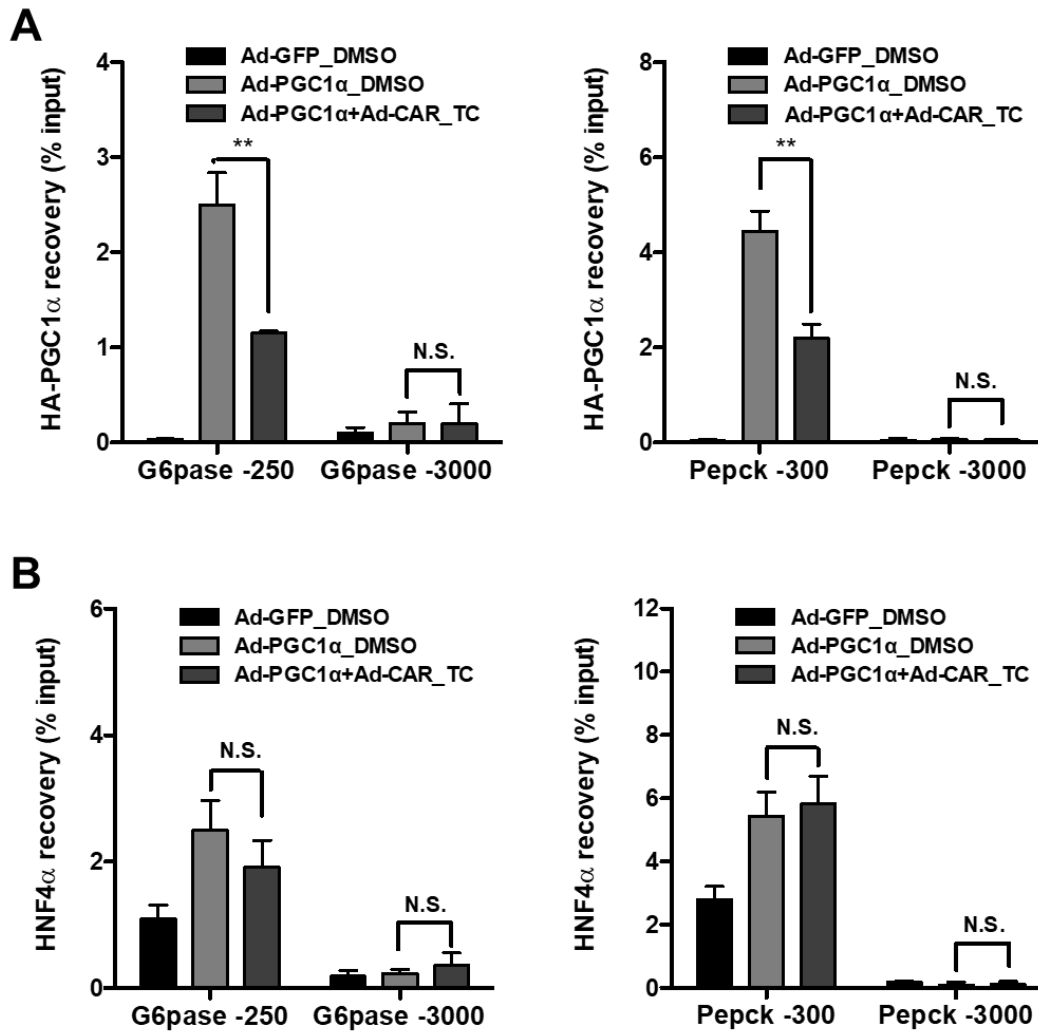


**Figure 8. CAR decreases the DNA-binding of PGC1 $\alpha$  on the gluconeogenic genes**

(A and B) Primary mouse hepatocytes were infected with Ad-HA-PGC1 $\alpha$  and/or Ad-CAR for 48 h, in the absence or presence of TCPOBOP (TC, 500 nM). PGC1 $\alpha$  (A) and HNF4 $\alpha$  (B) chromatin immunoprecipitation (ChIP) were facilitated by using anti-HA and anti-HNF4 $\alpha$  antibodies, respectively. \*\*,  $p < 0.01$ ; N.S., not significant.



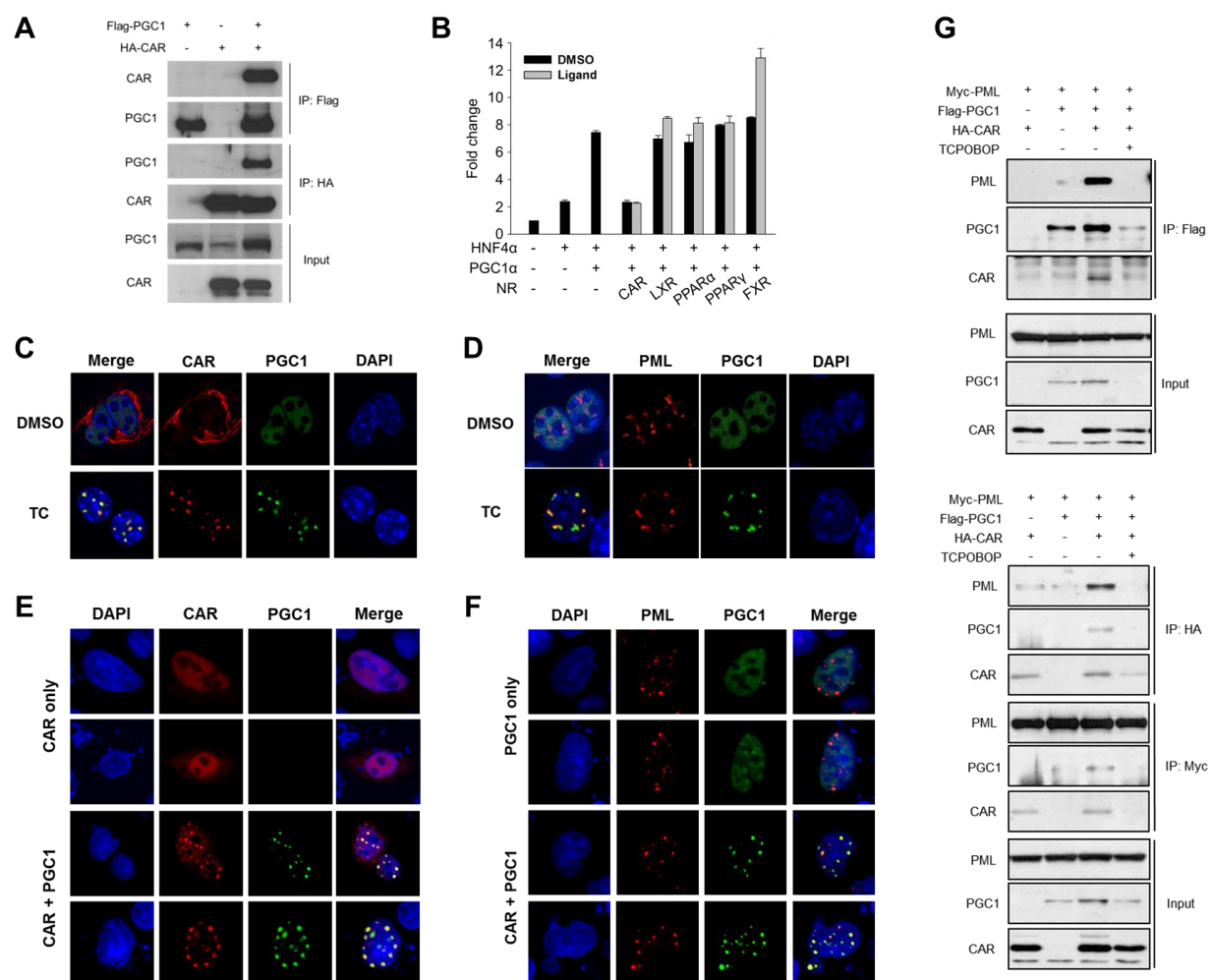


**Figure 9. Activation of CAR leads to the redistribution of PGC1α to PML-NBs**

(A) 293T cells were transfected with Flag-PGC1α and/or HA-CAR before subjecting to IP and Western blot as indicated. (B) 293T cells were co-transfected with G6pase luciferase reporter gene, HNF4α and PGC1α, together with a panel of nuclear receptors known to interact with PGC1α. Transfected cells were treated with cognate receptor agonists for 24 h before luciferase assay. (C and D) Mouse primary hepatocytes were infected with Ad-PGC1α and/or Ad-CAR for 48 h, in the absence or presence of TC (500 nM) before immunofluorescent detection of CAR and PGC1α (C) or PML and PGC1α (D). (E and F) HepG2 cells were co-transfected with PGC1α and CAR individually or in combination followed by immunofluorescent detection of CAR, PGC1α and the endogenous PML. (G) 293T cells were co-transfected with Myc-PML, Flag-PGC1α and HA-CAR before subjecting to IP and Western blot as indicated.

**CAR promotes ubiquitylation-proteasomal degradation of PGC1α, which is required for gluconeogenic suppression.** We noticed that treatment with TCPOBOP dramatically reduced the protein level of both CAR and PGC1α (Error! Reference source not found.G), suggesting a

ligand-dependent degradation of the CAR-PGC1 $\alpha$  complex upon their redistribution to the PML-NBs. Indeed, interaction of the CAR-PGC1 $\alpha$  complex to PML was associated with increased ubiquitylation of both CAR and PGC1 $\alpha$ , and their degradation was triggered by TCPOBOP (Figure 10A). In vivo treatment of HFD-fed mice with TCPOBOP significantly reduced the protein level of PGC1 $\alpha$ , CAR and PML in the liver (Figure 10B). Treatment of cells with the proteasome inhibitor MG132 inhibited the degradation of both PGC1 $\alpha$  and CAR, with PGC1 $\alpha$  enriched in the insoluble pellet fraction (Figure 10C). These results were consistent with the notion that PGC1 $\alpha$  has a tendency to form insoluble protein aggregates when poly-ubiquitinated [211]. The effect of proteasome inhibitor suggested the degradation of CAR and PGC1 $\alpha$  was achieved through the ubiquitylation-proteasome pathway.

Since the formation of CAR-PGC1 $\alpha$  complex was the prerequisite for their interaction with PML and subsequent degradation, we reasoned the binding between CAR and PGC1 $\alpha$  was necessary and sufficient to trigger the cascade. Indeed, mutation of CAR at the two conserved amino acid residues within H12/AF2 (E355A) and H3 (K187A) (coactivator-binding mutant, or CBM) that constitute the hydrophobic cleft for the binding of coregulators [212] disrupted the interaction between CAR and PGC1 $\alpha$  (**Error! Reference source not found.A**), which in turn abolished the CAR-induced ubiquitylation and degradation of PGC1 $\alpha$  (**Error! Reference source not found.B-C**). At the functional level, the suppressive effect of CAR on the PGC1 $\alpha$  responsive activation of the G6pase-luciferase reporter gene was nearly abolished by the CBM mutations (**Error! Reference source not found.D**).

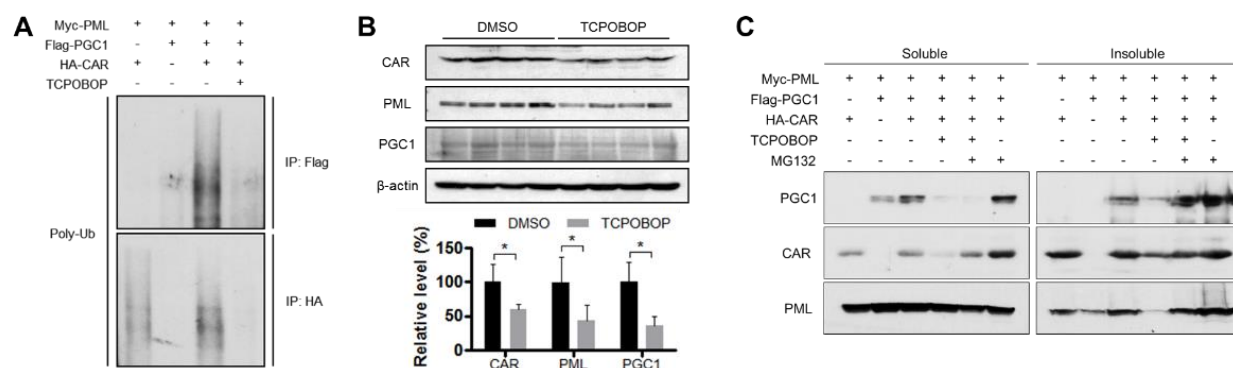


**Figure 10. CAR promotes ubiquitylation-proteasomal degradation of PGC1α**

(A) 293T cells were co-transfected with Myc-PML, Flag-PGC1α and HA-CAR before the detection of polyubiquitylation of PGC1, CAR and PML with a ubiquitin antibody. (B) Mice fed with HFD were treated with TCPOBOP (0.2 mg/kg, once per week) or vehicle for 12 weeks. Total liver lysates were analyzed by Western blot for the detection of endogenous PGC1α, CAR and PML (n=4 per group). The protein expression level was quantified by densitometry. (C) 293T cells were co-transfected with Myc-PML, Flag-PGC1α and HA-CAR and treated with TC (500 nM) or MG132 (10 μM) before subjecting to Western blotting. Proteins in both the soluble and insoluble fractions were analyzed. \*, p<0.05.

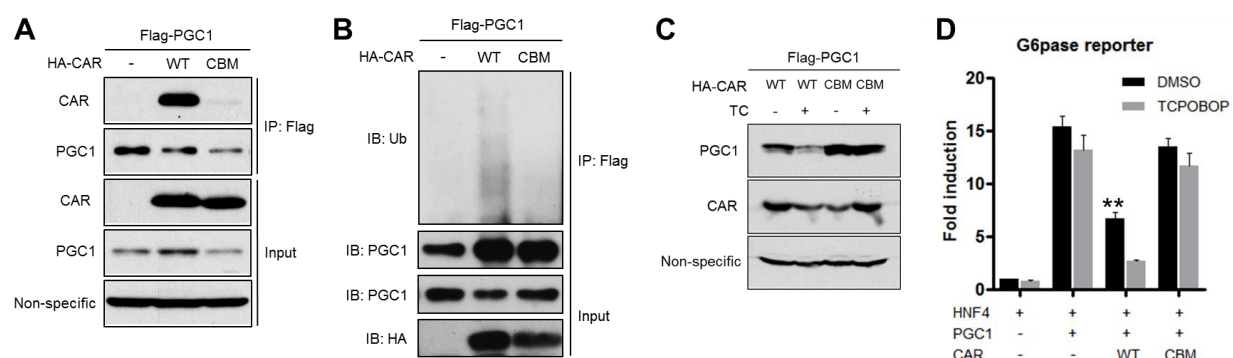


**Figure 11. CAR's interaction with PGC1α is essential for the ubiquitylation and degradation of PGC1α**

(A and B) 293T cells were co-transfected with Flag-PGC1α, HA-tagged WT CAR or CAR CBM mutant, followed by IP and Western blot to evaluate their interaction (A), and their polyubiquitylation was detected by Western blot with a ubiquitin antibody (B). "Non-specific" denotes the non-specific band detected by the PGC1 antibody used as loading control. (C) 293T cells were co-transfected with Flag-PGC1α, HA-tagged WT CAR or CAR CBM mutant, and treated with or without TC (500 nM). The expression of PGC1α and CAR was measured by Western blotting. "Non-specific" denotes the non-specific band detected by the PGC1 antibody used as loading control. (D) The suppressive effects of WT CAR or CAR CBM mutant on PGC1α activity were evaluated by G6pase luciferase reporter assay in 293T cells. \*\*, p<0.01 compared to control (HNH4+PGC1).

**PML-NBs are required for CAR to induce PGC1α degradation and suppress gluconeogenic gene expression.** The association between redistribution of CAR and PGC1α to the PML-NBs

and their degradation prompted us to determine whether PML-NBs were required for CAR-induced PGC1 $\alpha$  degradation and inhibition of gluconeogenesis. In Hepa1-6 cells stably expressing PML shRNA, the formation of PML-NBs was disrupted as expected, and PGC1 $\alpha$  remained evenly distributed in the nucleus when co-transfected with CAR (**Error! Reference source not found.A**, left panel). The inhibitory effect of CAR on PGC1 $\alpha$  responsive activation of the G6pase-lucifarease reporter gene was attenuated in PML knockdown cells (**Error! Reference source not found.A**, right panel). In contrast, overexpression of PML facilitated PML-NB formation and targeting of PGC1 $\alpha$  to PML-NBs (**Error! Reference source not found.B**, left panel). Interestingly, overexpression of PML had a marginal effect in enhancing CAR-induced suppression of PGC1 $\alpha$  activity (**Error! Reference source not found.B**, right panel), likely due to the abundance of the endogenous PML. In primary hepatocytes isolated from the PML<sup>-/-</sup> mice, CAR activation failed to induce the subnuclear redistribution of PGC1 $\alpha$  (**Error! Reference source not found.C**) and inhibition of the FSK-responsive induction of gluconeogenic genes (**Error! Reference source not found.D**). Moreover, treatment of primary mouse hepatocytes with As<sub>2</sub>O<sub>3</sub>, a PML degrading chemical [213], abolished the TCPOBOP responsive degradation of PGC1 $\alpha$  and CAR (**Error! Reference source not found.E**). In vivo treatment of HFD-fed PML<sup>-/-</sup> mice with TCPOBOP failed to reduce the protein level of PGC1 $\alpha$  and CAR (Figure 13A) and suppress the gluconeogenic gene expression (Figure 13B). Furthermore, the beneficial effect of TCPOBOP on glucose metabolism was completely abolished in the PML<sup>-/-</sup> mice, shown by the IPGTT assay (Figure 13C).

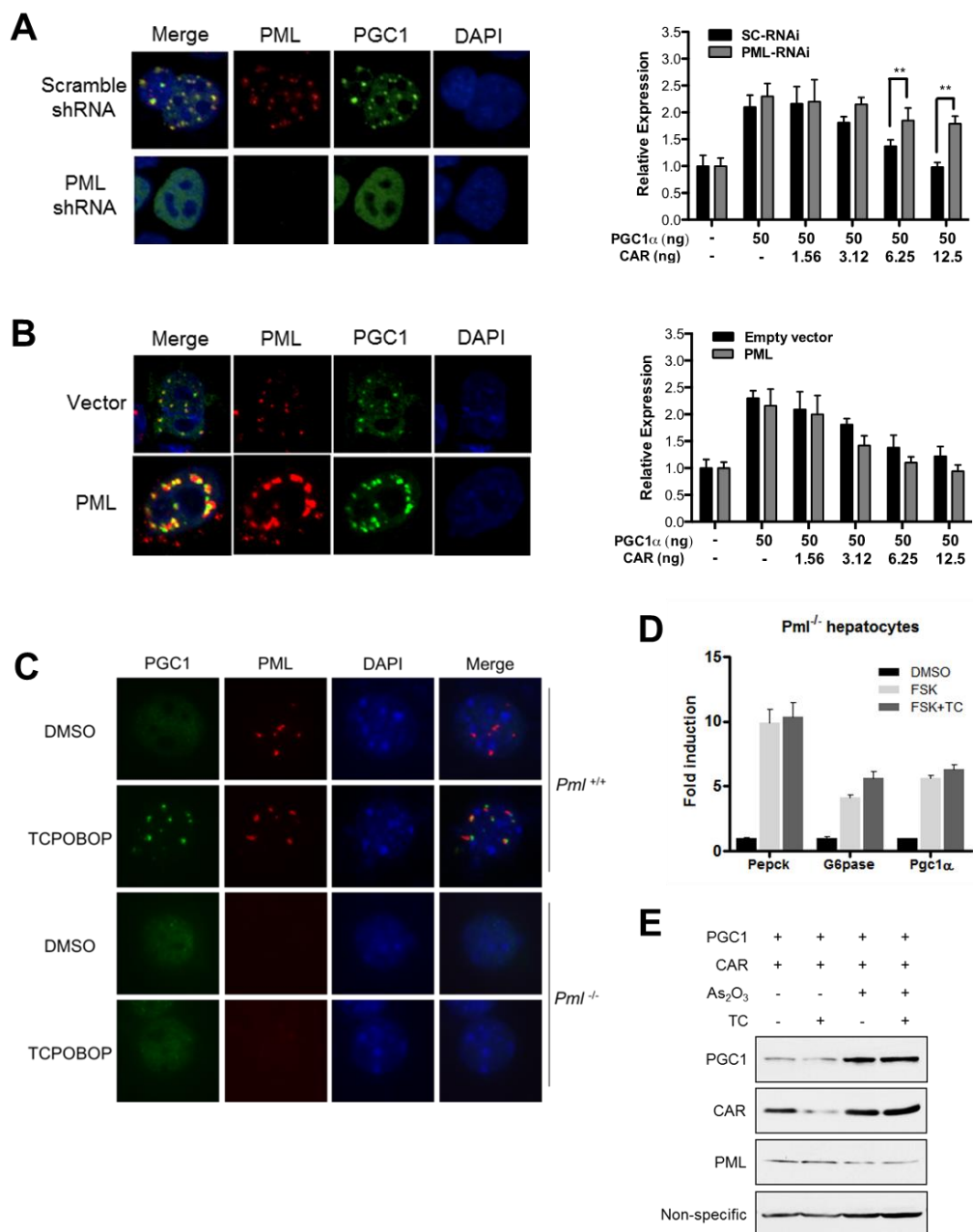


**Figure 12. PML-NBs are required for CAR to induce PGC1α degradation and suppress gluconeogenic gene expression in vitro**

(A) Immunofluorescent detection of PML and PGC1α in stable PML-knockdown Hepa1-6 cells generated by infecting cell with lenti-scramble or lenti-shPML and co-transfected with CAR and PGC1α (left panel). The effect of PML-knockdown on CAR-responsive inhibition of PGC1α activity was measured by the G6pase luciferase reporter gene assay (right panel). (B) Immunofluorescent detection of PML and PGC1α in Hepa1-6 cells co-transfected with CAR, PGC1α and PML or empty vector (left panel). The effect of PML overexpression on CAR-responsive inhibition of PGC1α activity was measured by the G6pase luciferase reporter gene assay (right panel). (C) Primary hepatocytes isolated from WT and *Pml*<sup>-/-</sup> mice were infected with Ad-HA-PGC1α and Ad-Flag-CAR and treated with DMSO or TC (500 nM) for 48 h before immunofluorescent detection of PGC1α and PML. (D) Primary hepatocytes from *Pml*<sup>-/-</sup> mice

were pretreated with TC (500 nM) or DMSO for 12 h before FSK (10  $\mu$ M) treatment for 2 h. Gene expression was measured by real-time PCR. (E) 293T cells were co-transfected with Flag-PGC1 $\alpha$  and HA-CAR and treated with TC (500 nM) and A<sub>2</sub>O<sub>3</sub> (10  $\mu$ M) as indicated. “Non-specific” denotes the non-specific band detected by the PGC1 antibody used as loading control. \*\*,  $p < 0.01$ .

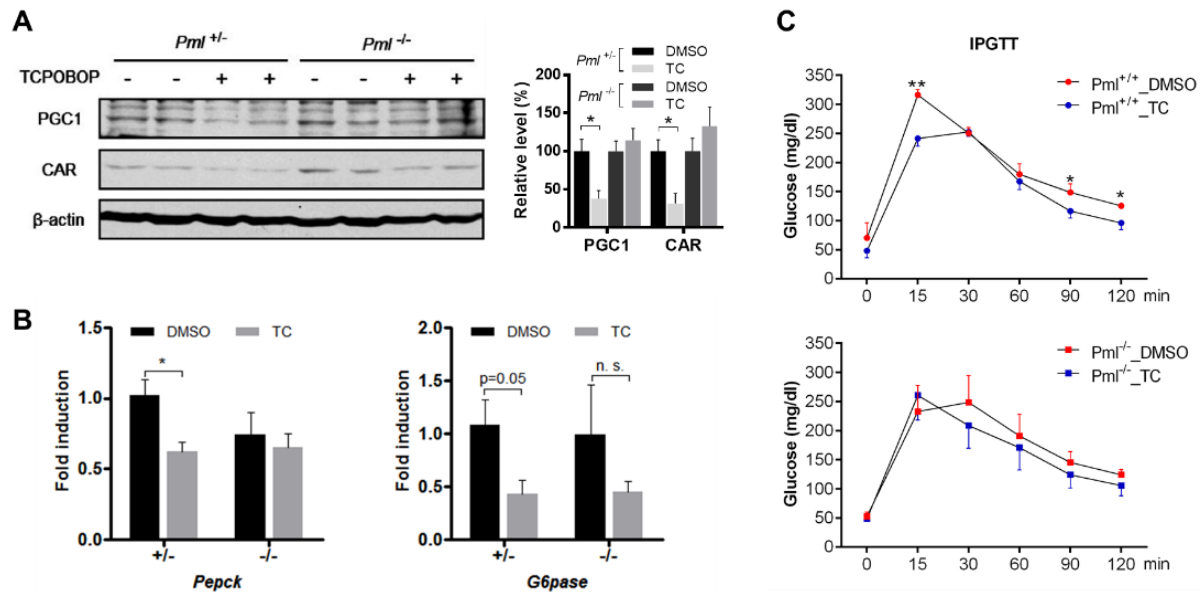


**Figure 13. PML-NBs are required for CAR to induce PGC1 $\alpha$  degradation and suppress gluconeogenic gene expression in vivo**

(A and B) *Pml*<sup>-/-</sup> mice and their heterozygous littermates were fed with HFD for 4 weeks (n=4 per group), followed by treatment with TC (0.25 mg/kg, once per week) or vehicle for additional two weeks. Total liver lysates were subjected to Western blot for the detection of endogenous PGC1 $\alpha$  and CAR (left panel). The quantification of the results is shown (right panel) (A). The same mice were used to measure the expression of *Pepck* and *G6pase* (B). (C) 6-week old WT and PML null mice (n=3-4 for each group) were fed with HFD for two weeks before weekly TCPOBOP injection (0.25 mg/kg body weight) for four weeks along with HFD feeding. IPGTT was performed two days after the final dosing. \*,  $p < 0.05$ ; \*\*,  $p < 0.01$ ; N.S., not significant.

**CAR recruits the CUL1 E3 ligase to promote the ubiquitylation of PGC1 $\alpha$ .** In understanding the mechanism by which CAR promotes PGC1 $\alpha$  ubiquitylation, we hypothesized that CAR may serve as an adaptor protein to present PGC1 $\alpha$  to an E3 ligase for ubiquitylation and subsequent degradation. Among a panel of E3 ubiquitin ligases, CAR showed ligand-independent interaction with CUL1 (Figure 14A), the major structural scaffold protein of the Skp1-CUL1-F-box protein (SCF) complex [214]. The interaction between CAR and CUL1 complex was further supported

by the coIP of CAR with Rbx1 and Skp1, another two core components of the CUL1 complex (Figure 14B). It has been reported that Rbx1 and CUL1 form a catalytic core complex that recruits a cognate E2 ubiquitin conjugating enzyme, and Skp1 serves as an adapter to bring the F-box protein together with a specific substrate and CUL1/Rbx1/E2 in the neighborhood [215]. We showed that CAR interacted with the N-terminal of CUL1 (Cul1NT) (Figure 14D). Interestingly, CAR retained its interaction with the mutant Cul1NT harboring mutations (Y46A/T47A/Y50A) that abolished the binding of CUL1 to Skp1 (Figure 14C-D). Furthermore, CAR interacted with both the wild type Skp1 and its CUL1-binding deficient mutant (Figure 14C and Figure 14E). Taken together, our results suggested that CAR formed a unique complex with CUL1, which was mediated through both CUL1 and Skp1 (Figure 14F).

We also showed that PGC1 $\alpha$  was coimmunoprecipitated with CUL1 in the presence of CAR in a ligand independent manner (Figure 15A), indicating that CAR is an adaptor protein that bridges PGC1 $\alpha$  and the CUL1 E3 complex. We then performed in vitro ubiquitylation to directly demonstrate that the CAR-recruited E3 complex is capable of catalyzing PGC1 $\alpha$  ubiquitylation. The CAR-containing CUL1 E3 ligase and PGC1 $\alpha$  were expressed in cells and purified by IP (Figure 15B). Incubation of purified PGC1 $\alpha$  with CAR-containing E3 ligase resulted in an increased PGC1 $\alpha$  poly-ubiquitylation (Figure 15C). In vivo ubiquitylation assay showed that CAR was able to induce the ubiquitylation of PGC1 $\alpha$ , which was largely abolished by the co-transfection of a dominant-negative CUL1 (DN-Cul1) (Figure 15D). At the functional level, co-transfection of DN-Cul1 (Figure 15E, left panel), or treatment with the CUL1 inhibitor MLN4924 [216] (Figure 15E, right panel) largely abolished the inhibition of PGC1 $\alpha$  activity by CAR in G6pase luciferase reporter gene assays. These results collectively suggested that CAR functions as an adaptor protein to present PGC1 $\alpha$  to the CUL1 E3 complex for ubiquitylation.

Interestingly, CAR-induced PGC1 $\alpha$  ubiquitylation seemed to be PML independent because the PGC1 $\alpha$  ubiquitylation was intact in the presence of As<sub>2</sub>O<sub>3</sub> (Figure 15F), suggesting PML-NBs might not be required for the ubiquitylation of PGC1 $\alpha$ , but were indispensable for its degradation.

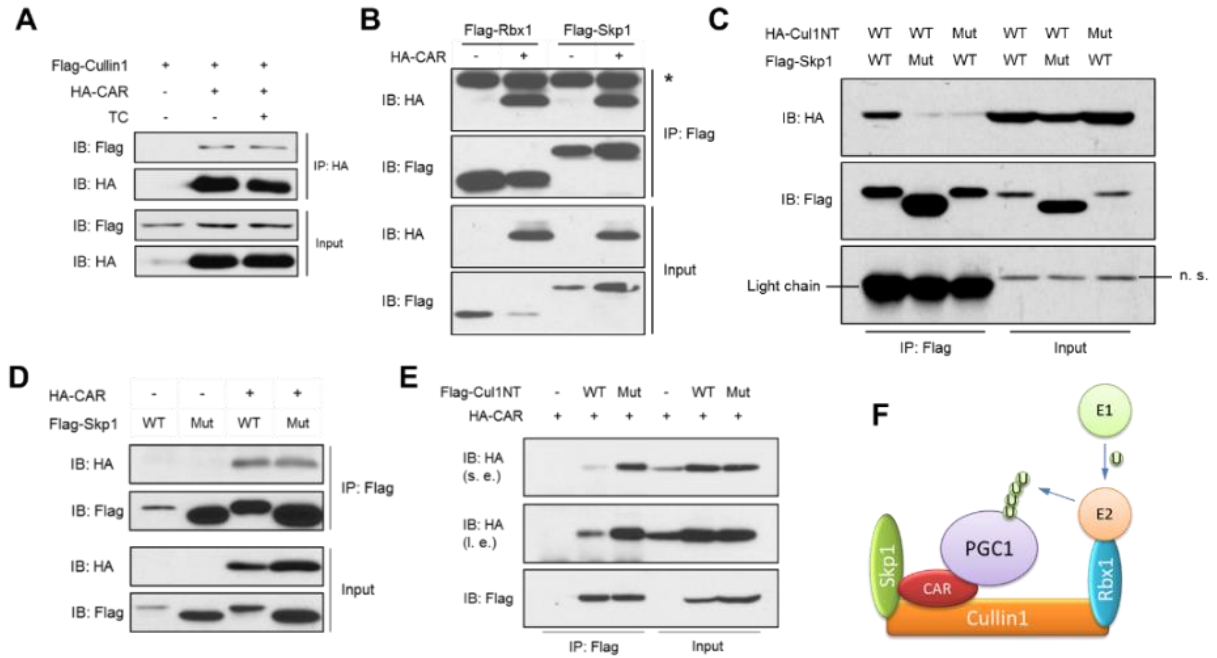


**Figure 14. CAR interacts with the CUL1 E3 ligase components and forms a unique complex**

(A) 293T cells were co-transfected with Flag-Cullin1 and HA-CAR and treated with or without TC (500 nM) as indicated before being subjected to IP and Western blot. (B) 293T cells were co-transfected with HA-CAR and Flag-Skp1 or Flag-Rbx1 as indicated before being subjected to IP and Western blot. The asterisk denotes the heavy chain of IgG. (C) 293T cells were transfected with plasmids as indicated. The protein-protein interaction was determined by IP and Western blot. (D) 293T cells were co-transfected with HA-CAR and Flag-Cul1NT WT or mutant (Y46A/T47A/Y50A) as indicated before being subjected to IP and Western blot. (E) 293T cells were co-transfected with HA-CAR and Flag-Skp1 WT or mutant (N108K, Y109N) as indicated before being subjected to IP and Western blot. (F) Proposed formation of CAR-associated E3 ligase and mechanism of CAR-mediated ubiquitylation of PGC1 $\alpha$ .



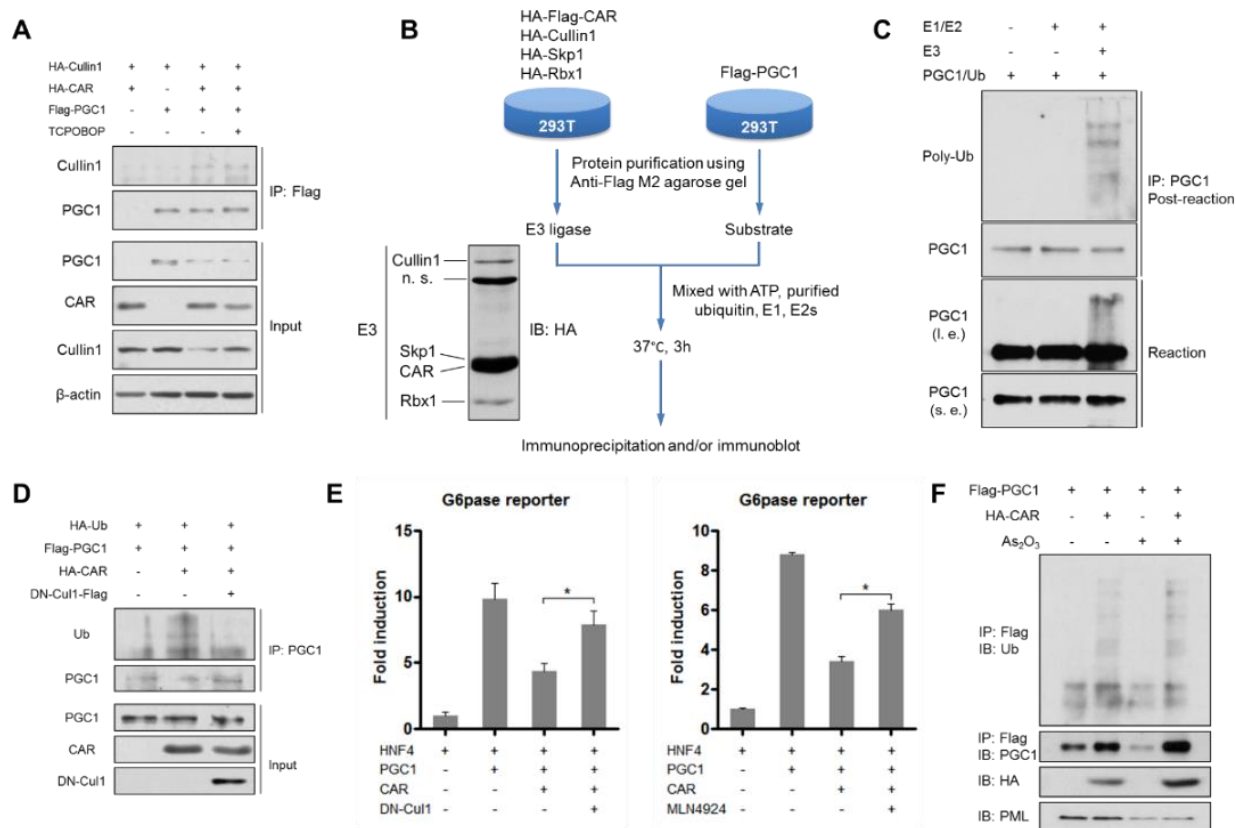


**Figure 15. CAR recruits the CUL1 E3 ligase to promote the ubiquitylation of PGC1 $\alpha$**   
 (A) 293T cells were co-transfected with HA-Cullin1, HA-CAR, and Flag-PGC1 $\alpha$  and treated with or without TC (500 nM) as indicated before being subjected to IP and Western blot. (B) Working flow of the in vitro ubiquitylation assay. CAR-associated E3 ligase was purified from 293T cells co-transfected with HA-Flag-CAR, HA-Cullin1, HA-Skp1 and HA-Rbx1 using anti-Flag M2 agarose gel. The component proteins were verified by Western blotting with the anti-HA antibody. The recombinant Flag-PGC1 $\alpha$  was purified from the 293T cells transfected with Flag-PGC1 $\alpha$  with anti-Flag M2 affinity gel. For the in vitro ubiquitylation reaction, the purified E3 complex and PGC1 $\alpha$  were incubated in the presence of ATP, ubiquitin, and E1/E2 (UbcH5a and UbcH3) followed by IP and/or Western blot as illustrated. (C) In vitro ubiquitylation of PGC1 $\alpha$  by CAR-containing Cullin1/SCF E3 ligase complex. CAR-containing CUL1/SCF E3 complex was purified and mixed with purified PGC1 $\alpha$  in the presence of E1, E2, ubiquitin, and ATP. (D) 293T cells were co-transfected with HA-ubiquitin (Ub), HA-CAR, Flag-PGC1 $\alpha$ , and dominant-negative CUL1 (DN-Cul1), followed by IP and Western blot as indicated. (E) Co-transfection of DN-Cul1 (left panel) or treatment with SCF inhibitor MLN4924 (right panel) abolished the inhibition of PGC1 $\alpha$  activity by CAR in G6pase reporter gene assay. (F) 293T cells were co-transfected with PGC1 $\alpha$  and CAR with or without As<sub>2</sub>O<sub>3</sub> treatment before IP and Western blot detection of PGC1 $\alpha$  and CAR proteins. \*, p<0.05.

**CAR-mediated inhibition of PGC1 $\alpha$  requires active AF2 domain, but is independent of DNA-binding.** The protein structure of CAR comprises N-terminal AF1 ligand-independent domain, DNA-binding domain (DBD), and ligand-binding domain (LBD), as a prototypical

nuclear receptor. Even without agonist binding, CAR exhibits high basal transcriptional activity. The reason behind this constitutive activity is that the last helix on the LBD (namely AF2 domain) is relatively short and stabilized in the active conformation, which makes the protein more accessible by the cofactors and results in constitutive activity without ligand-binding [25].

Our results suggested that the interaction between CAR and PGC1 $\alpha$  was sufficient to induce PGC1 $\alpha$  ubiquitylation, but the subsequent PGC1 $\alpha$  degradation (Figure 10C) and maximum inhibition of PGC1 $\alpha$  activity required the presence of CAR ligand (**Error! Reference source not found.A**). To determine whether the ligand-bound conformation of CAR was necessary to trigger PGC1 $\alpha$  degradation, we generated two CAR mutants with the Helix 12/AF2 deletion (D8) and Helix11-12 deletion (D30), respectively. Both D8 and D30 mutants retained their ability to interact with PGC1 $\alpha$  and PML (**Error! Reference source not found.**), to induce the redistribution of PGC1 $\alpha$  to PML-NBs (**Error! Reference source not found.B**), and to trigger PGC1 $\alpha$  ubiquitylation (**Error! Reference source not found.C**). However, both mutants failed to induce PGC1 $\alpha$  and CAR degradation in the presence of TCPOBOP (**Error! Reference source not found.D**), or to suppress PGC1 $\alpha$  responsive activation of the G6pase luciferase reporter gene (**Error! Reference source not found.E**).

We also generated the L346F mutant of CAR that was reported to stabilize the AF2 helix in the active conformation and mimic the TCPOBOP-bound receptor [25]. Compared to the WT CAR, transfection of the L346F mutant reduced the basal protein level of the co-transfected PGC1 $\alpha$ , and TCPOBOP had less effect in promoting PGC1 $\alpha$  and CAR degradation (**Error! Reference source not found.F**). The proteasome inhibitor lactacystin was able to stabilize the PGC1 $\alpha$  and CAR proteins regardless of the mutation of CAR (**Error! Reference source not found.F**). These results suggested that the L346F mutation destabilized both CAR and PGC1 $\alpha$ .

by enhancing their proteasome-mediated degradation. In the G6pase luciferase reporter gene assay, the L346F mutant was more efficient than WT CAR in inhibiting PGC1 $\alpha$  activity, and this inhibition cannot be further enhanced by TCPOBOP (**Error! Reference source not found.G**).

CAR is a transcriptional factor with intrinsic DNA-binding affinity. Previous reports have proposed the DNA-binding competition of CAR with FoxO1 or HNF4 $\alpha$  mediates the gluconeogenic suppressive effect [187, 188]. We then used the CC/AA DNA-binding deficient mutant of CAR [188] to determine whether the transcriptional targets of CAR are required for its inhibition of PGC1 $\alpha$ . The CC/AA mutant failed to transactivate the tk-PBRE luciferase reporter gene as expected (**Error! Reference source not found.A**). To our surprise, we found the CC/AA mutant retained its ability to induce the redistribution of PGC1 $\alpha$  to PML-NBs (**Error! Reference source not found.B**) and degradation of PGC1 $\alpha$  (**Error! Reference source not found.C**). Unlike the previous report that DNA-binding mutation impairs CAR-mediated inhibition of HNF-4 transactivation on the human CYP7A1 promoter reporter [188], the CC/AA mutant also retained the ability to suppress the PGC1 $\alpha$  responsive activation of the G6pase luciferase reporter gene (**Error! Reference source not found.D**). Collectively, CAR-mediated inhibition of PGC1 $\alpha$ , at least on the gluconeogenic transactivation, is DNA-binding independent.

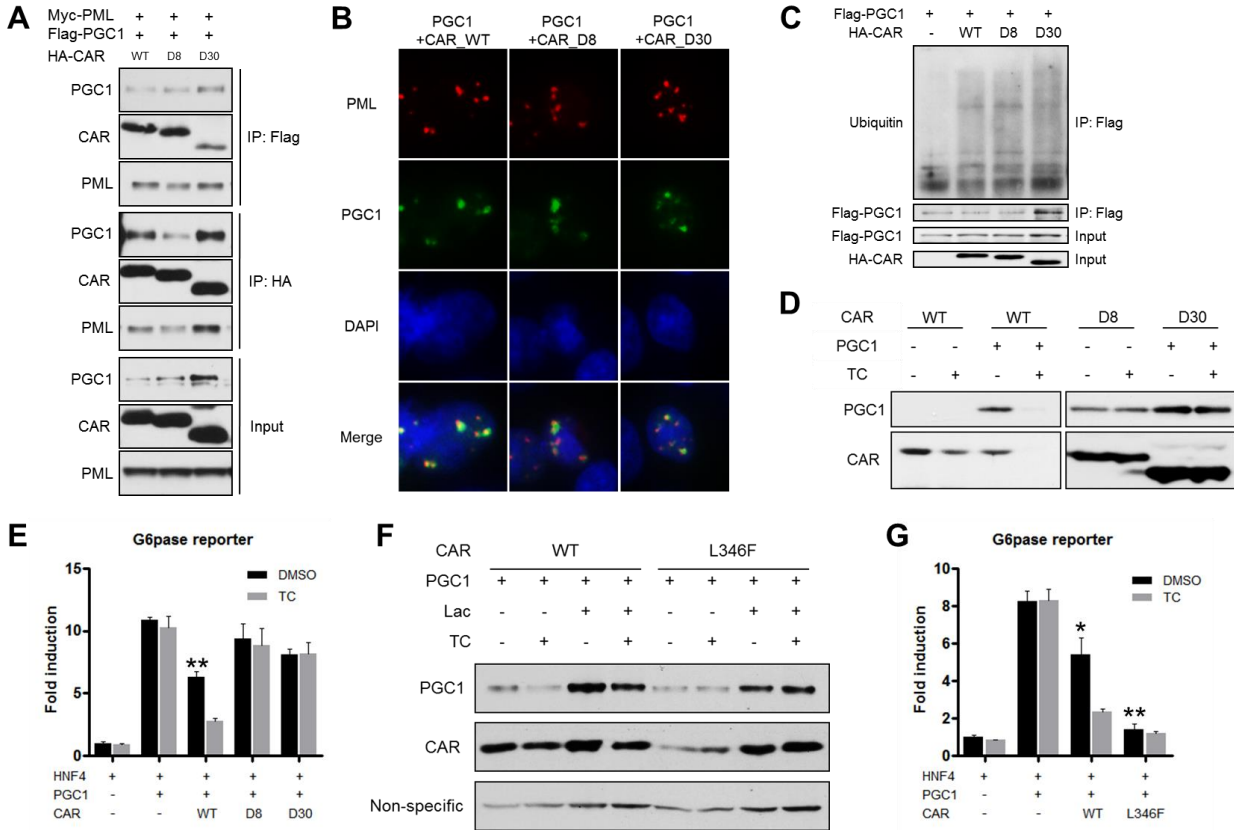


**Figure 16. CAR-mediated inhibition of PGC1 $\alpha$  requires active AF2 domain**

(A) 293T cells were co-transfected with Myc-PML, Flag-PGC1 $\alpha$  and HA-CAR or its mutants before being subjected to IP and Western blot as indicated. (B) 293T cells were co-transfected with PML, PGC1 $\alpha$ , WT CAR or its AF2-domain deletion mutants (D8 and D30), followed by immunofluorescent detection of PGC1 $\alpha$  and PML. (C) 293T cells were co-transfected with Flag-PGC1 $\alpha$  and HA-CAR or its mutants, the polyubiquitylation of PGC1 $\alpha$  was detected by IP followed by Western blot with a ubiquitin antibody. (D) Co-transfection of PGC1 $\alpha$  and WT CAR or D8 and D30 in 293T cells with or without TC (500 nM) treatment for 24 h, followed by Western blot to detect the protein level of PGC1 $\alpha$  and CAR. (E) The suppressive effect of CAR D8 and D30 on PGC1 $\alpha$  activity was measured by G6pase luciferase reporter assay. (F) Co-transfection of PGC1 $\alpha$  and WT CAR or L346F mutant in 293T cells with or without TC treatment (500 nM, 24 h), followed by Western blot to detect the protein level of PGC1 $\alpha$  and CAR. "Non-specific" denotes the non-specific band detected by the PGC1 antibody used as loading control. (G) The suppressive effect of CAR L346F mutant on PGC1 $\alpha$  activity was measured by G6pase luciferase reporter assay. \*,  $p < 0.05$ , \*\*,  $p < 0.01$  compared to control (HNF4+PGC1).

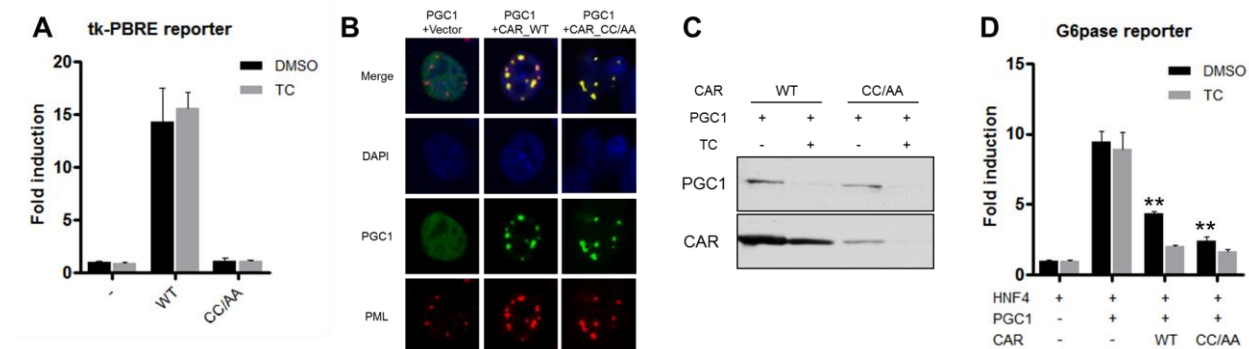


**Figure 17. CAR-mediated inhibition of PGC1 $\alpha$  is independent of DNA-binding**

(A) The transcriptional activity of WT CAR or CC/AA was measured by using the tk-PBRE reporter assay. PBRE, phenobarbital-response element. (B) HepG2 cells were co-transfected with PGC1 $\alpha$ , WT CAR or CC/AA, followed by immunofluorescent detection of PGC1 $\alpha$ , CAR and the endogenous PML. (C) Co-transfection of PGC1 $\alpha$  and WT CAR or CC/AA in 293T cells with or without TC treatment, followed by Western blot to detect PGC1 $\alpha$  and CAR. (D) The suppressive effect of WT CAR or CC/AA on PGC1 $\alpha$  activity was measured by G6pase luciferase reporter assay. \*\*,  $p < 0.01$  compared to control (HNF4+PGC1).

**N-terminal PGC1 $\alpha$  fragment is resistant to the inhibition by CAR.** Having determined the structural requirement of CAR for the inhibitory effect, we next characterized the structural determinant of PGC1 $\alpha$  for the CAR-mediated degradation. We generated PGC1 $\alpha$  mutants with truncation at the C-terminal (amino acids 1-400), mutations in the Leu-X-X-Leu-Leu (LXXLL) nuclear receptor recognition motif (L2/3A), deletion of RNA recognition motif (dRRM), or deletion of serine/arginine-rich domain (dRS) (**Error! Reference source not found.A**). The protein domain of PGC1 $\alpha$  required for its interaction with CAR were located at its C-terminal as shown by coIP (**Error! Reference source not found.B**). The N-terminal PGC1 $\alpha$  fragment failed to interact with CAR and showed resistance to CAR-induced degradation and inhibition of PGC1 $\alpha$  activity (**Error! Reference source not found.C-D**).

Crystal structure reveals that LBD amino acids on the CAR form a pocket which is responsible for high binding affinity for LXXLL motif. LXXLL is a conserved motif across the existing nuclear cofactors [217]. However, the LXXLL-containing N-terminal of PGC1 $\alpha$  does

not interact with CAR, suggesting some potential LXXLL-like motif exists in other domains that may be responsible for the interaction. Indeed, an earlier study has shown the protein region flanking the RS domain also interacts with CAR [208].

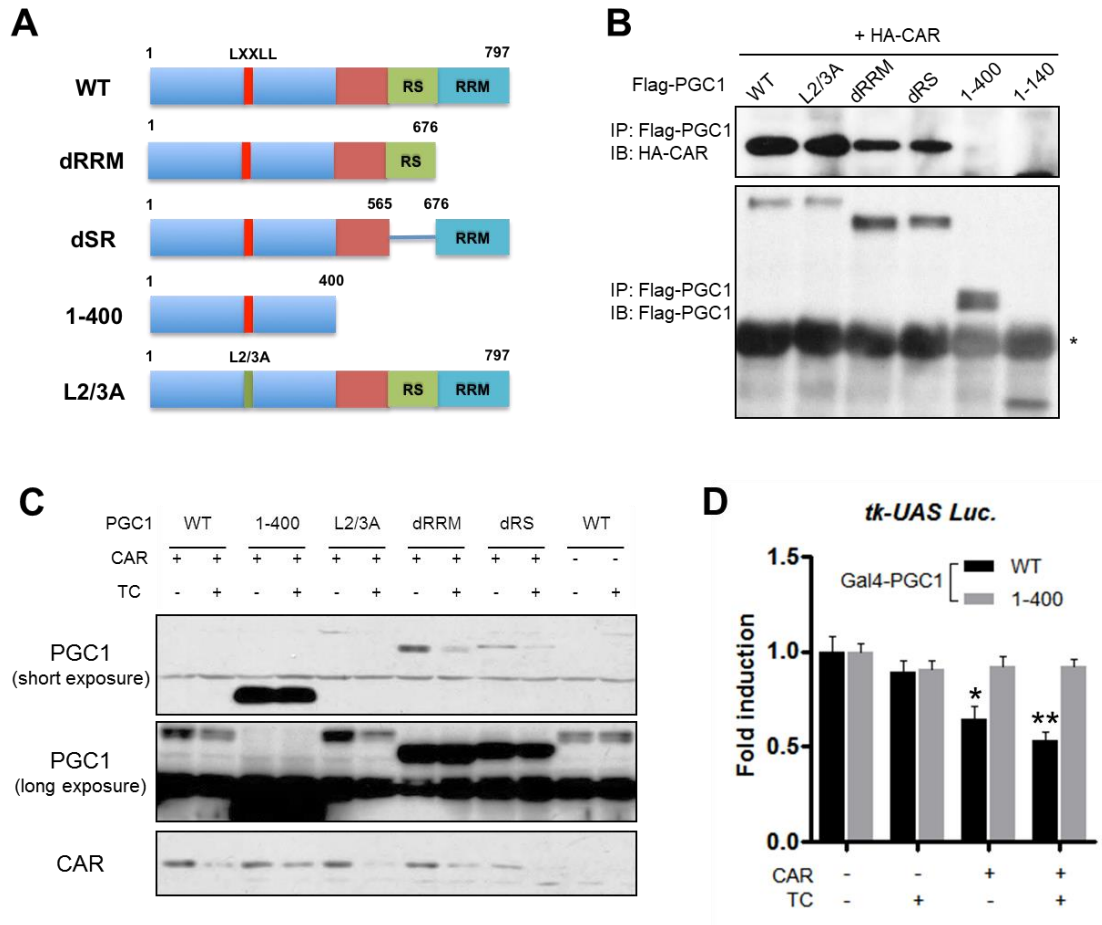


**Figure 18. N-terminal PGC1 $\alpha$  fragment is resistant to the inhibition by CAR**

(A) A diagram of PGC1 $\alpha$  mutants generated in the study. (B) 293T cells were co-transfected with CAR and WT or various PGC1 $\alpha$  mutants, followed by IP and Western blot to evaluate their interaction. (C) 293T cells co-transfected with CAR and WT or various PGC1 $\alpha$  mutants were treated with or without TC (500 nM) for 24 h. Cell lysates were subjected to Western blot analysis. (D) 293T cell were co-transfected with gal-responsive tk-UAS reporter gene and CAR, along with Gal4-PGC1 $\alpha$  WT or Gal4-PGC1 $\alpha$  (aa 1-400). Transfected cells were treated with or without TC (500 nM) for 24 h before luciferase assay. \*,  $p < 0.05$ , \*\*,  $p < 0.01$  compared to control in WT.

### 3.4 DISCUSSION AND CONCLUSION

As depicted in Figure 19, our results revealed a novel molecular mechanism by which CAR inhibits gluconeogenesis by post-translationally antagonizing PGC1 $\alpha$ , a key gluconeogenic transcriptional factor. In this model, following ligand activation, CAR translocates from the cytoplasm into the nucleus to serve as an adaptor protein to present PGC1 $\alpha$  to the CUL1 E3 ligase for ubiquitylation. The interaction between PML and the CAR-PGC1 $\alpha$  complex lead to the redistribution of PGC1 $\alpha$  and CAR to the PML-NBs where the degradation of PGC1 $\alpha$  occurs. As a result, CAR activation reduces the recruitment of PGC1 $\alpha$  to the gluconeogenic gene promoters and suppresses hepatic glucose production.

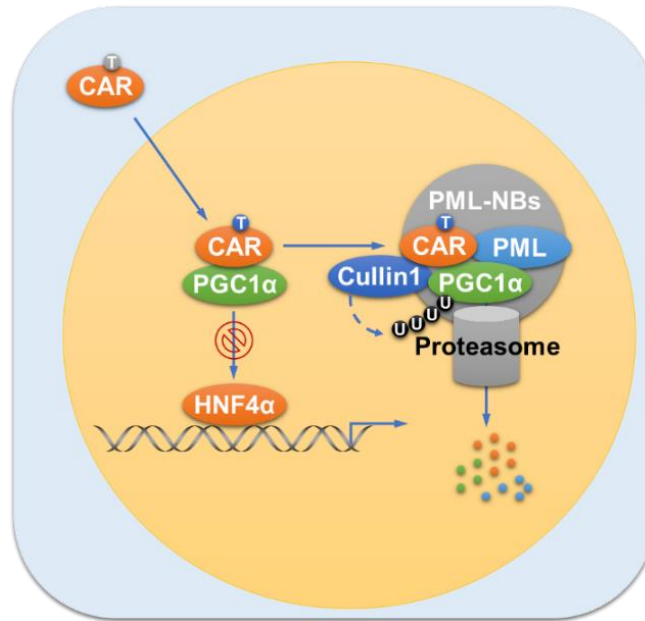


**Figure 19. Mechanism of CAR-mediated suppression of hepatic gluconeogenesis**

Hepatic gluconeogenic gene expression is facilitated by PGC1 $\alpha$ -mediated coactivation of transcription factors such as HNF4 and FoxO1 during fasting or under the diabetic condition. When bound by its ligand TCPOBOP, CAR enters the nucleus and physically interacts with PGC1 $\alpha$ . The CAR-PGC1 $\alpha$  interaction results in the targeting of both proteins to the PML-NBs, where CAR-associated CUL1 E3 ligase modifies PGC1 $\alpha$  with poly-ubiquitin chain and promotes the proteasomal degradation of PGC1 $\alpha$ . The gluconeogenic gene expression is inhibited due to the compromised availability of the PGC1 $\alpha$  protein.

One of our most interesting findings is the recruitment of the CUL1 E3 ligase complex by CAR. CAR is previously known as a master regulator of xenobiotic metabolism through its transcriptional regulation of drug metabolizing enzymes and transporters. To our knowledge, the recruitment of the CUL1 E3 ligase complex and subsequent ubiquitylation of PGC1 $\alpha$  is the first example that CAR controls the protein turnover of a gluconeogenic transcriptional factor, which may have accounted for the anti-diabetic activity of CAR that we and others have reported [132, 133]. The CUL1 E3 ligase/SCF complex and SCF-like complexes belong to the largest family of E3 ligases whose substrates include a broad range of proteins involved in cell cycle progression, signal transduction and gene transcription [218]. Cdc4, an F-box component of the SCF complex has been reported to target PGC1 $\alpha$  for proteasomal degradation in a phosphorylation-dependent manner [219]. In our study, we found no evidence that activation of CAR affected the phosphorylation of PGC1 $\alpha$ . Instead, our data suggested that CAR interacted with the SCF complex in a ligand-independent manner and served as an adaptor protein to bring PGC1 $\alpha$  to the SCF complex for ubiquitylation. Interestingly, the degradation of PGC1 $\alpha$  following ubiquitylation requires the presence of a CAR agonist, although the transcriptional targets of CAR are not required for the degradation because the DNA binding was dispensable. It is possible that the agonist-occupied conformation of CAR-PGC1 $\alpha$  is required to recruit additional proteasome activators and trigger the degradation.

PGC1 $\alpha$  is a transcriptional coactivator expressed in many tissues with high and fluctuating energy demands, such as the liver, skeletal muscle, heart, and brown adipose tissue. PGC1 $\alpha$  has been established as a master regulator of mitochondrial biogenesis and energy expenditure. As a critical metabolic orchestrator, the activity of PGC1 $\alpha$  is tightly regulated at both the transcriptional and post-translational levels. To date, post-translational modifications



(PTMs) on PGC1 $\alpha$ , including phosphorylation [220-226], SUMOylation [227], methylation [228], acetylation [204, 229], and GlcNAcylation [230], have been reported to weave a multifaceted and flexible system to regulate its activity, particularly in the liver tissue (Figure 20). PGC1 $\alpha$  is a short-lived protein with a high turnover rate [211], yet the regulation of PGC1 $\alpha$  protein stability in the liver is poorly understood. The MAPK p38 mediated phosphorylation of PGC1 $\alpha$  has been reported to increase its stability and is stimulatory for the gluconeogenesis [223]. GlcNAcylation, together with host cell factor C1 (HCF-1), recruits the deubiquitinase BRCA1-associated protein 1 (BAP1) to stabilize PGC1 $\alpha$  [230]. The stress-induced enzyme NADH quinone oxidoreductase 1 (NQO1) attenuates the degradation of PGC1 $\alpha$  in the hepatocytes [231]. However, the specific ubiquitin E3 ligase responsible for ubiquitylation of PGC1 $\alpha$  in the liver is still not clear, although several E3 ligases of PGC1 $\alpha$  were reported in other tissues [219, 232, 233].

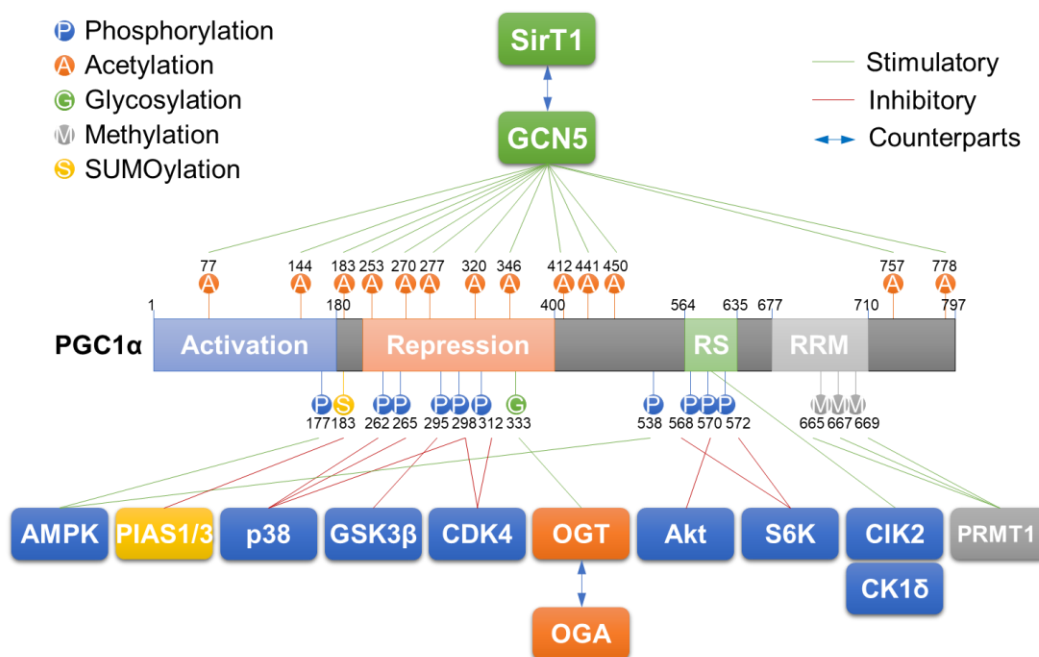


**Figure 20. Post-translational modifications of PGC1 $\alpha$**

Our results suggested that CAR can be defined as an E3 ligase for PGC1 $\alpha$  based on the experimental evidence. In addition, CAR also modulates PGC1 $\alpha$  activity by altering its subcellular localization and turnover rate by the nuclear proteasome machinery. This regulation of PGC1 $\alpha$  degradation by CAR was independent of phosphorylation. As the major gluconeogenic transcriptional factor, PGC1 $\alpha$  has been strongly associated with diabetes. The hepatic PGC1 $\alpha$  activity is robustly upregulated in the diabetic animal models and human patients, which may have contributed to increased hepatic glucose production and hyperglycemia. Since the expression of CAR is highly enriched in the liver, suppressing PGC1 $\alpha$  through CAR activation may provide a novel therapeutic strategy to specifically targeting the hepatic PGC1 $\alpha$  in diabetic conditions, without interfering with the metabolic benefits of PGC1 $\alpha$  in extrahepatic tissues, such as the skeletal muscle and heart.

Another interesting finding is the requirement of PML in the CAR-mediated PML-NBs-targeting and degradation of PGC1 $\alpha$ . PML-NBs are macromolecular nuclear structures implicated in the regulation of diverse cellular functions. The current models envision PML-NBs as a glue to recruit and concentrate partners along with many protein-modifying enzymes, and subsequently enhance post-translational modifications, leading to the activation, sequestration or degradation of proteins [195]. The PML-NBs is very likely the hub for the protein degradation in the nucleus, because they are enriched with 19S and 20S proteasomes and ubiquitin [234, 235]. Consistent with this concept, our study showed PML-NBs were indispensable for CAR-induced degradation of PGC1 $\alpha$ . Furthermore, PML-NBs were required for the suppression of gluconeogenesis by CAR, which is consistent with a recent report that PML ablation in mice induced hepatic gluconeogenic genes, leading to glucose intolerance and insulin resistance [198]. Yet a question remained with regards to how CAR facilitates the proteasomal degradation of

PGC1 $\alpha$  in the PML-NBs. Two pieces of evidence have suggested the direct interaction of CAR and proteasome. First, a component of the 26S proteasome, TBP7 (RPT3 in yeast), is bound with CAR [236]. Second, we found in our study that SUG1 (RPT6 in yeast), another 26S proteasome subunit, interacts with CAR by coIP analysis. Indeed, it has also been reported that proteasome inhibitors or overexpression of SUG1 attenuates TCPOBOP-induced CAR transcriptional activation [73, 237]. Both RPT3 and RPT6 are components of the 19S regulatory subcomplex which is recruited to an activated promoter. Therefore, it will be determined in the future whether the association between the 19S proteasome and CAR is a genomic event that is proteolysis-independent or ligand-activated CAR triggers the assembly of the 26S proteasome.

In summary, our study revealed a novel molecular mechanism through which CAR post-translationally antagonizes PGC1 $\alpha$ . CAR and PGC1 $\alpha$  are master regulators of drug metabolism and gluconeogenesis, respectively. Drug metabolism/detoxification is an essential cellular function that demands energy. Gluconeogenesis is also an energy-demanding process that requires a large amount of ATP to generate sufficient NADPH, a reducing power also needed for the cytochrome P450 enzymes to eliminate noxious chemicals. The negative regulation of PGC1 $\alpha$  by CAR may represent a cellular adaptive mechanism to cope with energy deficiency under energy-restricted conditions. We were aware that overexpression system used in this study has its limitation in terms of the physiological relevance. Although we also included data showing that the proposed mechanism can be applied to the endogenous proteins in addition to the dynamics of the transfected proteins, more work needs to be done in the future to further validate the molecular mechanism in the more physiologically relevant scenario.

## **4.0 AHR AND LIVER FIBROSIS**

### **4.1 RESEARCH BACKGROUND**

Liver fibrosis, defined as the excessive intercellular accumulation of extracellular matrix (ECM) proteins in the liver tissue, is strongly associated with chronic liver injury resulted from alcohol abuse, fatty liver diseases and viral infection [238]. Advanced liver fibrosis causes liver cirrhosis, leading to portal hypertension and liver failure. Liver fibrosis is also a risk factor often predisposing to hepatocellular carcinoma (HCC). The primary hepatic myofibroblasts, derived from activation of hepatic stellate cells (HSCs), are the major cell population responsible for the production of ECM components and pro-fibrogenic cytokines [239]. HSCs reside in the space of Disse between the sinusoidal endothelial cells and hepatic epithelial cells, and are characterized by the expression of desmin and glial fibrillary acidic protein (GFAP) in the quiescent state and  $\alpha$ -smooth muscle actin ( $\alpha$ -SMA) in the activated state [240]. The activation of HSCs is central to the pathogenesis of liver fibrosis. Thus, understanding the molecular basis of HSC activation will help to develop strategies to prevent and treat liver fibrosis. Among many proposed mechanisms, the TGF $\beta$  pathway that integrates a myriad of injury signals is pivotal for the HSC activation [241]. Emerging evidence has also stressed the role of Wnt signaling in potentiating HSC activation and its crosstalk with TGF $\beta$  pathway in the fibrotic diseases [242, 243]. However, how

Wnt signaling, particularly the  $\beta$ -catenin-mediated canonical pathway, promotes the fibrogenic progression is not fully understood.

The aryl hydrocarbon receptor (AhR), highly expressed in the liver, is a well-established xenobiotic receptor that senses environmental toxicants and regulates xenobiotic metabolism [244]. Many industrial pollutants, such as the polycyclic aromatic hydrocarbons (PAHs), have been reported as AhR ligands [12]. A prototypical xenobiotic activator and tool compound for AhR is 2,3,7,8-tetrachlorodibenzo-p-dioxin (TCDD or dioxin). As a ligand-dependent transcriptional factor, AhR signals through diverse protein partners and DNA-binding motifs [12]. For example, upon binding with TCDD, AhR translocates into the nucleus where it heterodimerizes with AhR nuclear translocator (ARNT) on the xenobiotic response elements (XREs) to regulate the transcription of multiple genes. The TCDD-responsive genes, by means of inflammatory response, xenobiotic catabolism, and metabolic reprogramming, collectively contribute to the overall toxicological outcome [245]. ChIP-sequencing analysis has revealed non-XRE binding of AhR in the genome likely through the crosstalk with other transcriptional factors (e.g. FoxA2), suggesting AhR-regulatory genes are not limited to those harboring XREs [246]. Subsequent studies, mainly through the characterization of AhR<sup>-/-</sup> mice, have implicated AhR and its endogenous ligands in physiological development and pathogenesis, including liver fibrosis [42, 43]. There are also cumulative evidence supporting the role of AhR in the homeostasis of energy metabolism, gut microbiota, stem cell differentiation, circadian rhythm, and adaptive immunity [247]. In addition to its function as a ligand-dependent transcriptional factor, AhR also participates in the proteasome-dependent proteolysis system by functioning as a substrate-specific adaptor component that targets selected proteins for degradation in the large E3 ubiquitin ligase complex CUL4B<sup>AhR</sup> [173]. The reported substrate proteins for CUL4B<sup>AhR</sup>

include estrogen receptor- $\alpha$  in the breast cancer cells, androgen receptor in the prostate cancer cells and  $\beta$ -catenin in the intestine [173, 174].

The role of AhR in liver fibrosis has been intriguing yet somewhat controversial. On one hand, AhR<sup>-/-</sup> mice exhibit spontaneous liver fibrosis [42]. On the other hand, treatment of mice with TCDD or constitutive activation of AhR in the hepatocytes sensitize mice to liver fibrosis [151, 248]. The liver is an organ composed of multiple cell types, with hepatocytes, HSCs and Kupffer cells being the most abundant cell populations. It is unclear whether AhR has a cell-type specific role in liver fibrosis. More specifically, it has not been reported whether and how AhR participates in HSC activation. In this study, we have demonstrated an unexpected role of AhR in preventing HSC activation and attenuating liver fibrosis. The ablation of AhR in HSCs sensitizes the mice to experimental liver fibrosis. The underlying mechanism for the anti-fibrotic activity of AhR have been carried out by negatively regulating the interaction of Smad3 and  $\beta$ -catenin thus attenuating TGF $\beta$ -mediated fibrogenesis.

## 4.2 MATERIALS AND METHODS

**Experimental Animals.** The wildtype (WT) C57BL/6J (000664), AhR<sup>fl/fl</sup> (STOCK AhR<sup>tm3.1Bra</sup>/J, 006203) [249], Albumin-Cre (B6.Cg-Tg(Alb-cre)21Mgn/J, 003574) [250], and LysM-Cre (B6.129P2-Lyz2<sup>tm1(cre)Ifo</sup>/J, 004781) mice [251] were purchased from the Jackson Laboratory (Bar Harbor, ME). The AhR<sup>-/-</sup> mice (C57BL/6-AhR<sup>tm1.2Arte</sup>, 9166) were from Taconic (Hudson, NY). Lrat-Cre mice were transferred from Dr. Robert F. Schwabe (Columbia University, New York, NY) [239]. AhR<sup>fl/fl</sup> mice were crossbred with Albumin-Cre, LysM-Cre, and Lrat-Cre mice, respectively, to generate cell type-specific AhR knockout mice. For the toxicological comparison

of TCDD and ITE, 6 weeks old male C57BL/6J mice were treated with vehicle (Veh) DMSO, TCDD (25 µg/kg), or ITE (10 mg/kg) once a week for two weeks by intraperitoneal injection. The animals were terminated 6 h after the third injection. For the carbon tetrachloride (CCl<sub>4</sub>) model of liver fibrosis, 9-10 weeks old male mice were intraperitoneally injected with CCl<sub>4</sub> (1 µl/g body weight, 1:3 diluted in corn oil, twice a week) for 4 weeks. The animals were terminated 72 h after the final CCl<sub>4</sub> injection. For the ITE therapeutic treatment, 200 µg ITE per mouse was administered every other day along with CCl<sub>4</sub> (0.5 µl/g body weight) in corn oil by intraperitoneal injection for 4 weeks. The animals were terminated 6 h after the final dosing of ITE. For the bile duct ligation (BDL) model of liver fibrosis, both male and female aged 8-9 weeks were anesthetized with ketamine (100 mg/kg) and xylazine (15 mg/kg) and surgically ligated at the common bile duct. The animals were terminated 14 days after surgery. All mice were housed in a pathogen-free animal facility under a standard 12h light-dark cycle with free access to food and water. The use of mice was performed in accordance with the University of Pittsburgh Institutional Animal Care and Use Committee.

**Histology.** Liver tissues were fixed overnight in 10% formalin phosphate followed by dehydration in alcohol and xylene. Dehydrated tissues were embedded in paraffin blocks. 5 µm paraffin sections were prepared using microtome, de-waxed and rehydrated before histological staining. For Hematoxylin & Eosin (H&E) Staining, hydrated tissue sections were stained in hematoxylin solution for 2 minutes, washed with tap water for 10 minutes, differentiated in 1% acetic acid solution for 1 minute, followed by 10 quick dips in eosin solution. For Sirius Red Staining, hydrated tissue sections were stained in 0.1% PicroSirius Red solution for 1h followed by two washes in 1% acetic acid solution. For Masson's Trichrome Staining, hydrated tissue

sections were re-fixed in Bouin's solution for 1h at 56°C, washed with running tap water for 10 minutes, stained in Weigert's iron hematoxylin solution for 10 minutes, washed with running tap water for 10 minutes, stained in Biebrich scarlet-acid fuchsin solution (Sigma-Aldrich, St. Louis, MO) for 15 minutes, washed briefly with distilled water, differentiated in phosphomolybdic-phosphotungstic acid solution (Sigma-Aldrich, St. Louis, MO) for 15 minutes, stained in aniline blue solution (Sigma-Aldrich, St. Louis, MO) for 10 minutes, and differentiated in 1% acetic acid solution for 5 minutes. Following the major staining procedures, all the sections were dehydrated in alcohol and xylene and mounted in Permount™ mounting medium (Thermo Fisher Scientific, Pittsburgh, PA) for microscopic analysis. Immunohistochemistry was performed using the VECTASTAIN ABC HRP Kit (Vector Laboratories, Burlingame, CA). Paraffin-embedded liver sections were de-waxed and rehydrated before staining. Antigen-retrieval was performed by incubating the sections in 10 mM citric acid solution (pH 6.0) at 95°C for 15 minutes. Potential endogenous peroxidase activity was reduced using 0.3% H<sub>2</sub>O<sub>2</sub> solution for 30 minutes. The specimens were then blocked in the serum from the species where the secondary antibody was produced for 1 hour before incubation with the primary antibodies (anti- $\alpha$ -SMA and anti-desmin) overnight at 4°C. The next day, the tissue samples were incubated with secondary antibody for 30 minutes followed by ABC reagents for 30 minutes. Positive staining was visualized using DAB Peroxidase (HRP) Substrate Kit (Vector Laboratories, Burlingame, CA). Nuclei were stained with hematoxylin QS (Vector Laboratories, Burlingame, CA). Following the major staining procedures, all the sections were dehydrated in alcohol and xylene and mounted in Permount™ mounting medium (Thermo Fisher Scientific, Pittsburgh, PA) for microscopic analysis. Quantification of Sirius Red and  $\alpha$ -SMA staining was performed by threshold analysis of randomly selected fields of view per slide (magnification 10X) and presented as percentage of



the positive staining versus the total area using Image J software (National Institutes of Health, Bethesda, MD).

**Measurement of ALT and AST.** The liver functional marker ALT and AST activity was measured using the kit from Stanbio Laboratory (Boerne, TX). The measurement was empirically modified according to the user manual supplied with the kit [252].

**Primary HSCs Isolation.** Primary mouse HSCs were isolated according to the previously reported protocol with minor modifications [253]. Briefly, in situ two-step perfusion was performed as previously described followed by a single-step Nycodenz gradient separation (Nycoprep™, Axis-Shield, Oslo, Norway) [254]. The purity of the isolated HSCs was >90% as determined by the vitamin A auto-fluorescence from the stellate cells. The primary human HSCs were isolated from the nonparenchymal fraction of in vitro digested human livers (Department of Surgery, University of Pittsburgh Medical Center, Pittsburgh, PA) following the same protocol as for primary mouse HSCs isolation. The primary HSCs were cultured in Dulbecco's modified Eagle's medium (DMEM) containing 10% FBS and Ampicillin/Streptomycin. For the adipogenic reversion of activated HSCs, cells were treated with MDI medium containing 3-Isobutyl-1-Methylxanthine (0.5 mM), Dexamethasone (1 μM), Insulin (10 μg/ml), and Rosiglitazone (10 μM) for 72h. The immortalized human stellate cell line LX2 was obtained from Dr. Scott Friedman (Mount Sinai School of Medicine, New York, NY). The LX2, 293A, and 293T cells were maintained in DMEM containing 10% FBS and Penicillin/Streptomycin.

**Adenovirus, Lentivirus, Plasmids and Cell Transfection.** Adenovirus-overexpressing mouse AhR and control GFP virus were a gift from Dr. Jodi A. Flaws (University of Illinois Urbana-Champaign, Urbana, IL) [255]. Adenovirus-overexpressing  $\beta$ -catenin (S33Y) and control GFP virus were a gift from Dr. Tong-Chuan He (The University of Chicago Medical Center, Chicago, IL) [256]. All the adenoviruses were amplified in 293A cells and purified using CsCl gradient ultracentrifugation based on the previously reported procedures with some minor modifications [257]. Lentiviral vector pCDH-puro (System Biosciences, Palo Alto, CA) carrying human full-length AhR (WT) and AhR with acidic domain deletion ( $\Delta$ Acidic, amino acids 500-600 deleted) were cloned using standard molecular cloning techniques. The lentiviral packaging vectors psPAX2 (#12260) and pMD2.G (#12259) were obtained from Addgene (Cambridge, MA). Lentiviruses production were performed in 293T cells by transfection with the lentiviral vectors (pCDH-AhR\_WT or pCDH-AhR\_ $\Delta$ Acidic) together with the packaging vectors psPAX2 and pMD2.G. Lentiviruses were collected from the culture supernatants 48h post-transfection and filtered through 0.45- $\mu$ m nitrocellulose membrane. To establish the stable cell lines, LX2 cells were infected with lentiviruses plus polybrene (8  $\mu$ g/ml) and selected with puromycin (0.5  $\mu$ g/ml). The HA-Smad2, HA-Smad3, and HA-Smad4 were cloned using standard molecular cloning techniques. Cell transfection was performed using TransIT®-LT1 or TransIT®-X2 (Mirus Bio, Madison, WI).

**Immunofluorescence.** Primary HSCs were grown on slide chambers and treated as desired. Cells were fixed in ice-cold methanol for 10 minutes followed by blocking with PBS/0.25% Triton X-100 (PBS-T) containing 5% donkey serum for 30 minutes. Slides were incubated in the PBS-T with primary antibody against  $\alpha$ -SMA or Ki67 overnight at 4°C followed by incubation

with fluorochrome-conjugated secondary antibody for 1 h at room temperature in the dark. Slides were mounted in DAPI-containing medium for microscopic analysis.

**Immunoprecipitation (IP) and Western Blot.** For IP, cells were lysed in non-denaturing immunoprecipitation buffer (150 mM NaCl, 50 mM Tris-HCl at pH 7.5, 1% NP-40) supplemented with a protease-inhibitor cocktail (Sigma-Aldrich, St. Louis, MO). The supernatants after sonication and centrifugation (14000g, 15 minutes, 4°C) were incubated with primary antibody against HA or Smad3 overnight at 4°C, followed by incubation with Protein A magnetic beads (New England Biolabs, Ipswich, MA) for 1 h at 4°C. The beads were washed six times with ice-cold immunoprecipitation buffer and eluted with protein loading buffer. The eluents were analyzed by Western blot. For Western blot analysis, liver tissues were homogenized in ice-cold RIPA buffer containing a protease inhibitor cocktail. Protein concentration was measured using Pierce™ BCA Protein Assay Kit (Thermo Fisher Scientific, Pittsburgh, PA). Cell lysates were prepared by adding protein loading buffer directly to the cells. Protein samples were heated for 10 minutes and loaded on the SDS-polyacrylamide gel for electrophoresis. The proteins were transferred on the nitrocellulose membrane and blocked with 5% non-fat milk in 1X Tris-buffered saline solution with Tween-20 (TBS-T). Primary antibodies were incubated overnight at 4°C followed by incubation of horseradish peroxidase (HRP)-conjugated secondary antibody on the next day before film development using HRP-based Pierce™ ECL Western Blot Substrate or SuperSignal™ West Pico PLUS Chemiluminescent Substrate (Thermo Fisher Scientific, Pittsburgh, PA). The densitometric analysis of Western blot was performed using Image Lab software (Bio-Rad Laboratories, Hercules, CA).

**Chromatin Immunoprecipitation (ChIP).** ChIP analysis was performed according to the previously reported protocol with minor modifications [258]. Briefly, LX2 cells were fixed in the formalin for 15 minutes followed by quenching with glycine for 5 minutes at room temperature. Cells were scraped/collected and washed with ice-cold PBS twice. Cell pellets were resuspended in the ChIP buffer (150 mM NaCl, 50 mM Tris-HCl at pH 7.5, 5 mM EDTA, 0.5% NP-40, 1% Triton X-100) supplemented with protease inhibitor cocktail followed by sonication. The sheared chromatin was cleared by centrifugation (12000g, 4°C, 10 minutes). Supernatants were incubated with normal rabbit IgG or primary antibody against p-Smad3 overnight at 4°C, followed by incubation with Protein A magnetic beads for another one hour at 4°C. The immunoprecipitates were washed in the ChIP buffer six times and eluted in 10% Chelex-100 by heating for 10 minutes. The resultant DNA was analyzed with quantitative real-time PCR using the following specific primers as previously reported [259, 260]:

COL1A1\_F: 5'-CATTCCCAGCTCCCCTCTCT-3',

COL1A1\_R: 5'-AGTCTACGTGGCAGGCAAGG-3';

COL1A2\_F: 5'-CCTGAGCCAGTAACCACTCC-3',

COL1A2\_R: 5'-CTTTCGAAGCTAACGTGGCAG-3';

PAI1\_F: 5'-GCAGGACATCCGGGAGAGA-3',

PAI1\_R: 5'-CCAATAGCCTTGGCCTGAGA-3'.

**Quantitative Real-Time PCR.** Total RNA was extracted from cells or tissues using TriPure isolation reagent from Sigma-Aldrich (St. Louis, MO). Reverse transcription was performed with high-capacity cDNA reverse transcription kit from Applied Biosystems (Thermo Fisher Scientific, Pittsburgh, PA). SYBR Green-based real-time PCR was performed with the

QuantStudio™ 6 Flex Real-Time PCR System from Applied Biosystems (Thermo Fisher Scientific, Pittsburgh, PA). Standard curve method was employed for data analysis with Cyclophilin as the housekeeping gene.

**Statistics.** Statistical analysis was performed using Prism GraphPad 7.0 (La Jolla, CA). All results were presented as means  $\pm$  SEM of at least three replicates. Statistical differences between groups were determined using unpaired two-tailed Student t test or one-way ANOVA with post-hoc Tukey test. P values less than 0.05 was considered statistically significant.

### 4.3 EXPERIMENTAL RESULTS

**Treatment of mice with the non-toxic AhR ligand ITE ameliorates CCl<sub>4</sub>-induced liver fibrosis.** The classical AhR ligand TCDD induces liver fibrosis in mice [248]. We speculated that the liver fibrosis is secondary to the TCDD-induced hepatotoxicity, so we decided to test 2-(1'H-indole-3'-carbonyl)-thiazole-4-carboxylic acid methyl ester (ITE), a tryptophan metabolite and endogenous AhR agonist that is believed to be non-toxic [261]. ITE showed comparable effect on the selected AhR target gene expression as TCDD (Figure 21A). When the hepatotoxicity was evaluated, we found that treatment of mice with TCDD for 2 weeks caused typical hepatotoxicity as indicated by neutrophil infiltration (Figure 21B), consistent with a previous report [249]. In contrast, the liver from the ITE-treated mice showed no signs of hepatotoxicity (Figure 21B). ITE did not induce the expression of fibrogenic genes as TCDD did (Figure 21C). To further prove that constitutive activation of AhR in the hepatocytes is sufficient to induce liver fibrosis, we used the constitutive activated AhR (CA-AhR) transgenic mice that

express CA-AhR only in the hepatocytes. We found similar liver fibrosis in those CA-AhR mice as in the TCDD-treated mice (Figure 21D). Consistently, the CA-AhR showed elevated fibrogenic gene expression in the liver (Figure 21E).

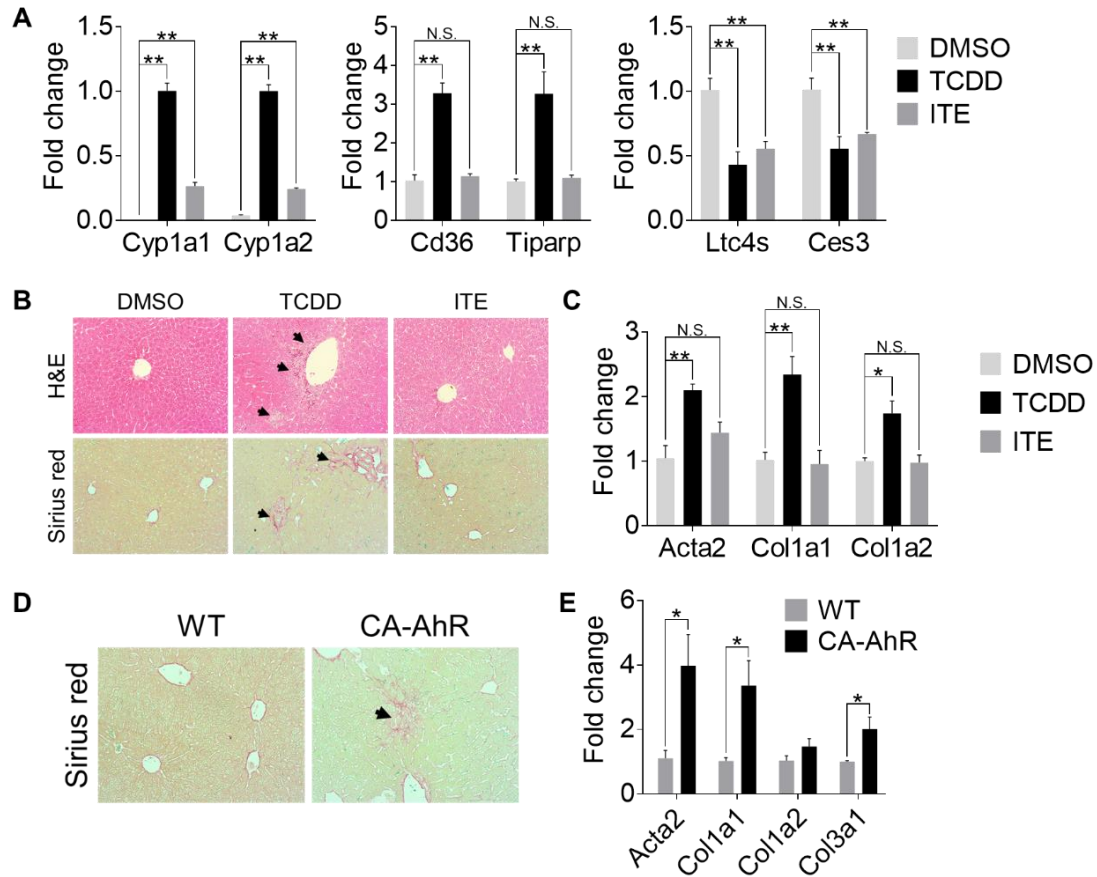


**Figure 21. Constitutive activation of AhR in the hepatocytes is sufficient to induce liver fibrosis** (A-C) 6 weeks old male C57BL/6J mice were treated with vehicle DMSO, TCDD (25  $\mu$ g/kg), or ITE (10 mg/kg) once a week for two weeks (n=4 per group). (A and B) Gene expression was determined by real-time PCR analysis. (C) Hematoxylin & Eosin (H&E) and Sirius red staining of liver tissue. Arrows indicate neutrophil infiltration in the H&E and collagen deposition in the Sirius red, respectively (magnification, 20X). (D and E) 6 weeks old WT and CA-AhR transgenic mice on normal chow. (D) Sirius red staining (magnification, 20X). (E) Gene expression in the liver was determined by real-time PCR analysis (n=5 per group). All the data were presented as mean  $\pm$  SEM (\*:  $p < 0.05$ , \*\*:  $p < 0.01$ ).

We then tested the effect of ITE on CCl<sub>4</sub>-induced liver fibrosis as outlined in Figure 22A. Comparable liver to body weight ratio suggested a similar CCl<sub>4</sub> toxicity between the two groups (Figure 22B). A dramatic induction of hepatic Cyp1a1 and Cyp1a2 by ITE suggested that ITE activated AhR efficiently in vivo (Figure 22C). Treatment of ITE ameliorated CCl<sub>4</sub>-induced liver fibrosis, which was supported by a significantly decreased collagen deposition and fibrogenesis as revealed by Masson's Trichrome and Sirius Red staining and immunohistochemical staining of  $\alpha$ -SMA (Figure 22D-E). The suppression of  $\alpha$ -SMA in ITE- and CCl<sub>4</sub>-treated mice was further verified by Western blotting (Figure 22F) and real-time PCR analysis (Figure 22G). Consistent with the relief of liver fibrosis, the levels of ALT and AST were decreased in ITE-treated mice compared to their vehicle-treated counterparts (Figure 22H).

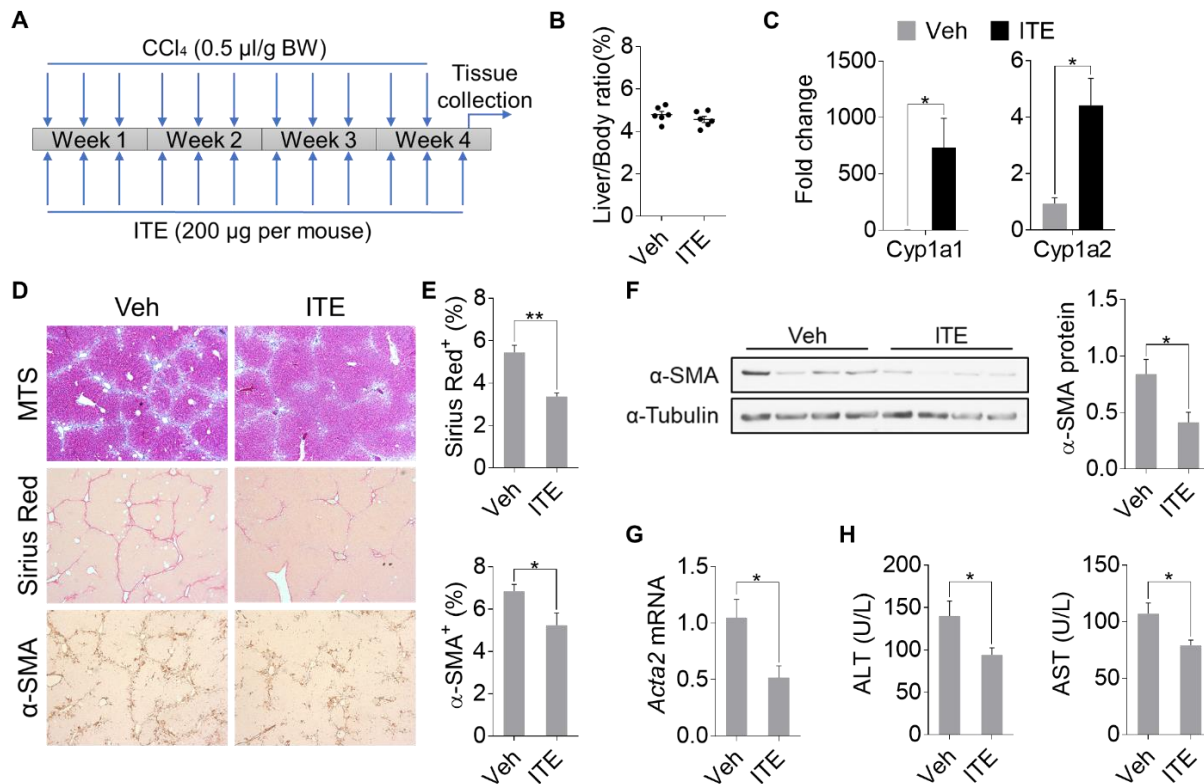


**Figure 22. Non-toxic AhR ligand, ITE, ameliorates CCl<sub>4</sub>-induced liver fibrosis**

8 weeks old male C57BL/6J mice were treated with DMSO (Veh) or ITE (200  $\mu$ g per mouse) together with CCl<sub>4</sub> (0.5  $\mu$ l/g body weight) three times a week for four weeks (n=6 per group). (A) Schematic diagram for mice treatment. (B) Liver to body ratio. (C) Cyp1a1 and Cyp1a2 expression was determined

by real-time PCR. (D) Histological analysis of liver by Masson's Trichrome and Sirius Red staining, and immunohistochemistry staining of  $\alpha$ -SMA (magnification, 5X). (E) Quantification of Sirius Red and  $\alpha$ -SMA positive areas. (F)  $\alpha$ -SMA protein level by Western blot and densitometric quantification. (G)  $\alpha$ -SMA gene Acta2 expression was determined by real-time PCR. (H) Serum ALT and AST activity. All the data were presented as mean  $\pm$  SEM (\*:  $p < 0.05$ , \*\*:  $p < 0.01$ ).

**AhR is highly expressed in HSCs and the expression of AhR inversely correlates with HSC activation.** The expression and role of AhR in HSCs are largely unknown. To investigate whether AhR in the HSCs mediates the anti-fibrotic effect of the endogenous ligand, we compared the expression of AhR in primary hepatocytes and HSCs isolated from the same mice. There was an approximately 4-fold increase in the mRNA expression of both AhR and its DNA-binding partner ARNT in HSCs compared to the hepatocytes (Figure 23A). The basal expression of Cyp1a1 and Cyp1b1, two typical AhR target genes, were also markedly higher in HSCs (Figure 23A). The higher expression of AhR protein in HSCs was verified by Western blot (Figure 23B). Our results were consistent with the recently reported quantitative proteomic study, in which HSCs were shown to express a higher level of AhR than the hepatocytes [262]. Treatment of primary HSCs isolated from WT mice with TCDD induced the expression of Cyp1a1, but this induction was abolished in HSCs isolated from the AhR<sup>-/-</sup> mice (Figure 23C). These results suggested that AhR is not only expressed, but also fully functional in HSCs. Moreover, we found the expression of AhR was inversely correlated with the activation of HSCs. In this experiment, primary mouse and human HSCs were subjected to spontaneous activation in culture. The expression of AhR in primary mouse (Figure 23D) and human (Figure 23E) HSCs decreased with the onset of HSC activation in a time-dependent manner.



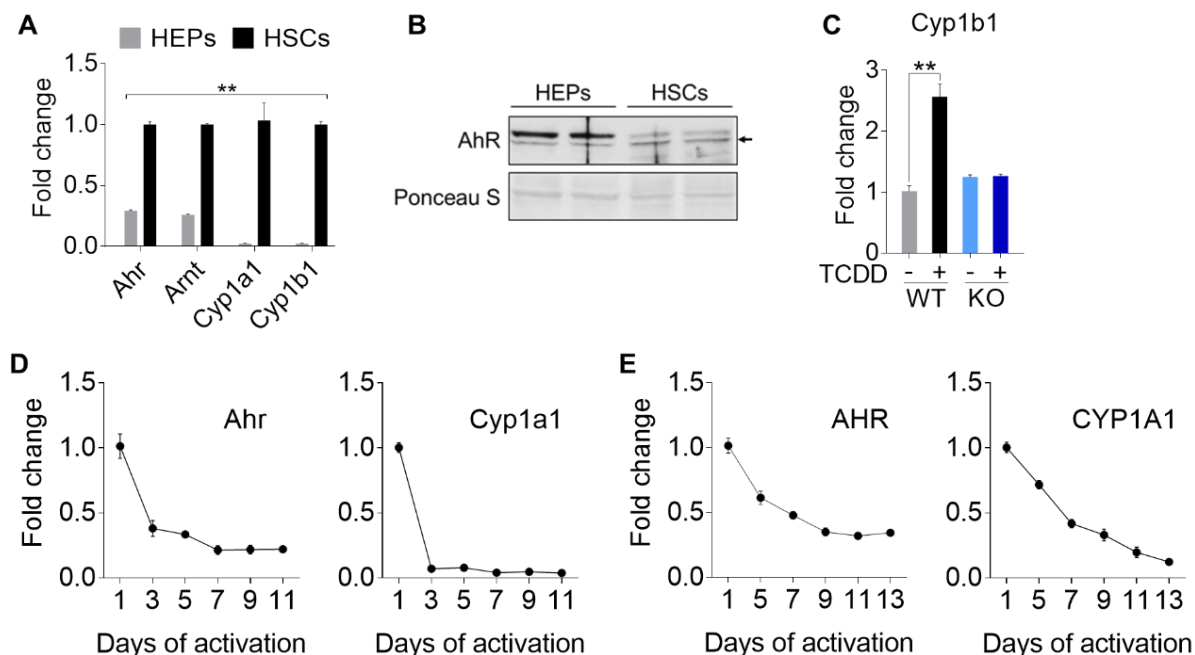


**Figure 23. AhR is highly expressed in HSCs and the expression of AhR declines with HSC activation**

(A and B) Primary mouse hepatocytes (HEPs) and HSCs were isolated from the same liver. (A) Gene expression was determined by real-time PCR (n=4). (B) AhR protein expression was detected by Western blot. Arrow designates the AhR band (95 KD). (C) Primary mouse HSCs were isolated from WT or AhR<sup>-/-</sup> mice (KO) and treated with TCDD (20 nM). Gene expression of Cyp1b1 was determined by real-time PCR (n=4). (D) Primary mouse HSCs were culture-activated for the indicated duration. Gene expression were determined by real-time PCR (n=4). (E) Primary human HSCs were culture-activated for the indicated duration. Gene expression were determined by real-time PCR (n=4). All the data were presented as mean  $\pm$  SEM (\*\*: p<0.01).

Although TGF $\beta$  can efficiently decrease the expression of AhR and its downstream target gene Cyp1b1 in the HSCs (Figure 24A), treatment of TGF $\beta$  receptor inhibitor, SB436542, was not able to reverse the reduction of AhR (Figure 24B). This may exclude the possibility that AhR is down-regulated through the autocrine TGF $\beta$  pathway. Instead, down-regulation of AhR along with HSCs activation may be dependent on HDAC-mediated pathway, because the treatment of the pan-HDAC inhibitors, TSA and SAHA, significantly rescued the expression of AhR in the activated HSCs (Figure 24C). Adipogenic differentiation phenocopies HSC deactivation to quiescence. To further prove that AhR expression is inversely correlated with activation status of

HSCs, we induced adipogenic differentiation of the fully activated HSCs with adipogenic medium. As expected, adipogenic medium-cultured HSCs had higher expression of AhR (Figure 24D).

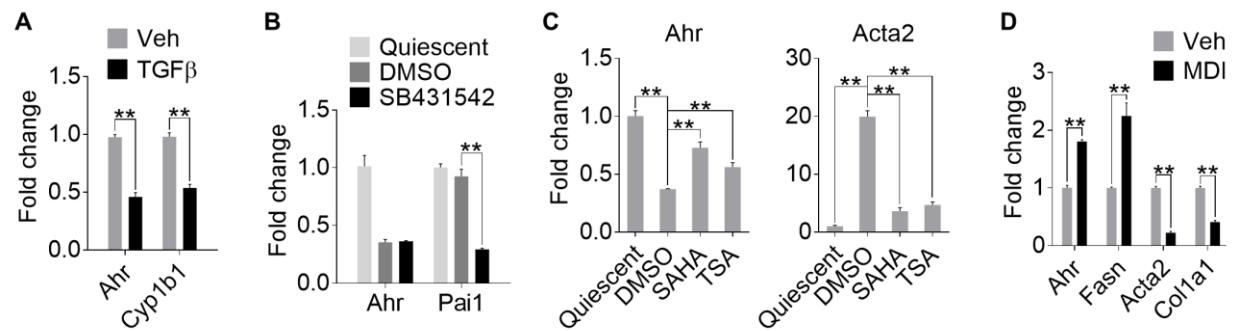


**Figure 24. The expression of AhR inversely correlates with HSC activation**

(A) Primary mouse HSCs were treated with TGFβ1 (2 ng/ml) for 24h. Gene expression was determined by real-time PCR (n=4). (B) Primary mouse HSCs were treated with SB431542 (10 μM) for 72h. Gene expression was determined by real-time PCR (n=4). (C) Primary mouse HSCs were treated with SAHA (10 μM) or TSA (10 μM) for 24h. Gene expression was determined by real-time PCR. (D) Fully activated HSCs were treated with MDI medium containing Dexmethasone (1 μM), 3-Isobutyl-1-methylxanthine (0.5 mM), Insulin (10 μg/ml), and Rosiglitazone (10 μM) for 72h. Gene expression was determined by real-time PCR (n=4). All the data were presented as mean ± SEM (\*\*: p<0.01).

**Pharmacological activation of AhR or forced expression of AhR inhibits spontaneous HSC activation.** In determining whether the expression of AhR in HSCs and the dynamics of AhR expression during HSC activation are functionally relevant, we found treatment of primary mouse HSCs with TCDD inhibited the expression of fibrogenic genes at both the protein (Figure 25A) and mRNA (Figure 25B) levels. A similar pattern of inhibition was observed in primary human HSCs treated with the human AHR activator 3-methylcholanthrene (3MC) (Figure 25C). The inhibitory effect of TCDD on the activation of mouse HSCs was AhR-dependent, because the inhibitory effect was abolished in HSCs isolated from the AhR<sup>-/-</sup> mice when the HSC activation was evaluated by cell morphology (Figure 25D) or the expression of fibrogenic marker genes (Figure 25E).

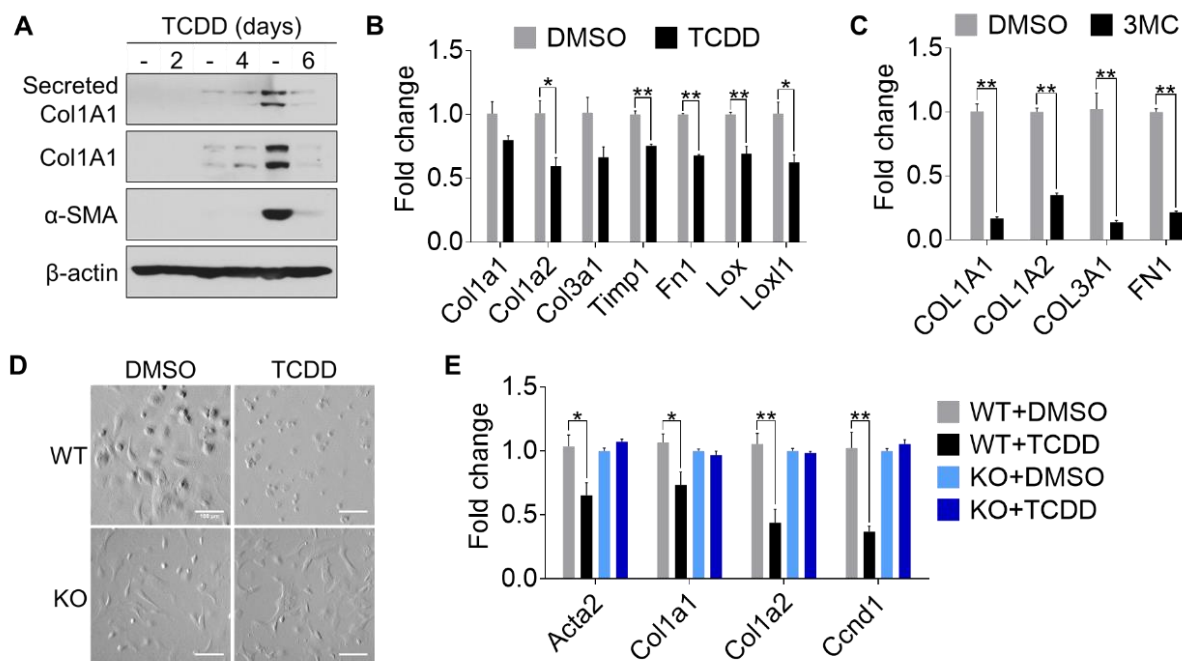


**Figure 25. Pharmacological activation of AhR inhibits spontaneous HSC activation**

(A) Primary mouse HSCs were treated with TCDD (50 nM) for 2, 4, and 6 days, respectively. Protein from whole cell lysate and secreted protein from culture medium were detected by Western blot. (B) Primary mouse HSCs were treated with TCDD (20 nM). Gene expression was determined by real-time PCR (n=3). (C) Primary human HSCs were treated with 3MC (2 μM) for 6 days. Gene expression was determined by real-time PCR (n=4). (D and E) Primary mouse HSCs were isolated from WT or KO mice and treated with TCDD (20 nM) for 6 days. Cell morphology was shown by light field microscopic imaging (D). Gene expression was determined by real-time PCR (n=4) (E). All the data were presented as mean  $\pm$  SEM (\*: p<0.05, \*\*: p<0.01).

Inhibition of HSC activation was also observed in primary HSCs transduced with adenovirus expressing the mouse AhR, as shown by the immunofluorescence of the fibrogenic marker α-SMA and the cell proliferation marker Ki67 (Figure 26A) and the expression of fibrogenic genes (Figure 26B). Adenoviral overexpression of AhR in the human primary HSCs achieved a similar inhibition of HSC activation (Figure 26C-D). These results suggested that the down-regulation of AhR may have contributed to the spontaneous activation of HSCs.

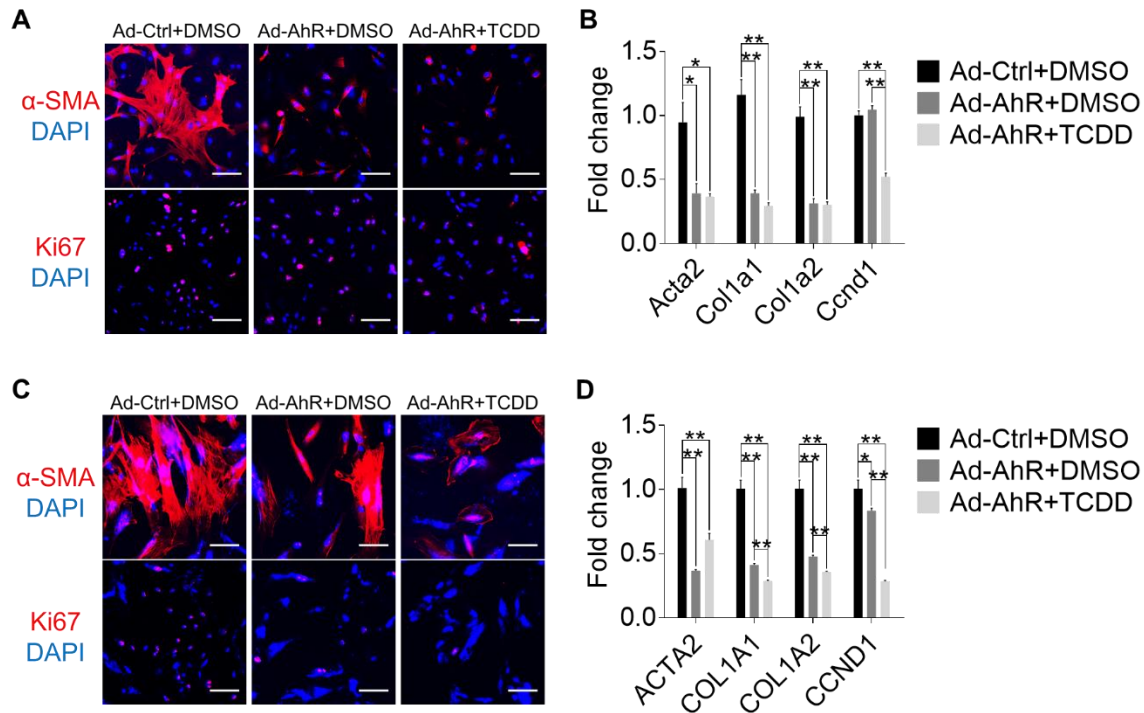


**Figure 26. Forced expression of AhR inhibits spontaneous HSC activation**

(A and B) AhR was overexpressed in the primary mouse HSCs using adenoviral vector overexpressing AhR and treated with or without TCDD (50 nM).  $\alpha$ -SMA and Ki67 were detected by immunofluorescent staining (A). Gene expression was determined by real-time PCR (n=3) (B). (C and D) Primary human HSCs were infected with adenoviral vector overexpressing AhR and treated with or without TCDD (50 nM).  $\alpha$ -SMA and Ki67 were detected by immunofluorescent staining (C). Gene expression was determined by real-time PCR (n=4) (D). Scale bar is 100  $\mu$ m in all the immunofluorescent images. All the data were presented as mean  $\pm$  SEM (\*: p<0.05, \*\*: p<0.01).

### Genetic ablation or pharmacological inhibition of AhR promotes HSC activation.

Consistent with our hypothesis that the down-regulation of AhR contributes to the activation of HSCs, HSCs isolated from AhR<sup>-/-</sup> mice showed enhanced spontaneous activation as shown by cell morphology (**Error! Reference source not found.A**) and the induction of fibrogenic marker genes throughout the spontaneous activation (**Error! Reference source not found.B**). Increased protein expression of  $\alpha$ -SMA and Col1A1 in AhR<sup>-/-</sup> HSCs was verified by Western blotting (**Error! Reference source not found.C**). Immunofluorescence verified the induction of  $\alpha$ -SMA and Ki67 in AhR<sup>-/-</sup> HSCs (**Error! Reference source not found.D**). In a pharmacological model

and consistent with the increased spontaneous activation in AhR<sup>-/-</sup> HSCs, treatment of HSCs isolated from WT mice with CH223191, an AhR antagonist [263], increased the expression of fibrogenic genes (**Error! Reference source not found.E**). The pro-fibrogenic effect of CH223191 was also observed in primary human HSCs (**Error! Reference source not found.F**). The activation of AhR<sup>-/-</sup> HSCs was attenuated when the expression of AhR was reconstituted by adenoviral infection, as shown by the protein expression of  $\alpha$ -SMA and CollA1 (**Error! Reference source not found.G**), the mRNA expression of fibrogenic genes (**Error! Reference source not found.H**), and the immunofluorescence of  $\alpha$ -SMA and Ki67 (**Error! Reference source not found.I**).

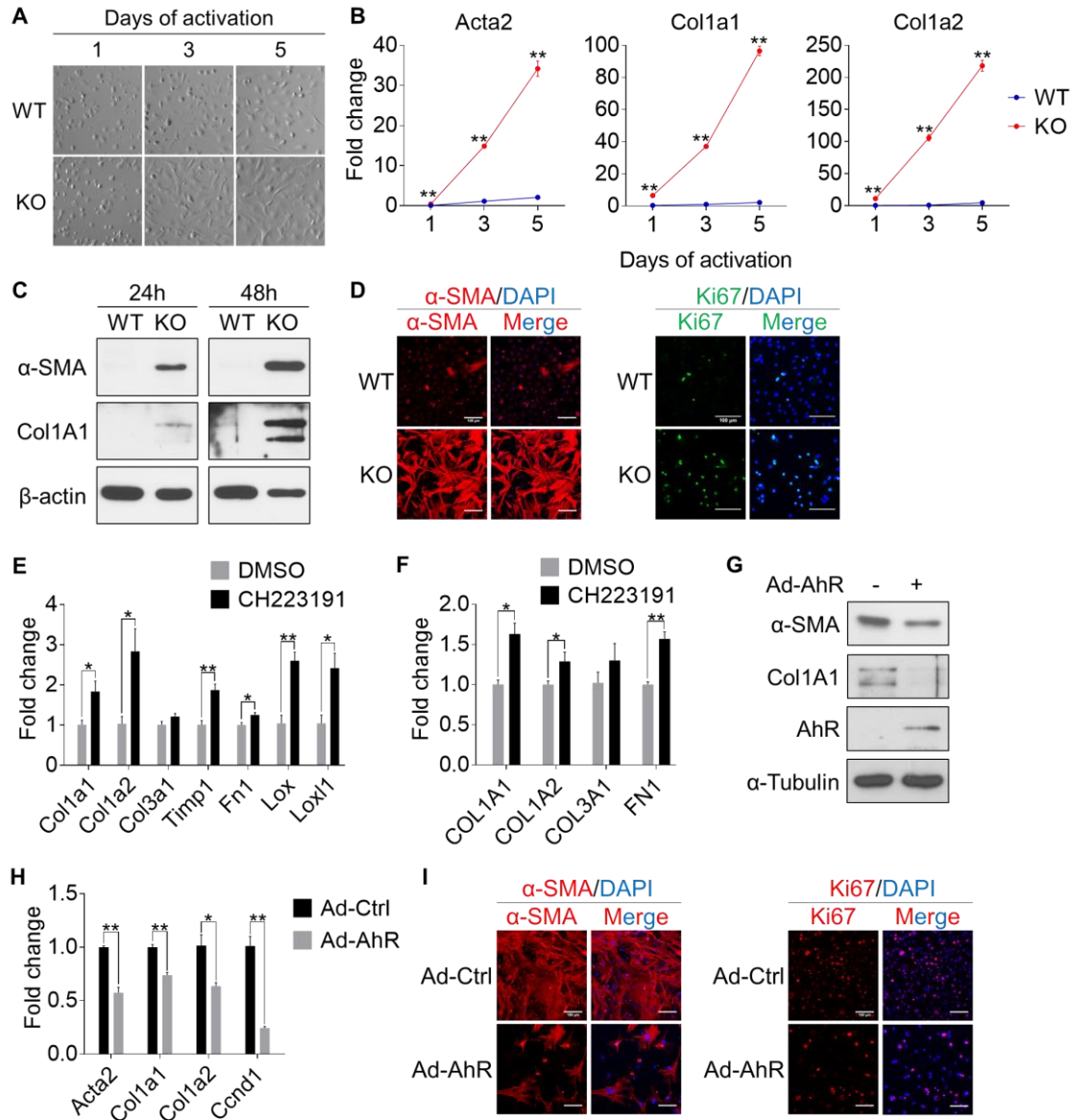


**Figure 27. Genetic ablation or pharmacological inhibition of AhR promotes HSC activation**

(A and B) Primary mouse HSCs were isolated from WT and KO mice and culture-activated for the indicated duration. Cell morphology was shown by light field microscopic imaging (A). Gene expression was determined by real-time PCR (n=4) (B). (C) Primary mouse HSCs were isolated from WT and KO mice and culture-activated for 24h and 48h. Protein expression was determined by Western blot. (D) Primary mouse HSCs were isolated from WT and KO mice and culture-activated for 48h.  $\alpha$ -SMA and Ki67 were detected by immunofluorescent staining. (E) Primary mouse HSCs were treated with CH223191 (10  $\mu$ M) for 6 days. Gene expression was determined by real-time PCR (n=3). (F) Primary human HSCs were treated with CH223191 (10  $\mu$ M). Gene expression was determined by real-time PCR (n=4). (G-I) Primary mouse HSCs isolated from KO mice were infected with adenoviral vector overexpressing AhR and treated with or without TCDD (50 nM). Protein expression was determined by Western blot (G). Gene expression was determined by real-time PCR (n=4) (H).  $\alpha$ -SMA and Ki67 were

detected with immunofluorescent staining (I). Scale bar is 100  $\mu$ m in all the immunofluorescent images. All the data were presented as mean  $\pm$  SEM (\*:  $p < 0.05$ , \*\*:  $p < 0.01$ ).

**Ablation of AhR in HSCs, but not in hepatocytes or Kupffer cells, sensitizes mice to spontaneous or CCl<sub>4</sub>- and BDL-induced liver fibrosis.** It has been reported that the whole body AhR<sup>-/-</sup> mice exhibited spontaneous periportal liver fibrosis [42, 43], which was independently verified by our own analysis by using the Masson's Trichrome staining and Sirius Red staining (Figure 28A). The liver is an organ of multiple cell types. To determine the loss of AhR in which cell type is responsible for the spontaneous liver fibrosis, we generated hepatocyte- (HEP-KO), Kupffer cell- (M $\Phi$ -KO), and HSC-specific (HSC-KO) AhR knockout mice by crossbreeding the AhR floxed (AhR<sup>fl/fl</sup>, fl/fl) mice with Albumin-Cre, LysM-Cre, and Lrat-Cre transgenic mice, respectively and as outlined in Figure 28B. The liver to body weight ratio was not significantly changed compared to the control mice (Figure 28C), indicating no liver developmental defect in those conditional knockout mice as seen in the AhR<sup>-/-</sup> mice. Compared to the AhR<sup>-/-</sup> mice, only the HSC-KO mice, but not the HEP-KO or M $\Phi$ -KO mice, showed spontaneous liver fibrosis yet with much less extent than AhR<sup>-/-</sup> as illustrated by Masson's Trichrome staining, Sirius Red staining, and immunohistochemistry of  $\alpha$ -SMA (Figure 28D).



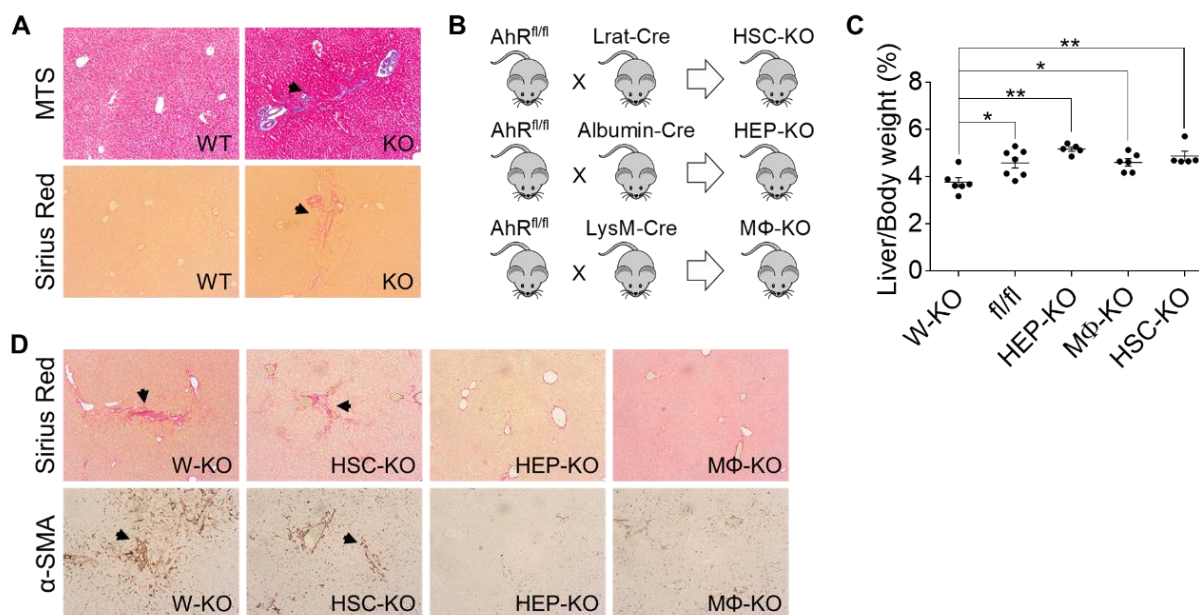


**Figure 28. Ablation of AhR in HSCs, but not in hepatocytes or Kupffer cells, sensitizes mice to spontaneous liver fibrosis**

(A) Histological analysis of liver, kidney, lung and heart by Masson's Trichrome and Sirius Red staining in WT and AhR<sup>-/-</sup> (KO) mice (magnification, 10X). (B) Breeding scheme for conditional AhR knockout mice. (C) Liver to body weight ratio. (D) Histological analysis of liver by Masson's Trichrome and Sirius Red staining and immunohistochemistry staining of  $\alpha$ -SMA in AhR<sup>-/-</sup> (W-KO), AhR<sup>fl/fl</sup> (fl/fl), hepatocyte- (HEP-KO), Kupffer cell- (MΦ-KO), and HSC-specific (HSC-KO) AhR knockout mice (magnification, 10X). All the data were presented as mean  $\pm$  SEM (\*:  $p < 0.05$ , \*\*:  $p < 0.01$ ).

We next went on to determine whether ablation of AhR in HSCs can sensitize mice to liver fibrosis induced by CCl<sub>4</sub> or BDL. Compared to the control AhR<sup>fl/fl</sup> mice (fl/fl), the HSC-KO mice exhibited more pronounced liver fibrosis in response to the CCl<sub>4</sub> challenge. These include increased collagen deposition and increased immunostaining of  $\alpha$ -SMA (Figure 29A). The HSC-KO mice also exhibited increased sensitivity to BDL-induced liver fibrosis (Figure 29B). The CCl<sub>4</sub>- and BDL-responsive induction of  $\alpha$ -SMA in the HSC-KO mice was verified by Western blotting (Figure 29C). Meanwhile, the HEP-KO mice were not more sensitive to CCl<sub>4</sub>-induced liver fibrosis (Figure 29D).



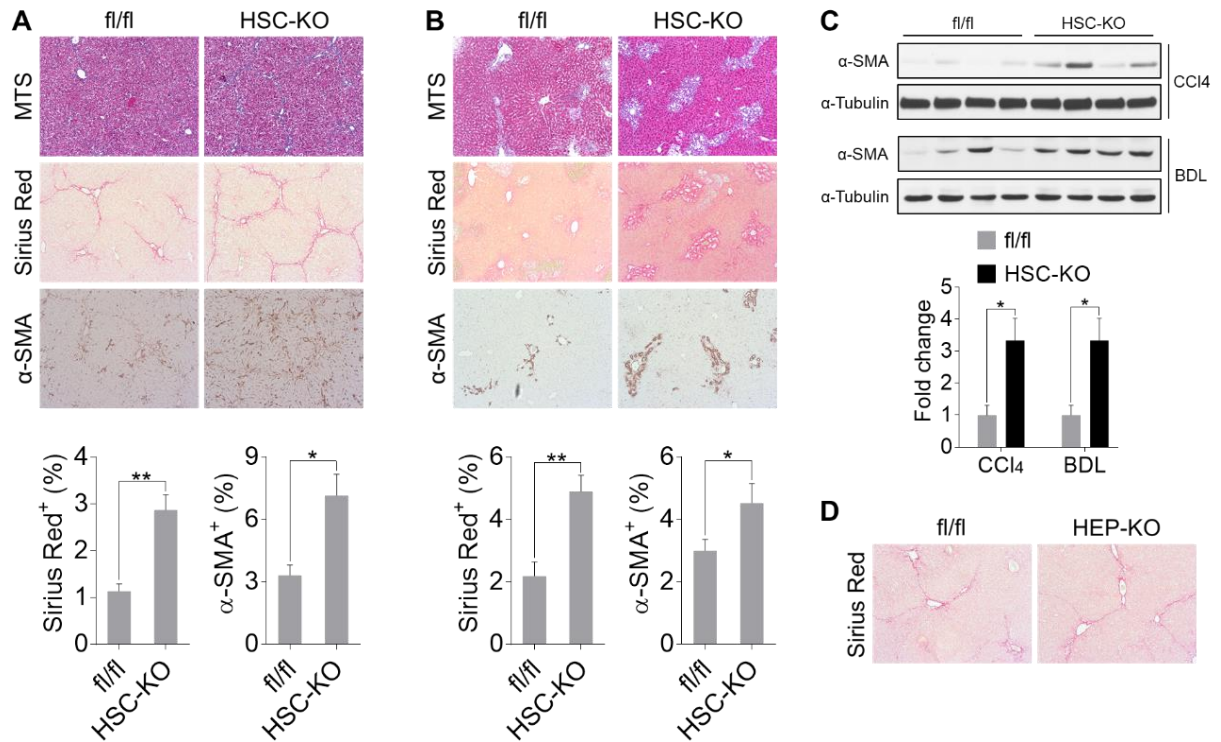


**Figure 29. Ablation of AhR in HSCs sensitizes mice to CCl<sub>4</sub>- and BDL-induced liver fibrosis** (A) 9-10 weeks old male AhR<sup>fl/fl</sup> and HSC-KO mice were treated with CCl<sub>4</sub> (1 μl/g body weight) twice a week for 4 weeks (n=5 per group). Top, histological analysis of liver by Masson's Trichrome (MTS) and Sirius Red staining, and immunohistochemistry staining of α-SMA (magnification, 10X). Bottom, quantification of Sirius Red and α-SMA positive staining. (B) 8-9 weeks old AhR<sup>fl/fl</sup> and HSC-KO mice were bile duct ligated for 2 weeks (n=7 for fl/fl, 6 for HSC-KO). Top, histological analysis of liver by Masson's Trichrome (MTS) and Sirius Red staining, and immunohistochemistry staining of α-SMA (magnification, 10X). Bottom, quantification of Sirius Red and α-SMA positive staining. (C) α-SMA protein expression in CCl<sub>4</sub>- and BDL-induced fibrotic liver were determined by Western blot. (D) 9-10 weeks old male AhR<sup>fl/fl</sup> and HEP-KO mice were treated with CCl<sub>4</sub> (1 μl/g body weight) twice a week for 4 weeks (n=5 per group). Representative Sirius Red staining was shown (magnification, 10X). All the data were presented as mean ± SEM (\*: p<0.05, \*\*: p<0.01).

**AhR attenuates TGFβ-stimulated fibrogenesis by disrupting the interaction between Smad3 and β-catenin.** TGFβ-Smad signaling stimulates liver fibrogenesis and is central to the activation of HSCs [264]. Having shown the inhibitory effect of AhR on the spontaneous activation of HSCs, we went on to determine whether AhR can also inhibit TGFβ-stimulated fibrogenesis in HSCs. Treatment of primary mouse HSCs with TGFβ induced the expression of fibrogenic genes as expected, but the inductions were largely attenuated when the cells were

treated with TCDD (Figure 30A). The TGF $\beta$  responsive induction of  $\alpha$ -SMA was also attenuated in TCDD-treated HSCs as shown by immunofluorescence (Figure 30B). Next, we overexpressed AhR in the human stellate cell line LX2 in which the endogenous AhR protein was not detectable thus not responsive to AhR ligands. The overexpression of AhR and the responsiveness of transfected cells to AhR ligands were verified. Overexpression of AhR in LX2 cells significantly attenuated the response to the TGF $\beta$  stimulation, and ligand treatment modestly enhanced the attenuation (Figure 30C-D). Consistent with the inhibition of fibrogenic gene expression, the TGF $\beta$  responsive recruitment of phosphorylated Smad3 onto the promoter regions of COL1A1, COL1A2, and PAI1 genes was attenuated by AhR overexpression as shown by chromatin precipitation (ChIP) analysis (Figure 30E).

To elucidate the molecular mechanism underlying the inhibitory effect of AhR on TGF $\beta$ -Smad stimulated fibrosis, we first checked the nuclear translocation of Smad proteins. Yet there were no significant changes for the nuclear translocation of Smad proteins (Figure 30F). We next examined the expression of negative regulators of the TGF $\beta$  signaling pathway, considering AhR is a transcriptional factor. There were no significant changes in the expression of genes that are involved in the protein degradation (Smurf1 and Smurf2), receptor antagonism (Bambi), nuclear transport (Xpo1, Xpo4, and Ranbp3), or transcriptional repressors (Tgif, Ski, and Skil) (Figure 30G).

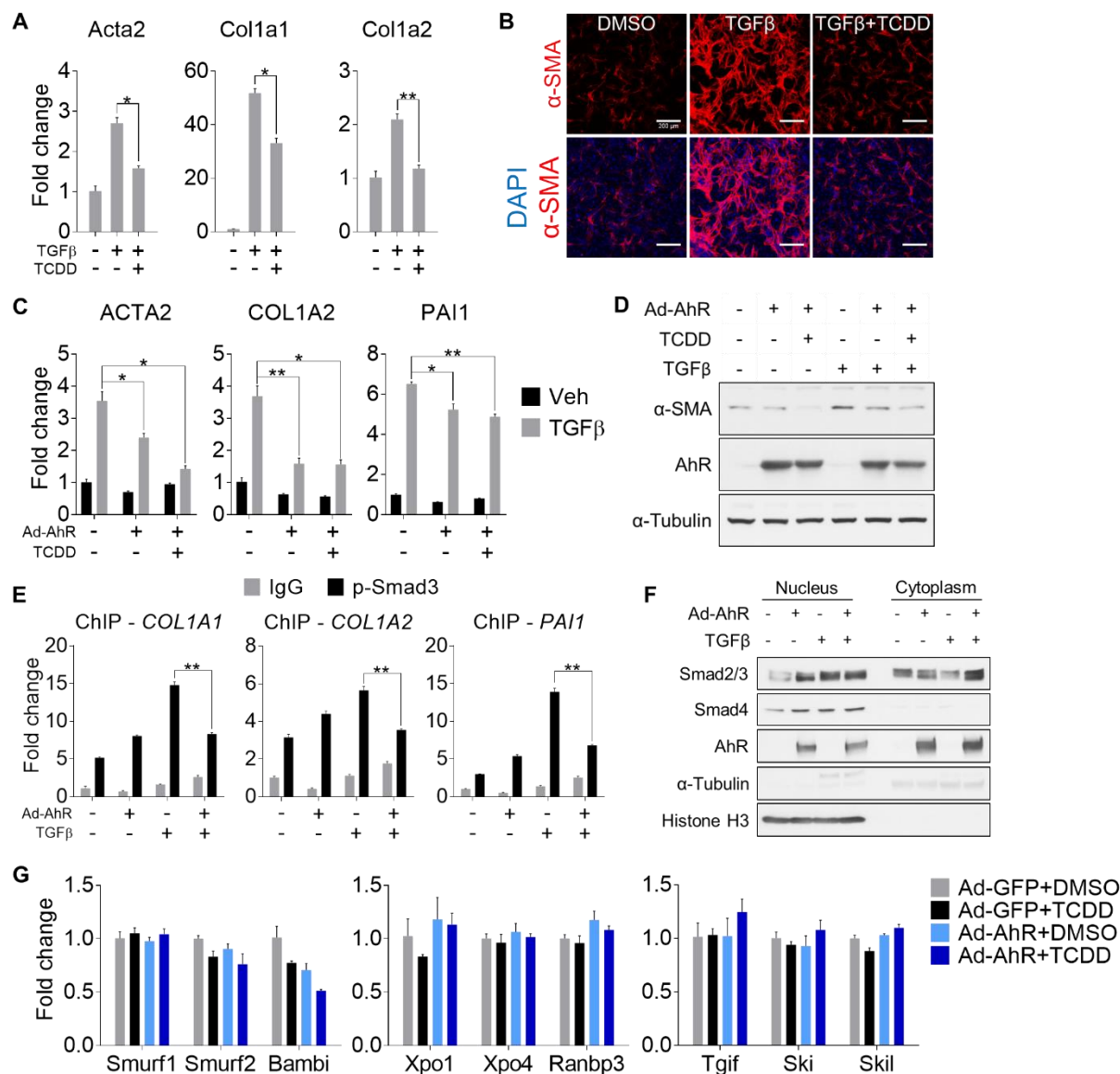


**Figure 30. AhR attenuates TGFβ-stimulated fibrogenesis**

(A) Primary mouse HSCs were treated with TGFβ1 (2 ng/ml) with or without TCDD (50 nM) for 24h as labelled. Gene expression was determined by real-time PCR (n=3). (B) Primary mouse HSCs were treated with TGFβ1 (2 ng/ml) with or without TCDD (50 nM) for 48h. α-SMA was detected with immunofluorescent staining, scale bar=200 μm. (C and D) LX2 cells were infected with adenoviral vector overexpressing AhR and treated with TCDD (50 nM) and/or TGFβ1 (5 ng/ml) as labelled for 24h. Gene expression was determined by real-time PCR (n=4) (C). Protein expression was detected by Western blot (D). (E) LX2 cells were infected with adenoviral vector overexpressing AhR were pre-treated with or without TCDD (50 nM) for 24h and then TGFβ1 (5 ng/ml) with or without TCDD (50 nM) for 4h. DNA binding of phosphorylated Smad3 on the promoter of human COL1A1, COL1A2 and PAI1 genes were determined by ChIP coupled with real-time PCR (n=4). (F) LX2 cells were infected with adenoviral vector overexpressing AhR and treated with TCDD (50 nM) before stimulated by TGFβ1 (5 ng/ml) with or without TCDD for 4h. Cytoplasmic and nuclear fractions were extracted for Western blot. (G) AhR was overexpressed in the primary mouse HSCs using adenoviral vector overexpressing AhR and treated

with or without TCDD (50 nM). Gene expression was determined by real-time PCR (n=3). All the data were presented as mean  $\pm$  SEM (\*:  $p<0.05$ , \*\*:  $p<0.01$ ).

We then determined whether AhR has a direct interaction with the Smad proteins. Coimmunoprecipitation (coIP) analysis showed that AhR can specifically interact with Smad3, but not Smad 2 and 4 (Figure 31A). We speculated that the AhR-Smad3 interaction may interfere with the accessibility of Smad3 to other Smad3-interacting transcriptional factors, including  $\beta$ -catenin, myocyte enhancer factor 2 (MEF2), serum response factor (SRF), and SP1. Only  $\beta$ -catenin exhibited substantial interaction with Smad3 and this interaction was not affected by the treatment of TGF $\beta$  as shown by coIP (Figure 31B). The interaction of  $\beta$ -catenin with Smad3 was decreased by the overexpression of AhR alone and was further reduced by the TCDD treatment, which coincided with increased binding of Smad3 to AhR (Figure 31C). As a control, the interaction of Smad3 with Smad4 remained intact in the presence of AhR (Figure 31C). Both AhR and  $\beta$ -catenin interact with Smad3 via the MH2 domain of Smad3 (Figure 31D). It has been reported that the coupling of Smads and  $\beta$ -catenin is required for optimal induction of ECM genes and fibrogenesis [265]. Our results suggested that AhR may attenuated TGF $\beta$  stimulated fibrosis by sequestering Smad3 from  $\beta$ -catenin. AhR decreased the  $\beta$ -catenin binding to Smad3 in a dose-dependent manner (Figure 31E), further supporting that AhR competes with  $\beta$ -catenin for the binding of Smad3. The inhibitory effect of AhR on the expression of  $\alpha$ -SMA was also dose-dependent (Figure 31F). Taken together, our results suggested that AhR attenuates TGF $\beta$  stimulated fibrogenesis by disrupting the binding between  $\beta$ -catenin and Smad3.

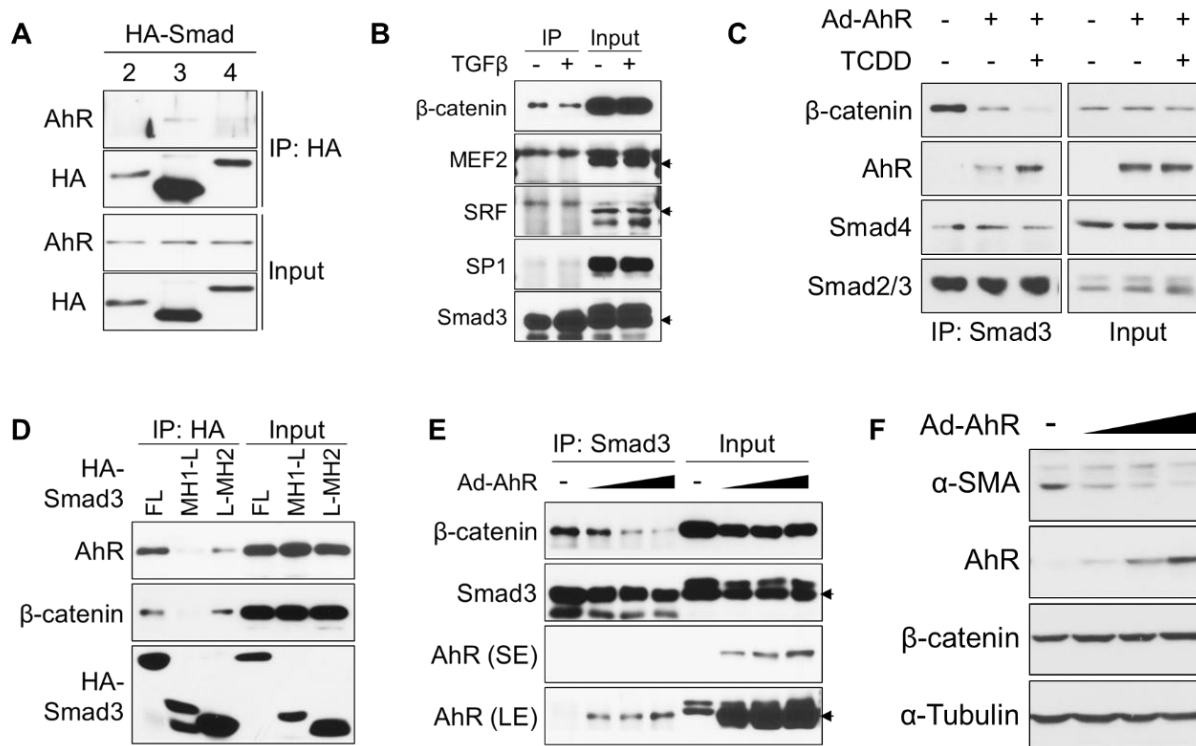


**Figure 31. AhR disrupts the interaction of Smad3 and  $\beta$ -catenin**

(A) Stable human AhR-expressing LX2 cells were transfected with HA-Smad2, HA-Smad3, or HA-Smad4. Protein interaction was determined by coimmunoprecipitation with HA antibody followed by Western blot analysis. (B) LX2 cells were stimulated with TGF $\beta$ 1 (5 ng/ml) for 3h before harvest. Protein interaction was determined by coimmunoprecipitation with anti-Smad3 followed by Western blot analysis. Arrows denote the protein bands. (C) LX2 cells were infected with adenoviral vector overexpressing AhR and treated with or without TCDD (50 nM). Protein interaction was determined by coimmunoprecipitation with Smad3 antibody followed by Western blot analysis. (D) LX2 cells with AhR overexpressed were transfected with HA-Smad3 plasmids (full length, FL; MH1 domain plus linker, MH1-L; Linker plus MH2 domain, L-MH2). Protein interaction was determined by coimmunoprecipitation with anti-HA followed by Western blot analysis. (E) LX2 were infected with increasing doses of Ad-AhR. Protein interaction was determined by coimmunoprecipitation with anti-Smad3 followed by Western blot analysis. Arrow denotes the Smad3 protein band. (F) LX2 were infected with Ad- $\beta$ -catenin (S33Y) with increasing doses of Ad-AhR. Protein expression was detected by Western blot.

**AhR impairs  $\beta$ -catenin-dependent stabilization of phosphorylated Smad2/3.**  $\beta$ -catenin is the effector of the canonical Wnt signaling pathway that is also responsive to the TGF $\beta$  stimulation [266]. However, how  $\beta$ -catenin potentiates the fibrogenesis mediated by the TGF $\beta$ -Smad axis and whether AhR can attenuated pro-fibrogenic activity of  $\beta$ -catenin are unknown. We first examined the kinetics of Smad2/3 phosphorylation. In the absence of AhR, overexpression of  $\beta$ -

catenin was efficient to prolong the duration of TGF $\beta$ -stimulated Smad2/3 phosphorylation, but this effect was largely diminished by the transfection of AhR (Figure 32A-B). The fibrogenic gene expression induced by  $\beta$ -catenin was also down-regulated by AhR in both LX2 cells (Figure 32C-D) and primary HSCs (Figure 32E).

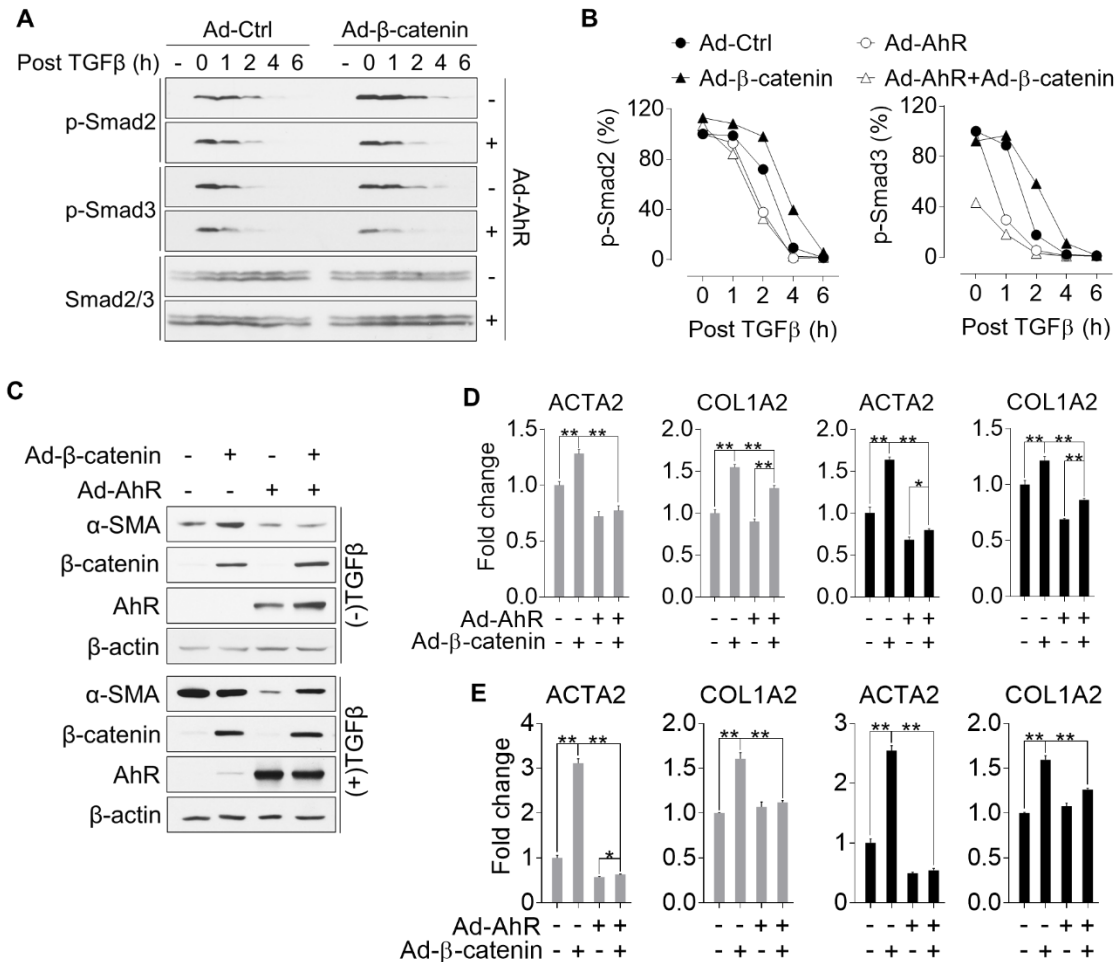


**Figure 32. AhR impairs  $\beta$ -catenin-dependent stabilization of phosphorylated Smad2/3**

(A and B) LX2 were infected with Ad-AhR and/or Ad- $\beta$ -catenin (S33Y) as labelled and were stimulated with TGF $\beta$ 1 (5 ng/ml) for 1h before harvest at multiple time points as labelled. Phosphorylated Smad2/3 was detected by Western blot (A) and quantified by densitometric analysis (B). (C and D) LX2 were infected with Ad-AhR and/or Ad- $\beta$ -catenin (S33Y) and treated with TCDD (50 nM) and TGF $\beta$ 1 (5 ng/ml) as labelled. Gene expression was determined by real-time PCR (Grey bars: no TGF $\beta$ 1, black bars: with TGF $\beta$ 1, n=4) (C). Protein expression was detected by Western blot (D). (E) Primary human HSCs were infected with Ad-AhR with or without Ad- $\beta$ -catenin (S33Y) and treated with TCDD (50 nM) for 24h (grey bars) or pre-treated with TCDD (50 nM) for 24h then TGF $\beta$ 1 (5 ng/ml) with or without TCDD (50 nM) for 24h (black bars). Gene expression was determined by real-time PCR. Grey bars, no TGF $\beta$ ; Black bars, with TGF $\beta$ . The data were presented by mean  $\pm$  SEM (\*: p<0.05, \*\*: p<0.01).

The stability of phosphorylated Smad2/3 is controlled by the ubiquitin-proteasomal degradation [267, 268]. Treatment of the ubiquitylation inhibitors (MLN4924 and Heclin) and/or proteasome inhibitors (MG132 and Lactacystin) in the AhR-overexpressing LX2 cells extended the duration of Smad2/3 phosphorylation (Figure 33A). For the expression of fibrogenic genes, MLN4924 (Figure 33B-C), but not Heclin (Figure 33D-E), significantly abolished the inhibitory effect of AhR. Similar as MLN4924, MG132 also significantly abolished the inhibitory effect of AhR (Figure 33F-G). Treatment of primary mouse (Figure 33H) and human (Figure 33I) HSCs with MLN4924 also attenuated the inhibitory effect of AhR on HSC activation. Taken together, it was suggested that the Cullin-RING E3 ligases (CRLs), but not the HECT E3 ligases, may play a role in mediating the inhibitory effect of AhR. Because AhR itself is a ubiquitylation E3 ligase for  $\beta$ -catenin in the intestinal cells as a substrate adaptor in the CUL4B ligase complex [174], we examined whether the E3 ligase activity of AhR is necessary for the inhibitory effect on the HSCs. The E3 ligase-deficient AhR mutant with the deletion of the acidic domain remained effective in decreasing the expression of fibrogenic genes (Figure 34A-B), indicating that the E3 ligase activity of AhR may be dispensable. In summary, our results suggested that  $\beta$ -catenin promotes HSC activation and fibrosis by stabilizing phosphorylated Smad2/3, which can be blocked by AhR.

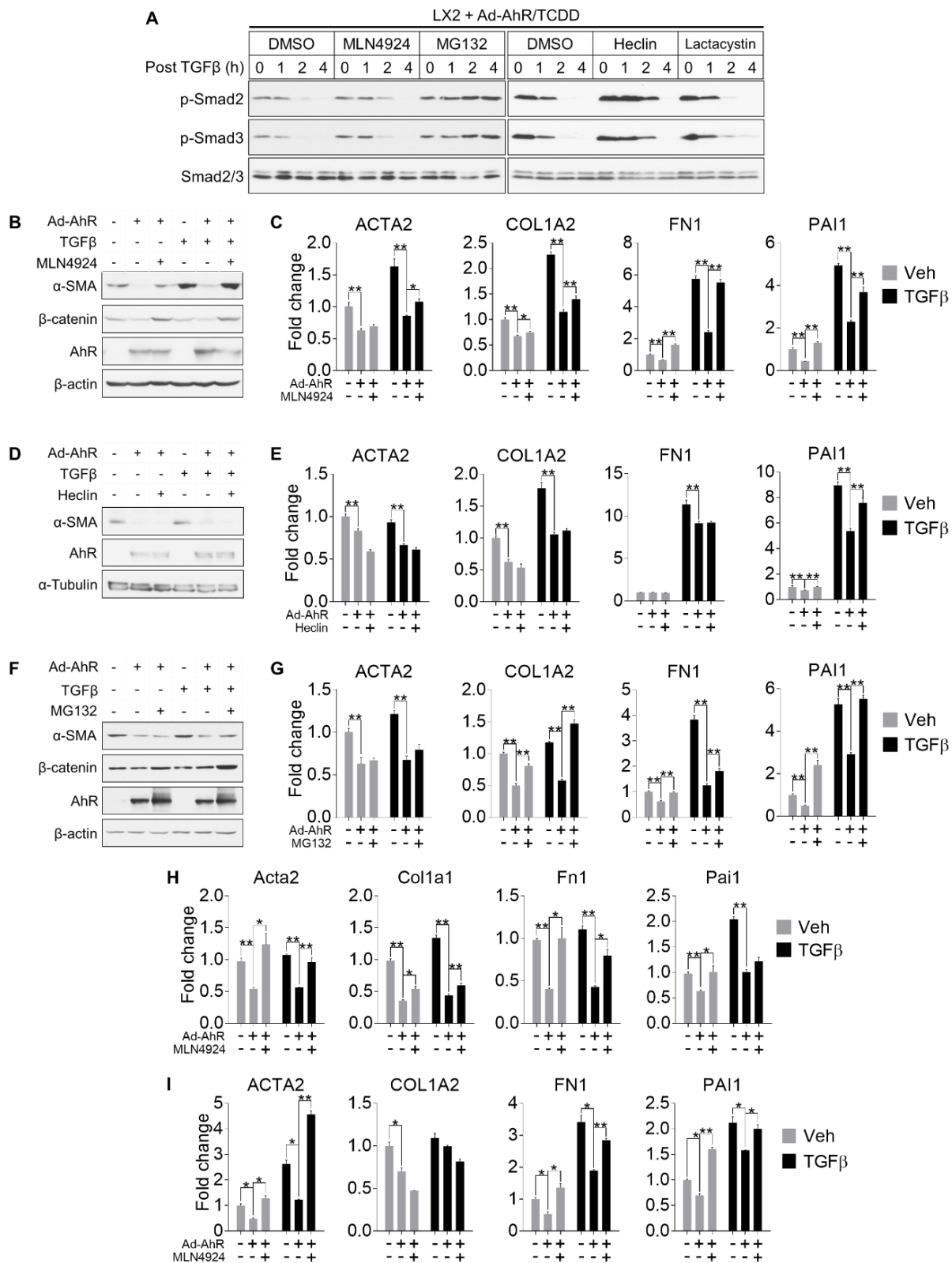


**Figure 33. CRLs play a role in the AhR-exerted inhibition of fibrogenesis in the HSCs**



(A) LX2 infected with Ad-AhR were stimulated with TGFβ1 (5 ng/ml) for 1h and were treated with MLN4924 (0.5 μM), MG132 (10 μM), Heclin (50 μM), or lactacystin (5 μM) before collected at multiple time points as labelled. Protein expression was detected by Western blot. (B and C) LX2 cells were infected with adenoviral vector overexpressing AhR and treated with TCDD (50 nM) with or without TGFβ1 (5 ng/ml) or MLN4924 (0.5 μM) for 24h as labelled. Protein expression was detected by Western blot (B). Gene expression was determined by real-time PCR (n=4) (C). (D and E) LX2 cells were infected with adenoviral vector overexpressing AhR and treated with TCDD (50 nM) with or without TGFβ1 (5 ng/ml) or Heclin (50 μM) as labelled. Protein expression was detected by Western blot (D). Gene expression was determined by real-time PCR (n=4) (E). (F and G) LX2 cells were infected with adenoviral vector overexpressing AhR and treated with TCDD (50 nM) with or without TGFβ1 (5 ng/ml) or MG132 (10 μM) for 6h as labelled. Protein expression was detected by Western blot (F). Gene expression was determined by real-time PCR (n=4) (G). (H) Primary mouse HSCs were infected with adenoviral vector overexpressing AhR and treated with TCDD (50 nM) with or without TGFβ1 (5 ng/ml) or MLN4924 (0.5 μM) as labelled. Gene expression was determined by real-time PCR (n=4). (I) Primary human HSCs were infected with adenoviral vector overexpressing AhR and treated with TCDD (50 nM) with or without TGFβ1 (5 ng/ml) or MLN4924 (0.5 μM) as labelled. Gene expression was determined by real-time PCR (n=4). All the data were presented by mean±SEM (\*: p<0.05, \*\*: p<0.01).

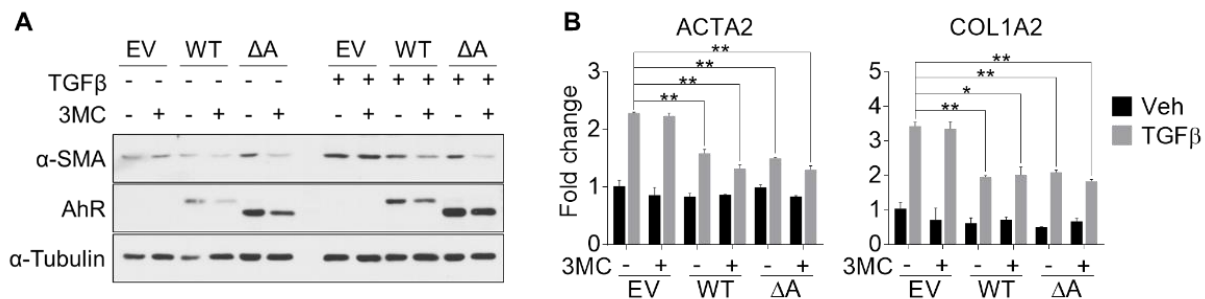


**Figure 34. AhR-mediated inhibition is independent of its E3 ligase activity**

LX2 cells stably expressing empty vector (EV), human AhR full length (WT), or AhR with acidic domain deleted (ΔA) were treated with 3MC (2 μM) and/or TGFβ1 (5 ng/ml) as labelled for 24h. Protein expression was detected by Western blot (A). Gene expression was determined by real-time PCR (n=3) (B). All the data were presented by mean ± SEM (\*: p<0.05, \*\*: p<0.01).

#### 4.4 DISCUSSION AND CONCLUSION

In this study, we have clarified the controversy for the role of AhR in liver fibrosis. We found the liver fibrosis observed in TCDD-treated mice might be secondary to inflammation, since the fibrils localize to the proximity of infiltrated neutrophils. It is therefore plausible that TCDD exacerbates experimental liver fibrosis [269, 270]. How TCDD induces the infiltration of

inflammatory cells and eventual liver toxicity is still not fully understood. Genetically engineered mouse model has shown TCDD-induced hepatotoxicity is dependent on DNA-binding of AhR [271]. Metabolomic disturbance due to the altered transcriptome by AhR might play a vital role in the inflammation and hepatotoxicity, as exemplified by two recent studies [272, 273]. In contrast, the physiological relevant AhR ligand ITE does not cause neutrophil infiltration hence no fibrosis was seen in the liver tissue. We argue that the discrepancy in the hepatotoxicity can be explained by the distinct transcriptional regulation by a specific ligand.

Furthermore, the “non-toxic” ITE was able to alleviate CCl<sub>4</sub>-induced fibrosis and improve liver function, suggesting the endogenous AhR signaling is generally protective against liver fibrosis. This agrees with the previous reports that AhR<sup>-/-</sup> mice has spontaneous periportal liver fibrosis [42, 43]. We observed the similar fibrotic liver phenotype in a different AhR<sup>-/-</sup> strain as well as in the HSC-KO mice, although the time of onset, the loci and degree of the fibrotic lesions varies between individual animals. When challenged with CCl<sub>4</sub> and BDL, the HSC-KO mice were distinguished with the control mice by enhanced fibrotic phenotype. We also have shown HSC-KO mice, but not HEP-KO or MΦ-KO, recapitulate the spontaneous liver fibrosis in the AhR<sup>-/-</sup>. This may suggest that the endogenous AhR signaling in the HSCs can restrict liver fibrosis. However, we cannot exclude the possibility that AhR signaling in the other cell types, particularly in the immune cells, may play a role in the development of liver fibrosis as well.

Although the identity of the endogenous “anti-fibrotic” AhR ligands remains unclear, they are presumably tryptophan metabolites. The speculation lies on the two lines of evidence. First, most of physiologically relevant AhR ligands identified so far have been tryptophan metabolites, such as kynurenine [274, 275]. Second, it has been reported that increased

tryptophan catabolism is associated with liver fibrosis caused by viral infection [276]. It would be of interest to find the endogenous ligands of AhR in the scenario of liver fibrosis using metabolomic approaches in the future. Regardless, exogenous supplementation of physiological AhR ligands could be a new class of therapeutics to treat fibrotic diseases. Several studies published during the preparation of this manuscript have shown the anti-fibrotic efficacy of AhR ligands in vitro or in vivo [277, 278]. In this study, we have also shown that the non-toxic AhR ligand ITE substantially decreased CCl<sub>4</sub>-induced liver fibrosis.

The TGF $\beta$ -Smad signaling pathway has been long implicated in multiple organ fibrosis including liver fibrosis [264]. In the liver fibrosis, TGF $\beta$  signal transduction in the HSCs, probably in other fibroblasts, is the central pathway that responds to injury signals from surrounding tissue and relays them to the transcriptional regulation leading to HSC activation [241, 279]. There is also evidence that pinpoint the importance of the canonical Wnt signaling in the fibrotic response [242]. The synergism of TGF $\beta$  and Wnt ligands and the concurrent nuclear entry in the fibrotic specimen suggest the intimate crosstalk between TGF $\beta$  and Wnt pathway in the fibrotic diseases [243]. However, how  $\beta$ -catenin, the canonical Wnt regulated transcriptional factor, regulates Smad proteins, particularly in the stellate cells, is still largely unknown.

In the present study, we proposed a molecular mechanism that  $\beta$ -catenin stabilizes the transcriptionally active phosphorylated Smad2/3 proteins and extends the duration of Smad2/3-dependent genomic activity. It has been reported that  $\beta$ -catenin interacts with the C-terminal MH2 domain of Smad3 [280]. This MH2 domain is also the binding site for the ubiquitylation E3 ligases [267, 268]. Therefore, it is reasonable to speculate that the stabilization of phosphorylated Smad2/3 protein by  $\beta$ -catenin could have been achieved through the prevention of ubiquitylation. In this study, we have also demonstrated that AhR competitively disrupts the

interaction of  $\beta$ -catenin and Smad3, impairs the stabilization of phosphorylated Smad2/3 by  $\beta$ -catenin, and thus inhibits TGF $\beta$ -induced fibrogenesis and HSC activation. This  $\beta$ -catenin- and Smad3-targeted inhibition by AhR could be an important negative regulation of HSC activation during the progression of liver fibrosis.

In summary, we have investigated the HSC-specific role of AhR in liver fibrosis and demonstrated that AhR is a suppresser of HSC activation by disrupting the  $\beta$ -catenin/Smad3 complex thus attenuating the fibrogenesis (Figure 35). Therefore, AhR-dependent therapeutic would be a novel strategy to prevent or treat liver fibrosis and likely other fibrotic diseases.

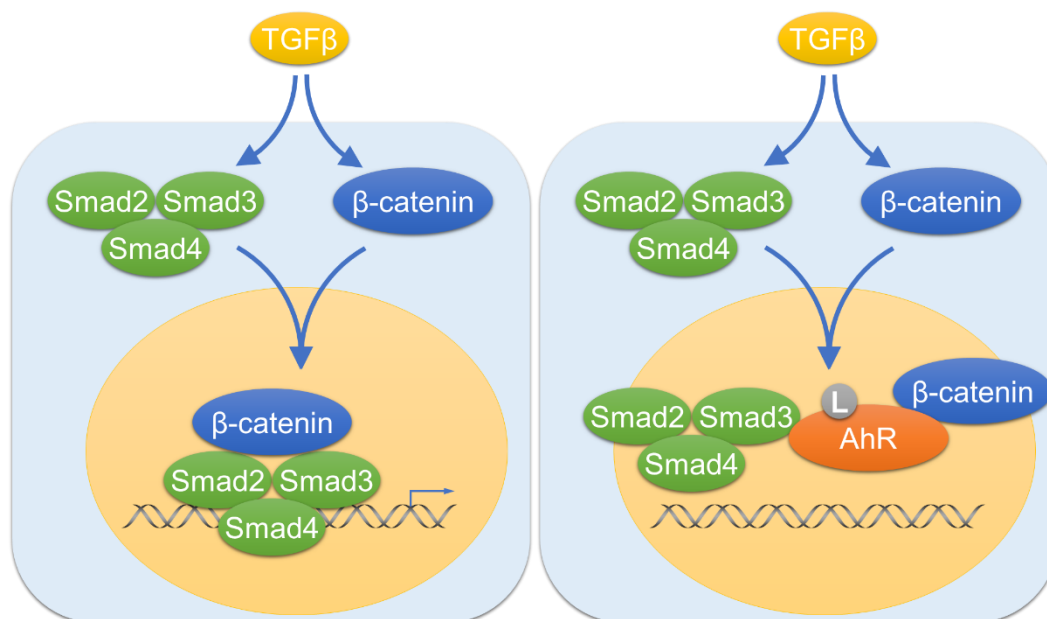


**Figure 35. Molecular mechanism for AhR-mediated suppression of fibrogenesis in HSCs**

Under fibrotic condition, activated HSCs are stimulated by TGF $\beta$  which induces the formation of complex containing Smad2/3, Smad4, and  $\beta$ -catenin. This complex optimally transduces fibrogenic genes in the HSCs. The presence of AhR signaling constrains the fibrogenic progression by interrupting the interaction of Smad3 and  $\beta$ -catenin, while loss of the AhR signaling enhances the fibrogenic activation.

## **5.0 SUMMARY**

### **5.1 NON-GENOMIC (NON-CANONICAL) FUNCTION OF XENOBIOTIC RECEPTORS**

The intrinsic transcriptional regulatory activity of xenobiotic receptors that controls xenobiotic responsive genes is the fundamental function of these xenobiotic sensors to mediate the therapeutic and toxicological effects. Moreover, the genomic function as a transcriptional factor is essential for not only the xenobiotic response but also physiological homeostasis, because there are other transcriptional targets of xenobiotic receptors that also participate in the metabolism of endobiotics. For example, the DNA-binding deficient AhR transgenic mice have defects in the liver development [271]. However, we have also noticed the non-genomic function of AhR as an E3 ligase which may be totally independent of its transcriptional activity [173]. In fact, these two activities seem exclusive to each other [175]. While numerous studies are focusing on the genomic function of xenobiotic receptors, the non-genomic function of xenobiotic receptors is poorly understood. Here we investigated the non-canonical functions of CAR and AhR in the liver glucose metabolism and liver fibrogenesis, respectively.

As described in the Chapter III, we found CAR forms a unique complex with Skp1/CUL1/Rbx1 and induces the ubiquitylation of PGC1 $\alpha$ . This E3 ligase activity is also DNA-binding independent. In vitro and in vivo ubiquitylation analysis suggest CAR is possibly a

substrate adaptor for the ubiquitylation of PGC1 $\alpha$ . However, unlike the canonical F-box proteins which usually only interact with CUL1, CAR interacts with both Skp1 and CUL1. This unique protein-protein interaction is a mimic of another nuclear receptor cryptochrome 2 (CRY2) in mediating the degradation of c-MYC by FBXL3 as described in a recent report [281]. In our study, we have no direct evidence on whether a F-box protein is involved, although a previous study has indicated the F-box protein Cdc4 is a E3 ligase adaptor for the ubiquitylation of PGC1 $\alpha$  [219]. In the Chapter IV, we have examined the role of AhR in the HSC activation and liver fibrogenesis. Although the E3 ligase activity of CUL4B<sup>AhR</sup> is not required for the inhibition of HSC activation, the inhibitory effect is achieved through protein-protein interaction between AhR and Smad3 which may be also independent of its genomic function as a transcriptional factor.

Such non-canonical ubiquitylation function is sporadically seen for other proteins. There are two examples: one is that the subunit of mammalian target of rapamycin (mTOR) complex 2, Rictor, forms a complex with CUL1 to induce the ubiquitylation of SGK1 [206]. Another one is that the G protein  $\beta$  subunit 2 (G $\beta$ 2) of the G protein-coupled receptors (GPCR) induces GRK2 ubiquitylation [282]. Altogether, our results and other studies highlight the unique function of transcriptional factors, protein kinases, or GPCR as a component of the UPS. These non-canonical activity is possibly due to the unique protein structure of the specific protein. Future study to capture the interactome of the E3 ligase with their substrates will unravel more such novel functions.

## 5.2 CAR IN THE REGULATION OF ENERGY METABOLISM

The role of CAR in energy metabolism did not receive much attention until several studies within the past few years demonstrating that CAR activation improves hyperglycemia and dyslipidemia, the hallmark of type 2 diabetes and the cause of diabetic complications. Activation of CAR by the synthetic agonist TCPOBOP increased insulin sensitivity, decreased circulating glucose level, and ameliorated liver steatosis in both diet- and leptin deficiency-induced obesity [181, 182]. Diabetic mice treated with TCPOBOP exhibited better glucose tolerance [181], primarily due to the suppression of hepatic gluconeogenesis rather than glucose disposal in the white adipose tissue and skeletal muscle, evidenced by a hyperinsulinemic-euglycemic clamp study in the *ob/ob* mice. In agreement with lower hepatic glucose production, the two rate-limiting gluconeogenic enzymes *Pepck* and *G6pase* were down-regulated by CAR activation. Several models were proposed to explain the inhibition of gluconeogenesis by CAR. In the first model, CAR competes with *FoxO1* and *HNF4 $\alpha$*  on the insulin responsive sequence (IRS) and DR1 element, respectively, on the promoters of *Pepck* and *G6pase* genes [187]. In the second model, CAR competitively binds to *NCoA2* (also known as *SRC2/GRIP1*) and *PGC1 $\alpha$* , which are two coactivators of *HNF4 $\alpha$* , thus diminishing the expression of gluconeogenic genes [188]. In the third model as proposed in this dissertation study (Chapter III), CAR is a ubiquitin E3 ligase that catalyzes the ubiquitylation of *PGC1 $\alpha$*  and transfers *PGC1 $\alpha$*  into the PML-NBs for proteasomal degradation. This mechanism seems independent of DNA-binding activity.

The LXR-SREBP pathway plays a central role in hepatic lipogenesis by transducing the genes involved in fatty acid biosynthesis and lipid uptake [283]. Crosstalk between CAR and LXR leads to mutual repression through “cofactor competition” [284]. Consequently, the expression of LXR target genes are down-regulated, including lipogenic genes (e.g. *Srebf1* and

Fasn). CAR can also directly bind to SREBP1, which suggests potential crosstalk between CAR and SREBP1 in the context of lipogenesis, although further functional and mechanistic characterization is needed to prove this association [285]. CAR can also influence lipid biosynthesis through downstream target genes. Insulin-induced gene-1 (Insig-1) is an endoplasmic reticulum-bound cholesterol sensor that suppresses the proteolytic activation of SREBPs when sterols are abundant [286]. CAR binds to the DR4 element on the Insig-1 promoter and directly induces the expression of Insig-1, therefore preventing SREBP1 from entering the nucleus to induce lipogenic genes [287].

Unlike Insig-1 that directly targets the activation of SREBP1, sulfotransferase 2B1b (Sult2B1b), another CAR responsive gene, inhibits Srebf1 expression and hepatic lipogenesis through enzymatic deactivation of LXR ligands. Sult2B1b belongs to the subfamily of cytosolic sulfotransferases, mediating the sulfonation of oxysterols such as 22-hydroxycholesterol, 24S-hydroxycholesterol, 25-hydroxycholesterol, 27-hydroxycholesterol, and 24, 25-epoxycholesterol [288]. These endogenous oxysterols are potent ligands for LXR activation. Sulfonation of oxysterols reduces their capacity to activate LXR and down-regulates the LXR-SREBP-mediated lipogenesis [289]. In line with this, TCPOBOP resulted reduction of lipogenic genes is abolished in Sult2B1b knockout mice [181]. Liver-specific overexpression of Sult2B1b, either by adenoviral delivery or transgenic strategy, ameliorates dyslipidemia in the diabetic mouse model [290, 291].

In addition to deactivating LXR ligands, the products of sulfonation (e.g. 25-hydroxycholesterol-3-sulfate) have the capability to decrease lipid accumulation and inflammation [292-295]. Cholesterol sulfates, which are converted from cholesterol by Sult2B1b, have also been reported to be potent agonists for ROR $\alpha$  [296]. Inhibitory crosstalk



between ROR $\alpha$  and LXR could be another reason for the down-regulation of lipid accumulation when Sult2B1b is overexpressed [297]. Our recent study has also demonstrated that the Sult2B1b and its product cholesterol sulfate were able to inhibit gluconeogenesis through deacetylation of HNF4 $\alpha$ , which leads the nuclear exclusion of HNF4 $\alpha$  [291]. Furthermore, the systemic metabolic benefit from CAR activation can be also achieved by the hepatic induction of irisin, a hormone proteolytically processed from fibronectin type III domain-containing protein 5 (FNDC5) and capable of inducing browning of adipose tissue [298].

Insulin resistance is associated with elevated plasma lipoproteins, very-low-density lipoprotein (VLDL) production, and plasma low-density lipoprotein (LDL) [299, 300]. Subsequent atherosclerotic lesions are a serious cause for the cardiovascular complications that arise in patients with type 2 diabetes. CAR activation has been shown to decrease VLDL secretion and plasma cholesterol concentration in apolipoprotein A-I (apoA-I) transgenic mice and Ldlr $^{-/-}$  mice, partially through the down-regulation of apoA-I and up-regulation of Vldlr, respectively [301, 302]. Excessive cholesterol levels in the liver are also eliminated in the form of bile salts into the feces [303]. In this process, the genes responsible for the conversion of cholesterol to bile salts and bile acid hydration, conjugation, and export are up-regulated in response to TCPOBOP in the liver. In the intestine, bile acid excretion is further facilitated by the inhibition of bile acid reabsorption machinery, most likely through the inhibition of LXR. In addition, VLDL secretion and lipid homeostasis are also maintained by HNF4 $\alpha$  [304]. The inhibitory effect of CAR on HNF4 $\alpha$  may explain its benefits on cholesterol metabolism. Overall, CAR activation attenuates the development of atherosclerotic lesions and has a therapeutic potential for prevention of diabetes-associated cardiovascular diseases.

Despite the fact that CAR activation lowers plasma cholesterol levels, the genes involved in de novo cholesterol biosynthesis are up-regulated by CAR activation [305]. Considering that hepatic cholesterol are prone to be metabolized into bile acids, the up-regulation of cholesterol biosynthesis could be a compensatory mechanism to maintain intracellular cholesterol homeostasis [306]. Interestingly, although de novo cholesterol and triglyceride biosynthesis share the same transcriptional factors such as SREBP, cholesterol biosynthesis seems to be selectively elevated. One explanation is that lipogenic genes are also directly regulated by other nuclear transcription factors, such as LXR and carbohydrate-responsive element-binding protein (ChREBP), but whether crosstalk between CAR and those transcription factors are necessary for the inhibitory effect on triglyceride accumulation needs to be further investigated [307, 308]. In addition, preferential de novo cholesterol biosynthesis can be achieved by selective activation of SREBP2 [309]. Whether CAR interplays with SREBP2 to activate cholesterol biosynthesis remains to be determined. Overall, activation of CAR ameliorates glucose and lipid metabolic disorders in the diabetic mouse models and improves diabetes-associated cardiovascular function through direct gene transduction or indirect mechanisms via protein-protein crosstalk. Development of potent and safe agonists of CAR for the treatment of type 2 diabetes is potentially important and clinically beneficial.

### **5.3 AHR IN THE HEPATIC TOXICITY AND HOMEOSTASIS**

AhR is a versatile factor participating in various biological processes, such as immune response, energy metabolism, and tumorigenesis [247]. The phenotypical observations in the AhR<sup>-/-</sup> mice strongly suggested the existence of endogenous ligands of AhR and their essential roles in the

development and homeostatic surveillance [42, 43]. For example, loss of AhR fails the closure of the ductus venosus (DV), suggesting AhR and presumably its endogenous ligands influence the vascular development [45, 310]. This vascular regulatory effect requires nuclear translocation and DNA-binding of AhR, indicating certain genes related to the DV closure are directly regulated by the AhR [271, 311]. A further study using AhR floxed mice has demonstrated the loss of AhR signaling in the endothelial cells is the cause for the portosystemic shunt (PSS) [249]. So far, quite a few physiologically relevant endogenous AhR ligands have been identified [312]. However, the chemical structure and affinity of these ligands are rather diverse. Even more interestingly, the effect of AhR ligands is cell type-specific. For instance, TCDD and ITE versus  $\beta$ -naphthoflavone ( $\beta$ -NF) and 6-formylindolo[3,2-b]carbazole (FICZ) have completely opposite effects in the classical autoimmune disease model, experimental autoimmune encephalomyelitis (EAE) [313, 314]. It is likely that TCDD, ITE, and kynurenine have preferential activity in the regulatory T cells ( $T_{reg}$ ) whereas FICZ is more potent to induce the differentiation of T cells producing interleukin-17 ( $T_H17$ ) [313-315].

More specifically, AhR plays a vital role in the hepatic function and pathogenesis. These functions are generally characterized based on experimental observations either from loss-of-function models (null and conditional knockout mice) or gain-of-function models (pharmacological activation by ligands and constitutive activation by genetic mutations). In theory, we can expect the opposite effect from loss-of-function and gain-of-function models. Intriguingly, sometimes AhR has seemingly a paradoxical role in the same disease model, exemplifying by the liver fibrosis and tumorigenesis in the liver and intestine. It was reported two decades ago that AhR<sup>-/-</sup> mice have mild periportal fibrosis [42, 43]. On the other hand, treatment of TCDD to the mice promotes liver fibrosis [248]. Moreover, constitutive activated

AhR (CA-AhR) and TCDD treatment exacerbate the fibrotic phenotype induced by MCD diet [151]. Similarly, both CA-AhR and AhR<sup>-/-</sup> mice are prone to hepatocarcinogenesis induced by N-Nitrosodiethylamine (DEN) [316, 317]. The reason behind the seemingly paradoxical role of AhR is complex and poorly understood, largely due to the promiscuous effects of AhR ligands, the unknown target cell type by these ligands, and the exact bioavailability of ligands to the AhR in a specific cell type.

In the present dissertation study, we used the same AhR floxed mice to discern the primary cell type that contributes to the spontaneous liver fibrosis observed in the AhR<sup>-/-</sup> mice. It was found that AhR in the HSCs plays a suppressive role in the liver fibrosis and might have contributed to the spontaneous liver fibrosis. Although the identity of the endogenous AhR ligand mediating the inhibitory effect is not known, this study is another example for the essential role of endogenous AhR signaling to maintain the homeostasis of hepatic function. The fact that hepatocyte-specific knockout of AhR did not alter the progress of liver fibrosis, indicating this is HSC-specific regulation. It has also been reported that loss of AhR in the hepatocytes exacerbated HFD-induced liver inflammation, suggesting endogenous AhR signaling in the hepatocytes is also essential for hepatic homeostasis in a context-dependent manner.

There are potentially multiple mechanisms underlying the ligand- and cell type-specific regulation by AhR. Metabolic rates, ligand binding sites, cell-specific proteome, and genetic variances are all profound factors in determining the subtle effects. Particularly, the dramatic difference in the metabolic rate of endogenous and xenobiotic AhR ligands may be an extremely critical determinant for the ligand- and cell type-specific effects. The toxicological effects of the environmental AhR activators have been widely investigated given its significant impact on the

human health. TCDD, the prototypical AhR ligand, has been a good tool to study the molecular mechanism with respect to the toxicity of AhR-activating pollutants. The half-life of TCDD in human serum was estimated to be over seven years [318], which renders the persistent activation of AhR and causes hepatotoxicity that induces fibrotic progression. The AhR-mediated hepatotoxicity of TCDD, characterized by hepatomegaly, hepatic steatosis, and inflammatory cell infiltration, is well established. Oxidative stress [319], NAD<sup>+</sup> depletion [152], and altered lipid metabolism [320] are proposed in the contribution to the liver toxicity. However, these general changes in the liver could be secondary to the toxicity. For instance, the proposed TiPARP-mediated NAD<sup>+</sup> depletion is still seen in the TiPARP<sup>-/-</sup> mice and these mice are even more sensitive to the TCDD-induced hepatic steatosis and overall lethality, indicating loss of NAD<sup>+</sup> is rather a toxicological consequence caused by TCDD intoxication [157].

The metabolic turnover rate of endogenous AhR ligands, on the other hand, is extremely high due to the rapid clearance by CYP1 enzymes, especially in the liver tissue [321]. This could be essentially important to better harness the risk of over-activating AhR by these ligands [322]. However, massive elimination of AhR ligands by the epithelial cells could also impact the physiological homeostasis by reducing the bioavailability of these ligands to the minor populations of cells [323]. In the liver, CYP1B1 expression is elevated in many end-stage liver diseases which are often associated with fibrosis [324]. Whether this up-regulation of CYP1B1 will dampen the bioavailability of endogenous AhR ligands to the HSCs as well as immune cells is worthy of further investigation. In summary, endogenous AhR signaling is the gatekeeper for the normal function of liver, whereas persistent activation of AhR disrupts hepatic homeostasis through mechanism to be further investigated.

## APPENDIX A

**Table 1. Antibody information**

<b>Antigen</b>	<b>Company</b>	<b>Identifier</b>	<b>Application*</b>	<b>Dilution</b>
AhR	Enzo Life Sciences	BML-SA550	WB	1:1000
$\alpha$ -SMA	Sigma	A2547	WB/IF	1:1000/1:500
$\alpha$ -SMA	Abcam	ab32575	IHC	1:500
$\alpha$ -Tubulin	Sigma	T6074	WB	1:10000
$\beta$ -actin	Sigma	A1978	WB	1:10000
$\beta$ -catenin	Cell Signaling	#9587	WB	1:1000
CAR	Santa Cruz	sc-13065	WB	1:500
Col1A1	Sigma	SAB1402151	WB	1:500
Desmin	Thermo Scientific	RB-9014	IHC	1:200
Flag	Sigma	F1804	WB/IP	1:1000/1:300
HA	Cell Signaling	#3724	WB	1:1000
HA	Thermo Scientific	26183	IP	1:300
HNF4 $\alpha$	Cell Signaling	#3113	ChIP	1:200
Ki67	Abcam	ab15580	IF	1:500
MEF2	Proteintech	10056-1-AP	WB	1:1000
Myc	Sigma	M4439	WB/IP	1:1000/1:300
Smad2	Cell Signaling	#5339	WB	1:1000
Smad3	Cell Signaling	#9523	WB	1:1000
Smad3	Santa Cruz	sc-101154	IP	1:100
Smad4	Cell Signaling	#9515	WB	1:1000
Sp1	Santa Cruz	sc-59	WB	1:500
SRF	Proteintech	16821-1-AP	WB	1:1000
p-Smad2	Cell Signaling	#3108	WB	1:1000
p-Smad3	Cell Signaling	#9520	WB/ChIP	1:1000/1:200
PGC-1	Santa Cruz	sc-13067	WB	1:500
PML	Millipore	05-718	WB	1:1000

\*: WB, Western blot; IF, Immunofluorescence; IP, Immunoprecipitation; IHC, Immunohistochemistry; ChIP, Chromatin immunoprecipitation.

## APPENDIX B

**Table 2. Real-time PCR primers sequences**

<b>Gene</b>	<b>Forward sequence (5' - 3')</b>	<b>Reverse sequence (5' - 3')</b>
Acta2	TGAAGATCCTGACTGAGCGT	TGATGTCACGGACAATCTCA
Ahr	ACGCACCAAAAGCAACACTA	GAGGGCACTCATAAGAGAAC
Arnt	TTTGCACAGGACAGAGATCC	GCTGGAGGAGATGCCTTTAC
Bambi	GCTCACCAAAAGGAGAGATCAG	TCGAGAAGTCTGGAGAAGCA
Ccnd1	TGAGAACAAGCAGACCATCC	TGAACTTCACATCTGTGGCA
Col1a1	ACTGCAACATGGAGACAGGTCAGA	ATCGGTCATGCTCTCTCCAAACCA
Col1a2	GAGGACTTGTTGGTGAGCCT	CTCACCTTGTTACCGGATT
Col3a1	CTGTAAACATGGAACTGGGGAA	CCATAGCTGAACTGAAAACCACC
Cyp1a1	GTTAACCATGACCGGGAAGT	GTGACCTTCTCACTCAAGCG
Cyp1b1	GAATCATGACCCAGCCAAGT	TAATGAAGCCGTCCTTGTC
Cyclophilin	TGGAGAGCACCAAGACAGACA	GCCCGTAGTGCTTCAGCTT
Fn1	GATGTCCGAACAGCTATTTACCA	CCTTGCGACTTCAGCCACT
G6pase	CTGTGAGACCGGACCAGGA	GACCATAACATAGTATACACCTGCTGC
Lox	CACAGAGGAGAGTGGCTGAA	AATCCCTGTGTGTGTGCAGT
Loxl1	CAGCGTGGGTAGTGTGTACC	TACAGATGGGCTCTCTGCAC
Pai1	CCGACAGAGACAATCCTCTTC	AGTTTCGTCCCAAATGAAGG
Pepck	GGCCACAGCTGCTGCAG	GGTCGCATGGCAAAGGG
Pgc1a	GACTCAGTGTACCACCGAAA	TGAACGAGAGCGCATCCT
Ranbp3	GAGCATGCCTTAGACCCTTC	AGATCTCCCTGCCAGTTCTC
Ski	ACTCAGCCCAGATTGAGGAC	CCTCACCACCTTCTCCAGAT
Skil	GCAGAAATGCACCTGTGACT	ATCTTGAGTTCTCTGCCTGT
Smurf1	TGGAGAACGAAGGAACAGTG	CTGCTGCACCAGTACCATCT
Smurf2	GCAACGTGTGGACATTCTTC	CCTTTGTTTCATAGCCTTCCG
Tgif	AGAGCTGAGGGATGGAGATG	AAGACCTTCCAGCTCCACAA
Timp1	GGTGTGCACAGTGTTTCCCTGTTT	TCCGTCCACAAACAGTGAGTGTC
Xpo1	TGGTTACAAAGCAACCATTGA	TCAGCTACCATCTGAGGATCA
Xpo4	CAAAGTTCTGATGGCACCAC	TGCAAATGGTGATTTGGACT
ACTA2	AAGAGGAATCCTGACCCTGAA	TGGTGATGATGCCATGTTCT
AHR	TAGTGGAGCCACAGCAACAG	TGCTGTGGACAATTGAAAGG
ARNT	GCAAACAGAATTGGACATGG	TGTTCTGGTCCTGTGGTTGT
CCND1	TGGTGAACAAGCTCAAGTGG	CTGGCATTCTTGAGAGGAAG
COL1A1	CGGTGTGACTCGTGCAGC	ACAGCCGCTTCACCTACAGC
COL1A2	TCAAACCTGGCTGCCAGCAT	CAAGAAACACGTCTGGCTAGG
COL3A1	CCCAGGGAAAGATGGCCCAA	CTCACCAGGGCTACCACGAG
CYP1A1	GCTCAGTACCTCAGCCACCT	CAGAGGCCAGAAGAACTCC
CYP1B1	ATGAACCAATCTGGATGCCT	GCAAGCATCTGATGACGACT

CYCLOPHILIN	TGGTGTTTGGCAAAGTGAAA	TCGAGTTGTCCACAGTCAGC
FN1	GCACCTGATGGTGAAGAAGA	GGAATAGCTGTGGACTGGGT
PAI1	CTGGTTCTGCCCAAGTTCTC	CTCGTGAAGTCAGCCTGAAA

---



## BIBLIOGRAPHY

1. Mackowiak, B. and H. Wang, *Mechanisms of xenobiotic receptor activation: Direct vs. indirect*. Biochimica et Biophysica Acta (BBA)-Gene Regulatory Mechanisms, 2016. **1859**(9): p. 1130-1140.
2. Tunkel, A.R., *Host Defense Mechanisms Against Infection*. The Merck Manual Online. 2016.
3. Delves, P.J., *Complement System*. The Merck Manual Online. 2017.
4. Takeuchi, O. and S. Akira, *Pattern recognition receptors and inflammation*. Cell, 2010. **140**(6): p. 805-820.
5. Zevini, A., D. O'laghner, and J. Hiscott, *Crosstalk between cytoplasmic RIG-I and STING sensing pathways*. Trends in immunology, 2017.
6. Rathinam, V.A. and K.A. Fitzgerald, *Inflammasome complexes: emerging mechanisms and effector functions*. Cell, 2016. **165**(4): p. 792-800.
7. Yang, J., Y. Zhao, and F. Shao, *Non-canonical activation of inflammatory caspases by cytosolic LPS in innate immunity*. Current opinion in immunology, 2015. **32**: p. 78-83.
8. Tolson, A.H. and H. Wang, *Regulation of drug-metabolizing enzymes by xenobiotic receptors: PXR and CAR*. Advanced drug delivery reviews, 2010. **62**(13): p. 1238-1249.
9. Chang, T.K. and D.J. Waxman, *Synthetic drugs and natural products as modulators of constitutive androstane receptor (CAR) and pregnane X receptor (PXR)*. Drug metabolism reviews, 2006. **38**(1-2): p. 51-73.
10. Chang, T.K., *Activation of pregnane X receptor (PXR) and constitutive androstane receptor (CAR) by herbal medicines*. The AAPS journal, 2009. **11**(3): p. 590.
11. Bersten, D.C., et al., *bHLH-PAS proteins in cancer*. Nature Reviews Cancer, 2013. **13**(12): p. 827-841.
12. Jackson, D., A. Joshi, and C. Elferink, *Ah receptor pathway intricacies; signaling through diverse protein partners and DNA-motifs*. Toxicology research, 2015. **4**(5): p. 1143-1158.
13. Kliewer, S.A., et al., *An orphan nuclear receptor activated by pregnanes defines a novel steroid signaling pathway*. Cell, 1998. **92**(1): p. 73-82.
14. Blumberg, B., et al., *SXR, a novel steroid and xenobioticsensing nuclear receptor*. Genes & development, 1998. **12**(20): p. 3195-3205.
15. Blumberg, B., et al., *BXR, an embryonic orphan nuclear receptor activated by a novel class of endogenous benzoate metabolites*. Genes & development, 1998. **12**(9): p. 1269-1277.
16. Barwick, J.L., et al., *Trans-species gene transfer for analysis of glucocorticoid-inducible transcriptional activation of transiently expressed human CYP3A4 and rabbit CYP3A6 in*

- primary cultures of adult rat and rabbit hepatocytes*. Molecular pharmacology, 1996. **50**(1): p. 10-16.
17. Quattrochi, L.C., et al., *A novel cis-acting element in a liver cytochrome P450 3A gene confers synergistic induction by glucocorticoids plus antiglyucocorticoids*. Journal of Biological Chemistry, 1995. **270**(48): p. 28917-28923.
  18. Xie, W., et al., *Humanized xenobiotic response in mice expressing nuclear receptor SXR*. Nature, 2000. **406**(6794): p. 435-438.
  19. Staudinger, J.L., et al., *The nuclear receptor PXR is a lithocholic acid sensor that protects against liver toxicity*. Proceedings of the National Academy of Sciences, 2001. **98**(6): p. 3369-3374.
  20. Watkins, R.E., et al., *The human nuclear xenobiotic receptor PXR: structural determinants of directed promiscuity*. Science, 2001. **292**(5525): p. 2329-2333.
  21. Baes, M., et al., *A new orphan member of the nuclear hormone receptor superfamily that interacts with a subset of retinoic acid response elements*. Molecular and cellular biology, 1994. **14**(3): p. 1544-1552.
  22. Choi, H.-S., et al., *Differential transactivation by two isoforms of the orphan nuclear hormone receptor CAR*. Journal of Biological Chemistry, 1997. **272**(38): p. 23565-23571.
  23. Forman, B.M., et al., *Androstane metabolites bind to and deactivate the nuclear receptor CAR- $\beta$* . Nature, 1998. **395**(6702): p. 612-615.
  24. Shan, L., et al., *Structure of the murine constitutive androstane receptor complexed to androstenol: a molecular basis for inverse agonism*. Molecular cell, 2004. **16**(6): p. 907-917.
  25. Suino, K., et al., *The nuclear xenobiotic receptor CAR: structural determinants of constitutive activation and heterodimerization*. Molecular cell, 2004. **16**(6): p. 893-905.
  26. Xu, R.X., et al., *A structural basis for constitutive activity in the human CAR/RXR $\alpha$  heterodimer*. Molecular cell, 2004. **16**(6): p. 919-928.
  27. Honkakoski, P. and M. Negishi, *Characterization of a phenobarbital-responsive enhancer module in mouse P450 Cyp2b10 gene*. Journal of Biological Chemistry, 1997. **272**(23): p. 14943-14949.
  28. Trottier, E., et al., *Localization of a phenobarbital-responsive element (PBRE) in the 5'-flanking region of the rat CYP2B2 gene*. Gene, 1995. **158**(2): p. 263-268.
  29. Park, Y., H. Li, and B. Kemper, *Phenobarbital induction mediated by a distal CYP2B2 sequence in rat liver transiently transfected in situ*. Journal of Biological Chemistry, 1996. **271**(39): p. 23725-23728.
  30. Honkakoski, P., et al., *The nuclear orphan receptor CAR-retinoid X receptor heterodimer activates the phenobarbital-responsive enhancer module of the CYP2B gene*. Molecular and Cellular Biology, 1998. **18**(10): p. 5652-5658.
  31. Wei, P., et al., *The nuclear receptor CAR mediates specific xenobiotic induction of drug metabolism*. Nature, 2000. **407**(6806): p. 920-923.
  32. Poland, A. and J.C. Knutson, *2, 3, 7, 8-Tetrachlorodibenzo-p-dioxin and related halogenated aromatic hydrocarbons: examination of the mechanism of toxicity*. Annual review of pharmacology and toxicology, 1982. **22**(1): p. 517-554.
  33. Sogawa, K., et al., *Location of regulatory elements responsible for drug induction in the rat cytochrome P-450c gene*. Proceedings of the National Academy of Sciences, 1986. **83**(21): p. 8044-8048.

34. Fujisawa-Sehara, A., et al., *Regulatory DNA elements localized remotely upstream from the drug-metabolizing cytochrome P-450c gene*. Nucleic acids research, 1986. **14**(3): p. 1465-1477.
35. Fujisawa-Sehara, A., et al., *Characterization of xenobiotic responsive elements upstream from the drug-metabolizing cytochrome P-450c gene: a similarity to glucocorticoid regulatory elements*. Nucleic acids research, 1987. **15**(10): p. 4179-4191.
36. Hoffman, E.C., et al., *Cloning of a factor required for activity of the Ah (dioxin) receptor*. Science, 1991. **252**(5008): p. 954-959.
37. Burbach, K.M., A. Poland, and C.A. Bradfield, *Cloning of the Ah-receptor cDNA reveals a distinctive ligand-activated transcription factor*. Proceedings of the National Academy of Sciences, 1992. **89**(17): p. 8185-8189.
38. Ema, M., et al., *cDNA cloning and structure of mouse putative Ah receptor*. Biochemical and biophysical research communications, 1992. **184**(1): p. 246-253.
39. Dolwick, K.M., et al., *Cloning and expression of a human Ah receptor cDNA*. Molecular pharmacology, 1993. **44**(5): p. 911-917.
40. Schulte, K.W., et al., *Structural basis for aryl hydrocarbon receptor-mediated gene activation*. Structure, 2017.
41. Seok, S.-H., et al., *Structural hierarchy controlling dimerization and target DNA recognition in the AHR transcriptional complex*. Proceedings of the National Academy of Sciences, 2017. **114**(21): p. 5431-5436.
42. Fernandez-Salguero, P., et al., *Immune system impairment and hepatic fibrosis in mice lacking the dioxin-binding Ah receptor*. Science, 1995. **268**(5211): p. 722-726.
43. Schmidt, J.V., et al., *Characterization of a murine Ahr null allele: involvement of the Ah receptor in hepatic growth and development*. Proceedings of the National Academy of Sciences, 1996. **93**(13): p. 6731-6736.
44. Mimura, J., et al., *Loss of teratogenic response to 2, 3, 7, 8-tetrachlorodibenzo-p-dioxin (TCDD) in mice lacking the Ah (dioxin) receptor*. Genes to cells, 1997. **2**(10): p. 645-654.
45. Lahvis, G.P., et al., *Portosystemic shunting and persistent fetal vascular structures in aryl hydrocarbon receptor-deficient mice*. Proceedings of the National Academy of Sciences, 2000. **97**(19): p. 10442-10447.
46. Butler, R., et al., *Uric acid stones in the urinary bladder of aryl hydrocarbon receptor (AhR) knockout mice*. Proceedings of the National Academy of Sciences, 2012. **109**(4): p. 1122-1126.
47. Huang, B., et al., *Dysregulation of Notch and ER $\alpha$  signaling in AhR $-/-$  male mice*. Proceedings of the National Academy of Sciences, 2016: p. 201613269.
48. Villa, M., et al., *The aryl hydrocarbon receptor controls cyclin O to promote epithelial multiciliogenesis*. Nature communications, 2016. **7**.
49. Baba, T., et al., *Intrinsic function of the aryl hydrocarbon (dioxin) receptor as a key factor in female reproduction*. Molecular and cellular biology, 2005. **25**(22): p. 10040-10051.
50. Xie, W., et al., *Reciprocal activation of xenobiotic response genes by nuclear receptors SXR/PXR and CAR*. Genes & Development, 2000. **14**(23): p. 3014-3023.
51. Xie, W. and R.M. Evans, *Orphan nuclear receptors: the exotics of xenobiotics*. Journal of Biological Chemistry, 2001. **276**(41): p. 37739-37742.
52. Guengerich, F.P., *Cytochrome P-450 3A4: regulation and role in drug metabolism*. Annual review of pharmacology and toxicology, 1999. **39**(1): p. 1-17.

53. Garte, S., *The role of ethnicity in cancer susceptibility gene polymorphisms: the example of CYP1A1*. Carcinogenesis, 1998. **19**(8): p. 1329-1332.
54. Miller, D.S., *Regulation of P-glycoprotein and other ABC drug transporters at the blood–brain barrier*. Trends in pharmacological sciences, 2010. **31**(6): p. 246-254.
55. Lo, R., et al., *Identification of aryl hydrocarbon receptor binding targets in mouse hepatic tissue treated with 2, 3, 7, 8-tetrachlorodibenzo-p-dioxin*. Toxicology and applied pharmacology, 2011. **257**(1): p. 38-47.
56. Nault, R., K.A. Fader, and T. Zacharewski, *RNA-Seq versus oligonucleotide array assessment of dose-dependent TCDD-elicited hepatic gene expression in mice*. BMC genomics, 2015. **16**(1): p. 373.
57. Cui, J.Y. and C.D. Klaassen, *RNA-Seq reveals common and unique PXR-and CAR-target gene signatures in the mouse liver transcriptome*. Biochimica et Biophysica Acta (BBA)-Gene Regulatory Mechanisms, 2016. **1859**(9): p. 1198-1217.
58. Cui, J.Y., et al., *ChIPing the cistrome of PXR in mouse liver*. Nucleic acids research, 2010. **38**(22): p. 7943-7963.
59. Smith, R.P., et al., *Genome-wide discovery of drug-dependent human liver regulatory elements*. PLoS genetics, 2014. **10**(10): p. e1004648.
60. Locker, J., et al., *A common set of immediate-early response genes in liver regeneration and hyperplasia*. Hepatology, 2003. **38**(2): p. 314-325.
61. Kawamoto, T., et al., *Phenobarbital-responsive nuclear translocation of the receptor CAR in induction of the CYP2B gene*. Molecular and Cellular Biology, 1999. **19**(9): p. 6318-6322.
62. Pratt, W.B. and D.O. Toft, *Steroid receptor interactions with heat shock protein and immunophilin chaperones*. Endocrine reviews, 1997. **18**(3): p. 306-360.
63. Yoshinari, K., et al., *Identification of the nuclear receptor CAR: HSP90 complex in mouse liver and recruitment of protein phosphatase 2A in response to phenobarbital*. FEBS letters, 2003. **548**(1): p. 17-20.
64. Squires, E.J., T. Sueyoshi, and M. Negishi, *Cytoplasmic localization of pregnane X receptor and ligand-dependent nuclear translocation in mouse liver*. Journal of Biological Chemistry, 2004. **279**(47): p. 49307-49314.
65. Chen, H.-S. and G.H. Perdew, *Subunit composition of the heteromeric cytosolic aryl hydrocarbon receptor complex*. Journal of Biological Chemistry, 1994. **269**(44): p. 27554-27558.
66. Kobayashi, K., et al., *Cytoplasmic accumulation of the nuclear receptor CAR by a tetratricopeptide repeat protein in HepG2 cells*. Molecular pharmacology, 2003. **64**(5): p. 1069-1075.
67. Carver, L.A. and C.A. Bradfield, *Ligand-dependent interaction of the aryl hydrocarbon receptor with a novel immunophilin homolog in vivo*. Journal of Biological Chemistry, 1997. **272**(17): p. 11452-11456.
68. Ma, Q. and J.P. Whitlock, *A novel cytoplasmic protein that interacts with the Ah receptor, contains tetratricopeptide repeat motifs, and augments the transcriptional response to 2, 3, 7, 8-tetrachlorodibenzo-p-dioxin*. Journal of Biological Chemistry, 1997. **272**(14): p. 8878-8884.
69. Meyer, B.K., et al., *Hepatitis B virus X-associated protein 2 is a subunit of the unliganded aryl hydrocarbon receptor core complex and exhibits transcriptional enhancer activity*. Molecular and cellular biology, 1998. **18**(2): p. 978-988.

70. Kanno, Y., et al., *Dependence on the microtubule network and 90-kDa heat shock protein of phenobarbital-induced nuclear translocation of the rat constitutive androstane receptor*. Molecular pharmacology, 2010. **77**(2): p. 311-316.
71. Ohno, M., et al., *The roles of co-chaperone CCRP/DNAJC7 in Cyp2b10 gene activation and steatosis development in mouse livers*. PloS one, 2014. **9**(12): p. e115663.
72. Nukaya, M., et al., *The aryl hydrocarbon receptor-interacting protein (AIP) is required for dioxin-induced hepatotoxicity but not for the induction of the Cyp1a1 and Cyp1a2 genes*. Journal of Biological Chemistry, 2010. **285**(46): p. 35599-35605.
73. Timsit, Y.E. and M. Negishi, *Coordinated Regulation of Nuclear Receptor CAR by CCRP/DNAJC7, HSP70 and the Ubiquitin-Proteasome System*. PloS one, 2014. **9**(5): p. e96092.
74. Sidhu, J.S. and C.J. Omiecinski, *An okadaic acid-sensitive pathway involved in the phenobarbital-mediated induction of CYP2B gene expression in primary rat hepatocyte cultures*. Journal of Pharmacology and Experimental Therapeutics, 1997. **282**(2): p. 1122-1129.
75. Negishi, M., *Phenobarbital meets phosphorylation of nuclear receptors*. Drug Metabolism and Disposition, 2017. **45**(5): p. 532-539.
76. Osabe, M. and M. Negishi, *Active ERK1/2 protein interacts with the phosphorylated nuclear constitutive active/androstane receptor (CAR; NR1I3), repressing dephosphorylation and sequestering CAR in the cytoplasm*. Journal of Biological Chemistry, 2011. **286**(41): p. 35763-35769.
77. Koike, C., R. Moore, and M. Negishi, *Extracellular signal-regulated kinase is an endogenous signal retaining the nuclear constitutive active/androstane receptor (CAR) in the cytoplasm of mouse primary hepatocytes*. Molecular pharmacology, 2007. **71**(5): p. 1217-1221.
78. Zelko, I., et al., *The peptide near the C terminus regulates receptor CAR nuclear translocation induced by xenochemicals in mouse liver*. Molecular and cellular biology, 2001. **21**(8): p. 2838-2846.
79. Mutoh, S., et al., *Phenobarbital Indirectly Activates the Constitutive Active Androstane Receptor (CAR) by Inhibition of Epidermal Growth Factor Receptor Signaling*. Science signaling, 2013. **6**(274): p. ra31.
80. Shizu, R., et al., *Phosphorylated nuclear receptor CAR forms a homodimer to repress its constitutive activity for ligand activation*. Molecular and Cellular Biology, 2017. **37**(10): p. e00649-16.
81. Saito, K., R. Moore, and M. Negishi, *p38 Mitogen-Activated Protein Kinase Regulates Nuclear Receptor CAR that Activates the CYP2B6 Gene*. Drug Metabolism and Disposition, 2013. **41**(6): p. 1170-1173.
82. Hori, T., R. Moore, and M. Negishi, *p38 MAP kinase links CAR activation and inactivation in the nucleus via phosphorylation at threonine 38*. Drug Metabolism and Disposition, 2016. **44**(6): p. 871-876.
83. Hosseinpour, F., et al., *Serine 202 regulates the nuclear translocation of constitutive active/androstane receptor*. Molecular pharmacology, 2006. **69**(4): p. 1095-1102.
84. Sueyoshi, T., et al., *PPP1R16A, the membrane subunit of protein phosphatase 1 $\beta$ , signals nuclear translocation of the nuclear receptor constitutive active/androstane receptor*. Molecular Pharmacology, 2008. **73**(4): p. 1113-1121.

85. Rencurel, F., et al., *AMP-activated protein kinase mediates phenobarbital induction of CYP2B gene expression in hepatocytes and a newly derived human hepatoma cell line*. Journal of Biological Chemistry, 2005. **280**(6): p. 4367-4373.
86. Rencurel, F., et al., *Stimulation of AMP-activated protein kinase is essential for the induction of drug metabolizing enzymes by phenobarbital in human and mouse liver*. Molecular pharmacology, 2006. **70**(6): p. 1925-1934.
87. Shindo, S., S. Numazawa, and T. Yoshida, *A physiological role of AMP-activated protein kinase in phenobarbital-mediated constitutive androstane receptor activation and CYP2B induction*. Biochem. J, 2007. **401**: p. 735-741.
88. Blättler, S.M., et al., *In the regulation of cytochrome P450 genes, phenobarbital targets LKB1 for necessary activation of AMP-activated protein kinase*. Proceedings of the National Academy of Sciences, 2007. **104**(3): p. 1045-1050.
89. Shizu, R., et al., *MicroRNA-122 down-regulation is involved in phenobarbital-mediated activation of the constitutive androstane receptor*. PloS one, 2012. **7**(7): p. e41291.
90. Hung, C.-M., et al., *Demethoxycurcumin modulates prostate cancer cell proliferation via AMPK-induced down-regulation of HSP70 and EGFR*. Journal of agricultural and food chemistry, 2012. **60**(34): p. 8427-8434.
91. Jung, J.H., et al., *Quercetin suppresses HeLa cell viability via AMPK-induced HSP70 and EGFR down-regulation*. Journal of cellular physiology, 2010. **223**(2): p. 408-414.
92. Kim, K.-y., et al., *Adiponectin-activated AMPK stimulates dephosphorylation of AKT through protein phosphatase 2A activation*. Cancer research, 2009. **69**(9): p. 4018-4026.
93. Ding, X. and J.L. Staudinger, *Repression of PXR-mediated induction of hepatic CYP3A gene expression by protein kinase C*. Biochemical pharmacology, 2005. **69**(5): p. 867-873.
94. Smutny, T., et al., *U0126, a mitogen-activated protein kinase kinase 1 and 2 (MEK1 and 2) inhibitor, selectively up-regulates main isoforms of CYP3A subfamily via a pregnane X receptor (PXR) in HepG2 cells*. Archives of toxicology, 2014. **88**(12): p. 2243-2259.
95. Sugatani, J., et al., *Threonine-290 regulates nuclear translocation of the human pregnane X receptor through its phosphorylation/dephosphorylation by Ca<sup>2+</sup>/calmodulin-dependent protein kinase II and protein phosphatase 1*. Drug Metabolism and Disposition, 2014. **42**(10): p. 1708-1718.
96. Whitelaw, M.L., et al., *Heat shock protein hsp90 regulates dioxin receptor function in vivo*. Proceedings of the National Academy of Sciences, 1995. **92**(10): p. 4437-4441.
97. Morales, J.L. and G.H. Perdew, *Carboxyl terminus of hsc70-interacting protein (CHIP) can remodel mature aryl hydrocarbon receptor (AhR) complexes and mediate ubiquitination of both the AhR and the 90 kDa heat-shock protein (hsp90) in vitro*. Biochemistry, 2007. **46**(2): p. 610-621.
98. Kazlauskas, A., L. Poellinger, and I. Pongratz, *Evidence that the co-chaperone p23 regulates ligand responsiveness of the dioxin (Aryl hydrocarbon) receptor*. Journal of Biological Chemistry, 1999. **274**(19): p. 13519-13524.
99. Nguyen, P.M., et al., *p23 co-chaperone protects the aryl hydrocarbon receptor from degradation in mouse and human cell lines*. Biochemical pharmacology, 2012. **84**(6): p. 838-850.
100. de Oliveira, S.K., et al., *Phosphodiesterase 2A forms a complex with the co-chaperone XAP2 and regulates nuclear translocation of the aryl hydrocarbon receptor*. Journal of Biological Chemistry, 2007. **282**(18): p. 13656-13663.

101. Enan, E. and F. Matsumura, *Identification of c-Src as the integral component of the cytosolic Ah receptor complex, transducing the signal of 2, 3, 7, 8-tetrachlorodibenzo-p-dioxin (TCDD) through the protein phosphorylation pathway*. Biochemical pharmacology, 1996. **52**(10): p. 1599-1612.
102. Patel, R.D., et al., *Aryl-hydrocarbon receptor activation regulates constitutive androstane receptor levels in murine and human liver*. Hepatology, 2007. **46**(1): p. 209-218.
103. Jung, D., D.J. Mangelsdorf, and U.A. Meyer, *Pregnane X receptor is a target of farnesoid X receptor*. Journal of Biological Chemistry, 2006. **281**(28): p. 19081-19091.
104. Pascussi, J.-M., et al., *Dexamethasone enhances constitutive androstane receptor expression in human hepatocytes: consequences on cytochrome P450 gene regulation*. Molecular Pharmacology, 2000. **58**(6): p. 1441-1450.
105. Pascussi, J.-M., et al., *Dexamethasone induces pregnane X receptor and retinoid X receptor- $\alpha$  expression in human hepatocytes: synergistic increase of CYP3A4 induction by pregnane X receptor activators*. Molecular Pharmacology, 2000. **58**(2): p. 361-372.
106. Pascussi, J.M., et al., *Dual effect of dexamethasone on CYP3A4 gene expression in human hepatocytes*. The FEBS Journal, 2001. **268**(24): p. 6346-6358.
107. Pascussi, J.M., et al., *Transcriptional analysis of the orphan nuclear receptor constitutive androstane receptor (NR1I3) gene promoter: identification of a distal glucocorticoid response element*. Molecular Endocrinology, 2003. **17**(1): p. 42-55.
108. Pascussi, J.-M., et al., *Interleukin-6 negatively regulates the expression of pregnane X receptor and constitutively activated receptor in primary human hepatocytes*. Biochemical and biophysical research communications, 2000. **274**(3): p. 707-713.
109. Assenat, E., et al., *Interleukin 1 $\beta$  inhibits CAR-induced expression of hepatic genes involved in drug and bilirubin clearance*. Hepatology, 2004. **40**(4): p. 951-960.
110. Bielefeld, K.A., C. Lee, and D.S. Riddick, *Regulation of aryl hydrocarbon receptor expression and function by glucocorticoids in mouse hepatoma cells*. Drug Metabolism and Disposition, 2008. **36**(3): p. 543-551.
111. Ooe, H., et al., *Thyroid hormone is necessary for expression of constitutive androstane receptor in rat hepatocytes*. Drug Metabolism and Disposition, 2009. **37**(9): p. 1963-1969.
112. Qatanani, M., J. Zhang, and D.D. Moore, *Role of the constitutive androstane receptor in xenobiotic-induced thyroid hormone metabolism*. Endocrinology, 2005. **146**(3): p. 995-1002.
113. Saito, K., et al., *Constitutive androstane/active receptor is a target of retinoic acid receptor in humans*. Biochemical pharmacology, 2010. **80**(1): p. 129-135.
114. Wang, T., et al., *Role of pregnane X receptor in control of all-trans retinoic acid (ATRA) metabolism and its potential contribution to ATRA resistance*. Journal of Pharmacology and Experimental Therapeutics, 2008. **324**(2): p. 674-684.
115. Wieneke, N., et al., *PPAR $\alpha$ -dependent induction of the energy homeostasis-regulating nuclear receptor NR1i3 (CAR) in rat hepatocytes: potential role in starvation adaptation*. FEBS letters, 2007. **581**(29): p. 5617-5626.
116. Ding, X., et al., *Regulation of constitutive androstane receptor and its target genes by fasting, cAMP, hepatocyte nuclear factor  $\alpha$ , and the coactivator peroxisome proliferator-activated receptor  $\gamma$  coactivator-1 $\alpha$* . Journal of biological chemistry, 2006. **281**(36): p. 26540-26551.

117. Buler, M., et al., *Energy sensing factors PGC-1 $\alpha$  and SIRT1 modulate PXR expression and function*. Biochemical pharmacology, 2011. **82**(12): p. 2008-2015.
118. FitzGerald, C.T., et al., *Differential regulation of mouse Ah receptor gene expression in cell lines of different tissue origins*. Archives of biochemistry and biophysics, 1996. **333**(1): p. 170-178.
119. Garrison, P.M., et al., *Effects of histone deacetylase inhibitors on the Ah receptor gene promoter*. Archives of biochemistry and biophysics, 2000. **374**(2): p. 161-171.
120. Mulero-Navarro, S., et al., *The dioxin receptor is silenced by promoter hypermethylation in human acute lymphoblastic leukemia through inhibition of Sp1 binding*. Carcinogenesis, 2006. **27**(5): p. 1099-1104.
121. Takahashi, Y., et al., *Characterization of Ah receptor promoter in human liver cell line, HepG2*. Pharmacogenetics and Genomics, 1994. **4**(4): p. 219-222.
122. Englert, N.A., et al., *Genetic and epigenetic regulation of AHR gene expression in MCF-7 breast cancer cells: role of the proximal promoter GC-rich region*. Biochemical pharmacology, 2012. **84**(5): p. 722-735.
123. Wolff, S., et al., *Cell-specific regulation of human aryl hydrocarbon receptor expression by transforming growth factor- $\beta$ 1*. Molecular pharmacology, 2001. **59**(4): p. 716-724.
124. Deer, E.L., et al., *Phenotype and genotype of pancreatic cancer cell lines*. Pancreas, 2010. **39**(4): p. 425.
125. Koliopanos, A., et al., *Increased arylhydrocarbon receptor expression offers a potential therapeutic target for pancreatic cancer*. Oncogene, 2002. **21**(39): p. 6059.
126. Jin, U.-H., S.-B. Kim, and S. Safe, *Omeprazole inhibits pancreatic cancer cell invasion through a nongenomic aryl hydrocarbon receptor pathway*. Chemical research in toxicology, 2015. **28**(5): p. 907-918.
127. Kimura, A., et al., *Aryl hydrocarbon receptor regulates Stat1 activation and participates in the development of Th17 cells*. Proceedings of the National Academy of Sciences, 2008. **105**(28): p. 9721-9726.
128. Vogel, C.F., et al., *Cross-talk between Aryl hydrocarbon receptor and the inflammatory response a role for nuclear factor- $\kappa$ B*. Journal of Biological Chemistry, 2014. **289**(3): p. 1866-1875.
129. Takwi, A., et al., *miR-137 regulates the constitutive androstane receptor and modulates doxorubicin sensitivity in parental and doxorubicin-resistant neuroblastoma cells*. Oncogene, 2013.
130. Takagi, S., et al., *Post-transcriptional regulation of human pregnane X receptor by micro-RNA affects the expression of cytochrome P450 3A4*. Journal of biological chemistry, 2008. **283**(15): p. 9674-9680.
131. Huang, T.-C., et al., *Silencing of miR-124 induces neuroblastoma SK-N-SH cell differentiation, cell cycle arrest and apoptosis through promoting AHR*. FEBS letters, 2011. **585**(22): p. 3582-3586.
132. Rentas, S., et al., *Musashi-2 attenuates AHR signalling to expand human haematopoietic stem cells*. Nature, 2016. **532**(7600): p. 508-511.
133. Boitano, A.E., et al., *Aryl hydrocarbon receptor antagonists promote the expansion of human hematopoietic stem cells*. Science, 2010. **329**(5997): p. 1345-1348.
134. Zhang, Y.-K.J., R.L. Yeager, and C.D. Klaassen, *Circadian expression profiles of drug-processing genes and transcription factors in mouse liver*. Drug Metabolism and Disposition, 2009. **37**(1): p. 106-115.



135. Yang, X., et al., *Nuclear receptor expression links the circadian clock to metabolism*. Cell, 2006. **126**(4): p. 801-810.
136. Carrier, F., et al., *Dioxin-dependent activation of murine Cyp1a-1 gene transcription requires protein kinase C-dependent phosphorylation*. Molecular and Cellular Biology, 1992. **12**(4): p. 1856-1863.
137. Berghard, A., et al., *Cross-coupling of signal transduction pathways: the dioxin receptor mediates induction of cytochrome P-450IA1 expression via a protein kinase C-dependent mechanism*. Molecular and Cellular Biology, 1993. **13**(1): p. 677-689.
138. Chen, Y.-H. and R.H. Tukey, *Protein kinase C modulates regulation of the CYP1A1 gene by the aryl hydrocarbon receptor*. Journal of Biological Chemistry, 1996. **271**(42): p. 26261-26266.
139. Long, W.P., et al., *Protein kinase C activity is required for aryl hydrocarbon receptor pathway-mediated signal transduction*. Molecular pharmacology, 1998. **53**(4): p. 691-700.
140. Pondugula, S.R., et al., *A phosphomimetic mutation at threonine-57 abolishes transactivation activity and alters nuclear localization pattern of human pregnane x receptor*. Drug Metabolism and Disposition, 2009. **37**(4): p. 719-730.
141. Lin, W., et al., *Cyclin-dependent kinase 2 negatively regulates human pregnane X receptor-mediated CYP3A4 gene expression in HepG2 liver carcinoma cells*. Journal of Biological Chemistry, 2008. **283**(45): p. 30650-30657.
142. Pondugula, S.R., et al., *PPM1A Phosphatase is Involved in Regulating PXR-Mediated CYP3A4 Gene Expression*. Drug Metabolism and Disposition, 2015: p. dmd. 114.062083.
143. Pondugula, S.R., et al., *Protein phosphatase 2C $\beta$ l regulates human pregnane X receptor-mediated CYP3A4 gene expression in HepG2 liver carcinoma cells*. Drug Metabolism and Disposition, 2010. **38**(9): p. 1411-1416.
144. Elias, A., et al., *Identification and characterization of phosphorylation sites within the pregnane X receptor protein*. Biochemical pharmacology, 2014. **87**(2): p. 360-370.
145. Lichti-Kaiser, K., C. Xu, and J.L. Staudinger, *Cyclic AMP-dependent protein kinase signaling modulates pregnane x receptor activity in a species-specific manner*. Journal of Biological Chemistry, 2009. **284**(11): p. 6639-6649.
146. Sidhu, J.S. and C.J. Omiecinski, *cAMP-associated inhibition of phenobarbital-inducible cytochrome P450 gene expression in primary rat hepatocyte cultures*. Journal of Biological Chemistry, 1995. **270**(21): p. 12762-12773.
147. Oesch-Bartlomowicz, B., et al., *Aryl hydrocarbon receptor activation by cAMP vs. dioxin: divergent signaling pathways*. Proceedings of the National Academy of Sciences of the United States of America, 2005. **102**(26): p. 9218-9223.
148. Biswas, A., et al., *Acetylation of pregnane X receptor protein determines selective function independent of ligand activation*. Biochemical and biophysical research communications, 2011. **406**(3): p. 371-376.
149. Pasquel, D., et al., *Acetylation of lysine 109 modulates pregnane X receptor DNA binding and transcriptional activity*. Biochimica et Biophysica Acta (BBA)-Gene Regulatory Mechanisms, 2016. **1859**(9): p. 1155-1169.
150. Diani-Moore, S., et al., *Identification of the aryl hydrocarbon receptor target gene TiPARP as a mediator of suppression of hepatic gluconeogenesis by 2, 3, 7, 8-tetrachlorodibenzo-p-dioxin and of nicotinamide as a corrective agent for this effect*. Journal of Biological Chemistry, 2010. **285**(50): p. 38801-38810.

151. He, J., et al., *Activation of the Aryl Hydrocarbon Receptor Sensitizes Mice to Nonalcoholic Steatohepatitis by Deactivating Mitochondrial Sirtuin Deacetylase Sirt3*. Molecular and cellular biology, 2013. **33**(10): p. 2047-2055.
152. Diani-Moore, S., et al., *NAD<sup>+</sup> loss, a new player in AhR biology: prevention of thymus atrophy and hepatosteatosis by NAD<sup>+</sup> repletion*. Scientific Reports, 2017. **7**.
153. Diani-Moore, S., et al., *Aryl hydrocarbon receptor activation by dioxin targets phosphoenolpyruvate carboxykinase (PEPCK) for ADP-ribosylation via 2, 3, 7, 8-tetrachlorodibenzo-p-dioxin (TCDD)-inducible poly (ADP-ribose) polymerase (TiPARP)*. Journal of Biological Chemistry, 2013. **288**(30): p. 21514-21525.
154. Bindesbøll, C., et al., *TCDD-inducible poly-ADP-ribose polymerase (TiPARP/PARP7) mono-ADP-ribosylates and co-activates liver X receptors*. Biochemical Journal, 2016. **473**(7): p. 899-910.
155. MacPherson, L., et al., *2, 3, 7, 8-Tetrachlorodibenzo-p-dioxin poly (ADP-ribose) polymerase (TiPARP, ARTD14) is a mono-ADP-ribosyltransferase and repressor of aryl hydrocarbon receptor transactivation*. Nucleic acids research, 2012. **41**(3): p. 1604-1621.
156. MacPherson, L., et al., *Aryl hydrocarbon receptor repressor and TiPARP (ARTD14) use similar, but also distinct mechanisms to repress aryl hydrocarbon receptor signaling*. International journal of molecular sciences, 2014. **15**(5): p. 7939-7957.
157. Ahmed, S., et al., *Loss of the Mono-ADP-ribosyltransferase, tiparp, increases sensitivity to dioxin-induced steatohepatitis and lethality*. Journal of Biological Chemistry, 2015. **290**(27): p. 16824-16840.
158. Lee, J.H., et al., *Differential SUMOylation of LXRA and LXRβ mediates transrepression of STAT1 inflammatory signaling in IFN-γ-stimulated brain astrocytes*. Molecular cell, 2009. **35**(6): p. 806-817.
159. Ghisletti, S., et al., *Parallel SUMOylation-dependent pathways mediate gene-and signal-specific transrepression by LXRs and PPARγ*. Molecular cell, 2007. **25**(1): p. 57-70.
160. Pascual, G., et al., *A SUMOylation-dependent pathway mediates transrepression of inflammatory response genes by PPAR-γ*. Nature, 2005. **437**(7059): p. 759-763.
161. Hu, G., C. Xu, and J.L. Staudinger, *Pregnane X receptor is SUMOylated to repress the inflammatory response*. Journal of Pharmacology and Experimental Therapeutics, 2010. **335**(2): p. 342-350.
162. Zhou, C., et al., *Mutual repression between steroid and xenobiotic receptor and NF-κB signaling pathways links xenobiotic metabolism and inflammation*. The Journal of clinical investigation, 2006. **116**(8): p. 2280.
163. Cui, W., et al., *SUMOylation and ubiquitylation circuitry controls pregnane X receptor biology in hepatocytes*. Drug Metabolism and Disposition, 2015. **43**(9): p. 1316-1325.
164. Oshima, M., et al., *SUMO modification regulates the transcriptional repressor function of aryl hydrocarbon receptor repressor*. Journal of Biological Chemistry, 2009. **284**(17): p. 11017-11026.
165. Xing, X., et al., *SUMOylation of AhR modulates its activity and stability through inhibiting its ubiquitination*. Journal of cellular physiology, 2012. **227**(12): p. 3812-3819.
166. Tojo, M., et al., *The aryl hydrocarbon receptor nuclear transporter is modulated by the SUMO-1 conjugation system*. Journal of Biological Chemistry, 2002. **277**(48): p. 46576-46585.
167. Kwon, Y.T. and A. Ciechanover, *The ubiquitin code in the ubiquitin-proteasome system and autophagy*. Trends in biochemical sciences, 2017.

168. Buetow, L. and D.T. Huang, *Structural insights into the catalysis and regulation of E3 ubiquitin ligases*. Nature Reviews Molecular Cell Biology, 2016.
169. Rape, M., *Ubiquitylation at the crossroads of development and disease*. Nature Reviews Molecular Cell Biology, 2017.
170. Petroski, M.D. and R.J. Deshaies, *Function and regulation of cullin–RING ubiquitin ligases*. Nature reviews Molecular cell biology, 2005. **6**(1): p. 9-20.
171. Davarinios, N.A. and R.S. Pollenz, *Aryl hydrocarbon receptor imported into the nucleus following ligand binding is rapidly degraded via the cytoplasmic proteasome following nuclear export*. Journal of Biological Chemistry, 1999. **274**(40): p. 28708-28715.
172. Ma, Q. and K.T. Baldwin, *2, 3, 7, 8-Tetrachlorodibenzo-p-dioxin-induced Degradation of Aryl Hydrocarbon Receptor (AhR) by the Ubiquitin-Proteasome Pathway ROLE OF THE TRANSCRIPTION ACTIVATON AND DNA BINDING OF AhR*. Journal of Biological Chemistry, 2000. **275**(12): p. 8432-8438.
173. Ohtake, F., et al., *Dioxin receptor is a ligand-dependent E3 ubiquitin ligase*. Nature, 2007. **446**(7135): p. 562-566.
174. Kawajiri, K., et al., *Aryl hydrocarbon receptor suppresses intestinal carcinogenesis in ApcMin/+ mice with natural ligands*. Proceedings of the National Academy of Sciences, 2009. **106**(32): p. 13481-13486.
175. Luecke-Johansson, S., et al., *A molecular mechanism to switch the aryl hydrocarbon receptor from a transcription factor to an E3 ubiquitin ligase*. Molecular and Cellular Biology, 2017. **37**(13): p. e00630-16.
176. Staudinger, J.L., et al., *Post-translational modification of pregnane x receptor*. Pharmacological research, 2011. **64**(1): p. 4-10.
177. Rana, R., et al., *RBCK1, an E3 ubiquitin ligase, interacts with and ubiquinates the human pregnane X receptor*. Drug Metabolism and Disposition, 2013. **41**(2): p. 398-405.
178. Ong, S.S., et al., *Stability of the human pregnane X receptor is regulated by E3 ligase UBR5 and serine/threonine kinase DYRK2*. Biochemical Journal, 2014. **459**(1): p. 193-203.
179. Sugatani, J., et al., *Threonine-408 regulates the stability of human pregnane X receptor through Its phosphorylation and the CHIP/chaperone-autophagy pathway*. Drug Metabolism and Disposition, 2016. **44**(1): p. 137-150.
180. Willson, T.M. and S.A. Kliewer, *PXR, CAR and drug metabolism*. Nature reviews Drug discovery, 2002. **1**(4): p. 259-266.
181. Dong, B., et al., *Activation of nuclear receptor CAR ameliorates diabetes and fatty liver disease*. Proceedings of the National Academy of Sciences, 2009. **106**(44): p. 18831-18836.
182. Gao, J., et al., *The constitutive androstane receptor is an anti-obesity nuclear receptor that improves insulin sensitivity*. Journal of Biological Chemistry, 2009. **284**(38): p. 25984-25992.
183. Masuyama, H. and Y. Hiramatsu, *Treatment with a constitutive androstane receptor ligand ameliorates the signs of preeclampsia in high-fat diet-induced obese pregnant mice*. Molecular and cellular endocrinology, 2012. **348**(1): p. 120-127.
184. Lahtela, J., P. Särkkä, and E. Sotaniemi, *Phenobarbital treatment enhances insulin mediated glucose metabolism in man*. Research communications in chemical pathology and pharmacology, 1984. **44**(2): p. 215-226.

185. Lahtela, J.T., A.J. Arranto, and E.A. Sotaniemi, *Enzyme inducers improve insulin sensitivity in non-insulin-dependent diabetic subjects*. Diabetes, 1985. **34**(9): p. 911-916.
186. Sotaniemi, E.A., et al., *Treatment of noninsulin-dependent diabetes mellitus with enzyme inducers*. Clinical Pharmacology & Therapeutics, 1983. **33**(6): p. 826-835.
187. Kodama, S., et al., *Nuclear receptors CAR and PXR cross talk with FOXO1 to regulate genes that encode drug-metabolizing and gluconeogenic enzymes*. Molecular and cellular biology, 2004. **24**(18): p. 7931-7940.
188. Miao, J., et al., *Functional inhibitory cross-talk between constitutive androstane receptor and hepatic nuclear factor-4 in hepatic lipid/glucose metabolism is mediated by competition for binding to the DR1 motif and to the common coactivators, GRIP-1 and PGC-1 $\alpha$* . Journal of Biological Chemistry, 2006. **281**(21): p. 14537-14546.
189. Puigserver, P., *Tissue-specific regulation of metabolic pathways through the transcriptional coactivator PGC1- $\alpha$* . International journal of obesity, 2005. **29**: p. S5-S9.
190. Yoon, J.C., et al., *Control of hepatic gluconeogenesis through the transcriptional coactivator PGC-1*. Nature, 2001. **413**(6852): p. 131-138.
191. Puigserver, P., et al., *Insulin-regulated hepatic gluconeogenesis through FOXO1–PGC-1 $\alpha$  interaction*. Nature, 2003. **423**(6939): p. 550-555.
192. Puigserver, P. and B.M. Spiegelman, *Peroxisome proliferator-activated receptor- $\gamma$  coactivator 1 $\alpha$  (PGC-1 $\alpha$ ): transcriptional coactivator and metabolic regulator*. Endocrine reviews, 2003. **24**(1): p. 78-90.
193. Daitoku, H., et al., *Regulation of PGC-1 promoter activity by protein kinase B and the forkhead transcription factor FKHR*. Diabetes, 2003. **52**(3): p. 642-649.
194. Finck, B.N. and D.P. Kelly, *PGC-1 coactivators: inducible regulators of energy metabolism in health and disease*. Journal of Clinical Investigation, 2006. **116**(3): p. 615-622.
195. Lallemand-Breitenbach, V., *PML nuclear bodies*. Cold Spring Harbor perspectives in biology, 2010. **2**(5): p. a000661.
196. Carracedo, A., et al., *A metabolic prosurvival role for PML in breast cancer*. The Journal of clinical investigation, 2012. **122**(9): p. 3088.
197. Ito, K., et al., *A PML-PPAR-[delta] pathway for fatty acid oxidation regulates hematopoietic stem cell maintenance*. Nature medicine, 2012. **18**(9): p. 1350-1358.
198. Cheng, X., et al., *Ablation of promyelocytic leukemia protein (PML) re-patterns energy balance and protects mice from obesity induced by a Western diet*. Journal of Biological Chemistry, 2013. **288**(41): p. 29746-29759.
199. Wang, Z.G., et al., *Role of PML in cell growth and the retinoic acid pathway*. Science, 1998. **279**(5356): p. 1547-1551.
200. Monsalve, M., et al., *Direct coupling of transcription and mRNA processing through the thermogenic coactivator PGC-1*. Molecular cell, 2000. **6**(2): p. 307-316.
201. Puigserver, P., et al., *A cold-inducible coactivator of nuclear receptors linked to adaptive thermogenesis*. Cell, 1998. **92**(6): p. 829-839.
202. Jin, J., et al., *Identification of Substrates for F-Box Proteins*. Methods in enzymology, 2005. **399**: p. 287-309.
203. Schilling, M.M., et al., *Gluconeogenesis: Re-evaluating the FOXO1–PGC-1 $\alpha$  connection*. Nature, 2006. **443**(7111): p. E10-E11.
204. Lerin, C., et al., *GCN5 acetyltransferase complex controls glucose metabolism through transcriptional repression of PGC-1 $\alpha$* . Cell metabolism, 2006. **3**(6): p. 429-438.

205. Koo, S.-H., et al., *The CREB coactivator TORC2 is a key regulator of fasting glucose metabolism*. *Nature*, 2005. **437**(7062): p. 1109-11.
206. Gao, D., et al., *Rictor forms a complex with Cullin-1 to promote SGK1 ubiquitination and destruction*. *Molecular cell*, 2010. **39**(5): p. 797-808.
207. Herzig, S., et al., *CREB regulates hepatic gluconeogenesis through the coactivator PGC-1*. *Nature*, 2001. **413**(6852): p. 179-183.
208. Shiraki, T., et al., *Activation of Orphan Nuclear Constitutive Androstane Receptor Requires Subnuclear Targeting by Peroxisome Proliferator-activated Receptor  $\gamma$  Coactivator-1 $\alpha$  A POSSIBLE LINK BETWEEN XENOBIOTIC RESPONSE AND NUTRITIONAL STATE*. *Journal of Biological Chemistry*, 2003. **278**(13): p. 11344-11350.
209. Bernardi, R. and P.P. Pandolfi, *Structure, dynamics and functions of promyelocytic leukaemia nuclear bodies*. *Nature reviews Molecular cell biology*, 2007. **8**(12): p. 1006-1016.
210. Zhong, S., et al., *A role for PML and the nuclear body in genomic stability*. *Oncogene*, 1999. **18**(56): p. 7941-7947.
211. Sano, M., et al., *Intramolecular control of protein stability, subnuclear compartmentalization, and coactivator function of peroxisome proliferator-activated receptor  $\gamma$  coactivator 1 $\alpha$* . *Journal of Biological Chemistry*, 2007. **282**(35): p. 25970-25980.
212. Dussault, I., et al., *A structural model of the constitutive androstane receptor defines novel interactions that mediate ligand-independent activity*. *Molecular and cellular biology*, 2002. **22**(15): p. 5270-5280.
213. Zhang, X.-W., et al., *Arsenic trioxide controls the fate of the PML-RAR $\alpha$  oncoprotein by directly binding PML*. *Science*, 2010. **328**(5975): p. 240-243.
214. Ravid, T. and M. Hochstrasser, *Diversity of degradation signals in the ubiquitin–proteasome system*. *Nature Reviews Molecular Cell Biology*, 2008. **9**(9): p. 679-689.
215. Zheng, N., et al., *Structure of the Cull1–Rbx1–Skp1–F boxSkp2 SCF ubiquitin ligase complex*. *Nature*, 2002. **416**(6882): p. 703-709.
216. Soucy, T.A., et al., *An inhibitor of NEDD8-activating enzyme as a new approach to treat cancer*. *Nature*, 2009. **458**(7239): p. 732-736.
217. Plevin, M.J., M.M. Mills, and M. Ikura, *The LxxLL motif: a multifunctional binding sequence in transcriptional regulation*. *Trends in biochemical sciences*, 2005. **30**(2): p. 66-69.
218. Deshaies, R., *SCF and Cullin/Ring H2-based ubiquitin ligases*. *Annual review of cell and developmental biology*, 1999. **15**(1): p. 435-467.
219. Olson, B.L., et al., *SCFCdc4 acts antagonistically to the PGC-1 $\alpha$  transcriptional coactivator by targeting it for ubiquitin-mediated proteolysis*. *Genes & development*, 2008. **22**(2): p. 252-264.
220. Li, X., et al., *Akt/PKB regulates hepatic metabolism by directly inhibiting PGC-1 $\alpha$  transcription coactivator*. *Nature*, 2007. **447**(7147): p. 1012-1016.
221. Rodgers, J.T., et al., *Cdc2-like kinase 2 is an insulin-regulated suppressor of hepatic gluconeogenesis*. *Cell metabolism*, 2010. **11**(1): p. 23-34.
222. Lustig, Y., et al., *Separation of the gluconeogenic and mitochondrial functions of PGC-1 $\alpha$  through S6 kinase*. *Genes & development*, 2011. **25**(12): p. 1232-1244.

223. Puigserver, P., et al., *Cytokine stimulation of energy expenditure through p38 MAP kinase activation of PPAR $\gamma$  coactivator-1*. Molecular cell, 2001. **8**(5): p. 971-982.
224. Jäger, S., et al., *AMP-activated protein kinase (AMPK) action in skeletal muscle via direct phosphorylation of PGC-1 $\alpha$* . Proceedings of the National Academy of Sciences, 2007. **104**(29): p. 12017-12022.
225. Bhalla, K., et al., *Cyclin D1 represses gluconeogenesis via inhibition of the transcriptional coactivator PGC1 $\alpha$* . Diabetes, 2014. **63**(10): p. 3266-3278.
226. Li, S., et al., *Circadian metabolic regulation through crosstalk between casein kinase 1 $\delta$  and transcriptional coactivator PGC-1 $\alpha$* . Molecular endocrinology, 2011. **25**(12): p. 2084-2093.
227. Rytinki, M.M. and J.J. Palvimo, *SUMOylation attenuates the function of PGC-1 $\alpha$* . Journal of Biological Chemistry, 2009. **284**(38): p. 26184-26193.
228. Teyssier, C., et al., *Activation of nuclear receptor coactivator PGC-1 $\alpha$  by arginine methylation*. Genes & development, 2005. **19**(12): p. 1466-1473.
229. Rodgers, J.T., et al., *Nutrient control of glucose homeostasis through a complex of PGC-1 $\alpha$  and SIRT1*. Nature, 2005. **434**(7029): p. 113-118.
230. Ruan, H.-B., et al., *O-GlcNAc transferase/host cell factor C1 complex regulates gluconeogenesis by modulating PGC-1 $\alpha$  stability*. Cell metabolism, 2012. **16**(2): p. 226-237.
231. Adamovich, Y., et al., *The protein level of PGC-1 $\alpha$ , a key metabolic regulator, is controlled by NADH-NQO1*. Molecular and cellular biology, 2013. **33**(13): p. 2603-2613.
232. Shin, J.-H., et al., *PARIS (ZNF746) repression of PGC-1 $\alpha$  contributes to neurodegeneration in Parkinson's disease*. Cell, 2011. **144**(5): p. 689-702.
233. Wei, P., et al., *RNF34 is a cold-regulated E3 ubiquitin ligase for PGC-1 $\alpha$  and modulates brown fat cell metabolism*. Molecular and cellular biology, 2012. **32**(2): p. 266-275.
234. Lafarga, M., et al., *Clastosome: a subtype of nuclear body enriched in 19S and 20S proteasomes, ubiquitin, and protein substrates of proteasome*. Molecular biology of the cell, 2002. **13**(8): p. 2771-2782.
235. von Mikecz, A., *The nuclear ubiquitin-proteasome system*. Journal of cell science, 2006. **119**(10): p. 1977-1984.
236. Choi, H.-S., W. Seol, and D.D. Moore, *A component of the 26S proteasome binds an orphan member of the nuclear hormone receptor superfamily*. The Journal of steroid biochemistry and molecular biology, 1996. **56**(1): p. 23-30.
237. Chen, T., et al., *Proteasomal interaction as a critical activity modulator of the human constitutive androstane receptor*. Biochemical Journal, 2014. **458**(1): p. 95-107.
238. Bataller, R. and D.A. Brenner, *Liver fibrosis*. Journal of clinical investigation, 2005. **115**(2): p. 209.
239. Mederacke, I., et al., *Fate tracing reveals hepatic stellate cells as dominant contributors to liver fibrosis independent of its aetiology*. Nature communications, 2013. **4**.
240. Friedman, S.L., *Hepatic stellate cells: protean, multifunctional, and enigmatic cells of the liver*. Physiological reviews, 2008. **88**(1): p. 125-172.
241. Tsuchida, T. and S.L. Friedman, *Mechanisms of hepatic stellate cell activation*. Nature Reviews Gastroenterology & Hepatology, 2017.
242. Akhmetshina, A., et al., *Activation of canonical Wnt signalling is required for TGF- $\beta$ -mediated fibrosis*. Nature communications, 2012. **3**: p. 735.

243. Piersma, B., R.A. Bank, and M. Boersema, *Signaling in fibrosis: TGF- $\beta$ , WNT, and YAP/TAZ converge*. *Frontiers in medicine*, 2015. **2**: p. 59.
244. Beischlag, T.V., et al., *The aryl hydrocarbon receptor complex and the control of gene expression*. *Critical Reviews™ in Eukaryotic Gene Expression*, 2008. **18**(3).
245. Denison, M.S., et al., *Exactly the same but different: promiscuity and diversity in the molecular mechanisms of action of the aryl hydrocarbon (dioxin) receptor*. *Toxicological sciences*, 2011: p. kfr218.
246. Lo, R. and J. Matthews, *High-resolution genome-wide mapping of AHR and ARNT binding sites by ChIP-Seq*. *Toxicological sciences*, 2012: p. kfs253.
247. Nebert, D.W., *Aryl hydrocarbon receptor (AHR): “pioneer member” of the basic-helix/loop/helix per-Arnt-sim (bHLH/PAS) family of “sensors” of foreign and endogenous signals*. *Progress in Lipid Research*, 2017.
248. Pierre, S., et al., *Aryl Hydrocarbon Receptor–Dependent Induction of Liver Fibrosis by Dioxin*. *toxicological sciences*, 2014. **137**(1): p. 114-124.
249. Walisser, J.A., et al., *Aryl hydrocarbon receptor-dependent liver development and hepatotoxicity are mediated by different cell types*. *Proceedings of the National Academy of Sciences of the United States of America*, 2005. **102**(49): p. 17858-17863.
250. Postic, C., et al., *Dual roles for glucokinase in glucose homeostasis as determined by liver and pancreatic  $\beta$  cell-specific gene knock-outs using Cre recombinase*. *Journal of Biological Chemistry*, 1999. **274**(1): p. 305-315.
251. Clausen, B., et al., *Conditional gene targeting in macrophages and granulocytes using LysMcre mice*. *Transgenic research*, 1999. **8**(4): p. 265-277.
252. Lu, P., et al., *Activation of aryl hydrocarbon receptor dissociates fatty liver from insulin resistance by inducing FGF21*. *Hepatology*, 2015.
253. Mederacke, I., et al., *High-yield and high-purity isolation of hepatic stellate cells from normal and fibrotic mouse livers*. *Nature protocols*, 2015. **10**(2): p. 305-315.
254. Gao, J., et al., *CAR Suppresses Hepatic Gluconeogenesis by Facilitating the Ubiquitination and Degradation of PGC1 $\alpha$* . *Molecular Endocrinology*, 2015. **29**(11): p. 1558-1570.
255. Ziv-Gal, A., et al., *In vitro re-expression of the aryl hydrocarbon receptor (Ahr) in cultured Ahr-deficient mouse antral follicles partially restores the phenotype to that of cultured wild-type mouse follicles*. *Toxicology in Vitro*, 2015. **29**(2): p. 329-336.
256. Tang, N., et al., *BMP-9-induced osteogenic differentiation of mesenchymal progenitors requires functional canonical Wnt/ $\beta$ -catenin signalling*. *Journal of cellular and molecular medicine*, 2009. **13**(8b): p. 2448-2464.
257. Luo, J., et al., *A protocol for rapid generation of recombinant adenoviruses using the AdEasy system*. *Nature protocols*, 2007. **2**(5): p. 1236-1247.
258. Nelson, J.D., O. Denisenko, and K. Bomsztyk, *Protocol for the fast chromatin immunoprecipitation (ChIP) method*. *NATURE PROTOCOLS-ELECTRONIC EDITION-*, 2006. **1**(1): p. 179.
259. Lönn, P., et al., *PARP-1 attenuates Smad-mediated transcription*. *Molecular cell*, 2010. **40**(4): p. 521-532.
260. Ding, N., et al., *A vitamin D receptor/SMAD genomic circuit gates hepatic fibrotic response*. *Cell*, 2013. **153**(3): p. 601-613.
261. Song, J., et al., *A ligand for the aryl hydrocarbon receptor isolated from lung*. *Proceedings of the National Academy of Sciences*, 2002. **99**(23): p. 14694-14699.

262. Azimifar, S.B., et al., *Cell-Type-Resolved Quantitative Proteomics of Murine Liver*. Cell metabolism, 2014. **20**(6): p. 1076-1087.
263. Kim, S.-H., et al., *Novel compound 2-methyl-2H-pyrazole-3-carboxylic acid (2-methyl-4-o-tolylazo-phenyl)-amide (CH-223191) prevents 2, 3, 7, 8-TCDD-induced toxicity by antagonizing the aryl hydrocarbon receptor*. Molecular pharmacology, 2006. **69**(6): p. 1871-1878.
264. Leask, A. and D.J. Abraham, *TGF- $\beta$  signaling and the fibrotic response*. The FASEB Journal, 2004. **18**(7): p. 816-827.
265. Ge, W.-S., et al.,  *$\beta$ -catenin is overexpressed in hepatic fibrosis and blockage of Wnt/ $\beta$ -catenin signaling inhibits hepatic stellate cell activation*. Molecular medicine reports, 2014. **9**(6): p. 2145-2151.
266. Jian, H., et al., *Smad3-dependent nuclear translocation of  $\beta$ -catenin is required for TGF- $\beta$ 1-induced proliferation of bone marrow-derived adult human mesenchymal stem cells*. Genes & development, 2006. **20**(6): p. 666-674.
267. Fukuchi, M., et al., *Ligand-dependent degradation of Smad3 by a ubiquitin ligase complex of ROC1 and associated proteins*. Molecular biology of the cell, 2001. **12**(5): p. 1431-1443.
268. Gao, S., et al., *Ubiquitin ligase Nedd4L targets activated Smad2/3 to limit TGF- $\beta$  signaling*. Molecular cell, 2009. **36**(3): p. 457-468.
269. Ozeki, J., et al., *Aryl hydrocarbon receptor ligand 2, 3, 7, 8-tetrachlorodibenzo-p-dioxin enhances liver damage in bile duct-ligated mice*. Toxicology, 2011. **280**(1): p. 10-17.
270. Lamb, C.L., et al., *2, 3, 7, 8-Tetrachlorodibenzo-p-dioxin (TCDD) increases necroinflammation and hepatic stellate cell activation but does not exacerbate experimental liver fibrosis in mice*. Toxicology and applied pharmacology, 2016. **311**: p. 42-51.
271. Bunker, M.K., et al., *Abnormal liver development and resistance to 2, 3, 7, 8-tetrachlorodibenzo-p-dioxin toxicity in mice carrying a mutation in the DNA-binding domain of the aryl hydrocarbon receptor*. Toxicological Sciences, 2008. **106**(1): p. 83-92.
272. Matsubara, T., et al., *Metabolomics identifies an inflammatory cascade involved in dioxin-and diet-induced steatohepatitis*. Cell metabolism, 2012. **16**(5): p. 634-644.
273. Takeda, T., et al., *Dioxin-induced increase in leukotriene B4 biosynthesis through the aryl hydrocarbon receptor and its relevance to hepatotoxicity owing to neutrophil infiltration*. Journal of Biological Chemistry, 2017: p. jbc. M116. 764332.
274. Murray, I.A., A.D. Patterson, and G.H. Perdew, *Aryl hydrocarbon receptor ligands in cancer: friend and foe*. Nature Reviews Cancer, 2014. **14**(12): p. 801-814.
275. Opitz, C.A., et al., *An endogenous tumour-promoting ligand of the human aryl hydrocarbon receptor*. Nature, 2011. **478**(7368): p. 197-203.
276. Jenabian, M.-A., et al., *Liver fibrosis is strongly associated with an enhanced level of immunosuppressive tryptophan catabolism independently of HCV viremia in ART-treated HIV/HCV co-infected patients*. BMC Infectious Diseases, 2014. **14**(2): p. 1-2.
277. Woeller, C.F., et al., *The aryl hydrocarbon receptor and its ligands inhibit myofibroblast formation and activation: implications for thyroid eye disease*. The American journal of pathology, 2016. **186**(12): p. 3189-3202.
278. Monteleone, I., et al., *Aryl hydrocarbon receptor-driven signals inhibit collagen synthesis in the gut*. European journal of immunology, 2016. **46**(4): p. 1047-1057.



279. Seki, E. and D.A. Brenner, *Recent advancement of molecular mechanisms of liver fibrosis*. Journal of hepato-biliary-pancreatic sciences, 2015. **22**(7): p. 512-518.
280. Zhang, M., et al., *Smad3 prevents  $\beta$ -catenin degradation and facilitates  $\beta$ -catenin nuclear translocation in chondrocytes*. Journal of Biological Chemistry, 2010. **285**(12): p. 8703-8710.
281. Huber, A.-L., et al., *CRY2 and FBXL3 cooperatively degrade c-MYC*. Molecular cell, 2016. **64**(4): p. 774-789.
282. Zha, Z., et al., *A non-canonical function of G $\beta$  as a subunit of E3 ligase in targeting GRK2 ubiquitylation*. Molecular cell, 2015. **58**(5): p. 794-803.
283. Horton, J.D., J.L. Goldstein, and M.S. Brown, *SREBPs: activators of the complete program of cholesterol and fatty acid synthesis in the liver*. Journal of Clinical Investigation, 2002. **109**(9): p. 1125-1131.
284. Zhai, Y., et al., *A functional cross-talk between liver X receptor- $\alpha$  and constitutive androstane receptor links lipogenesis and xenobiotic responses*. Molecular pharmacology, 2010. **78**(4): p. 666-674.
285. Roth, A., et al., *Sterol regulatory element binding protein 1 interacts with pregnane X receptor and constitutive androstane receptor and represses their target genes*. Pharmacogenetics and genomics, 2008. **18**(4): p. 325-337.
286. Yang, T., et al., *Crucial step in cholesterol homeostasis: sterols promote binding of SCAP to INSIG-1, a membrane protein that facilitates retention of SREBPs in ER*. Cell, 2002. **110**(4): p. 489-500.
287. Roth, A., et al., *Regulatory cross-talk between drug metabolism and lipid homeostasis: constitutive androstane receptor and pregnane X receptor increase Insig-1 expression*. Molecular pharmacology, 2008. **73**(4): p. 1282-1289.
288. Falany, C.N., *Enzymology of human cytosolic sulfotransferases*. The FASEB Journal, 1997. **11**(4): p. 206-216.
289. Chen, W., et al., *Enzymatic reduction of oxysterols impairs LXR signaling in cultured cells and the livers of mice*. Cell metabolism, 2007. **5**(1): p. 73-79.
290. Bai, Q., et al., *Sulfation of 25-hydroxycholesterol by SULT2B1b decreases cellular lipids via the LXR/SREBP-1c signaling pathway in human aortic endothelial cells*. Atherosclerosis, 2011. **214**(2): p. 350-356.
291. Shi, X., et al., *Cholesterol Sulfate and Cholesterol Sulfotransferase Inhibit Gluconeogenesis by Targeting Hepatocyte Nuclear Factor 4a*. Molecular and cellular biology, 2014. **34**(3): p. 485-497.
292. Xu, L., et al., *5-Cholesten-3 $\beta$ , 25-Diol 3-Sulfate Decreases Lipid Accumulation in Diet-Induced Nonalcoholic Fatty Liver Disease Mouse Model*. Molecular pharmacology, 2013. **83**(3): p. 648-658.
293. Xu, L., et al., *Regulation of hepatocyte lipid metabolism and inflammatory response by 25-hydroxycholesterol and 25-hydroxycholesterol-3-sulfate*. Lipids, 2010. **45**(9): p. 821-832.
294. Ma, Y., et al., *25-Hydroxycholesterol-3-sulfate regulates macrophage lipid metabolism via the LXR/SREBP-1 signaling pathway*. American Journal of Physiology-Endocrinology And Metabolism, 2008. **295**(6): p. E1369-E1379.
295. Xu, L., et al., *25-Hydroxycholesterol-3-sulfate attenuates inflammatory response via PPAR $\gamma$  signaling in human THP-1 macrophages*. American Journal of Physiology-Endocrinology And Metabolism, 2012. **302**(7): p. E788-E799.

296. Kallen, J.A., et al., *X-ray structure of the hROR $\alpha$  LBD at 1.63 Å: structural and functional data that cholesterol or a cholesterol derivative is the natural ligand of ROR $\alpha$* . Structure, 2002. **10**(12): p. 1697-1707.
297. Xiao, L., X. Xie, and Y. Zhai, *Functional crosstalk of CAR–LXR and ROR–LXR in drug metabolism and lipid metabolism*. Advanced drug delivery reviews, 2010. **62**(13): p. 1316-1321.
298. Mo, L., et al., *Irisin is regulated by CAR in liver and is a mediator of hepatic glucose and lipid metabolism*. Molecular Endocrinology, 2016. **30**(5): p. 533-542.
299. Haidari, M., et al., *Fasting and Postprandial Overproduction of Intestinally Derived Lipoproteins in an Animal Model of Insulin Resistance EVIDENCE THAT CHRONIC FRUCTOSE FEEDING IN THE HAMSTER IS ACCOMPANIED BY ENHANCED INTESTINAL DE NOVO LIPOGENESIS AND ApoB48-CONTAINING LIPOPROTEIN OVERPRODUCTION*. Journal of Biological Chemistry, 2002. **277**(35): p. 31646-31655.
300. Federico, L.M., et al., *Intestinal Insulin Resistance and Aberrant Production of Apolipoprotein B48 Lipoproteins in an Animal Model of Insulin Resistance and Metabolic Dyslipidemia Evidence for Activation of Protein Tyrosine Phosphatase-1B, Extracellular Signal–Related Kinase, and Sterol Regulatory Element–Binding Protein-1c in the Fructose-Fed Hamster Intestine*. Diabetes, 2006. **55**(5): p. 1316-1326.
301. Masson, D., et al., *Activation of the constitutive androstane receptor decreases HDL in wild-type and human apoA-I transgenic mice*. Journal of lipid research, 2008. **49**(8): p. 1682-1691.
302. Sberna, A.-L., et al., *Constitutive Androstane Receptor Activation Decreases Plasma Apolipoprotein B–Containing Lipoproteins and Atherosclerosis in Low-Density Lipoprotein Receptor–Deficient Mice*. Arteriosclerosis, thrombosis, and vascular biology, 2011. **31**(10): p. 2232-2239.
303. Sberna, A.L., et al., *Constitutive androstane receptor activation stimulates faecal bile acid excretion and reverse cholesterol transport in mice*. Journal of hepatology, 2011. **55**(1): p. 154-161.
304. Hayhurst, G.P., et al., *Hepatocyte nuclear factor 4 $\alpha$  (nuclear receptor 2A1) is essential for maintenance of hepatic gene expression and lipid homeostasis*. Molecular and cellular biology, 2001. **21**(4): p. 1393-1403.
305. Tojima, H., et al., *Ligand dependent hepatic gene expression profiles of nuclear receptors CAR and PXR*. Toxicology letters, 2012. **212**(3): p. 288-297.
306. Režen, T., et al., *Effect of CAR activation on selected metabolic pathways in normal and hyperlipidemic mouse livers*. BMC genomics, 2009. **10**(1): p. 384.
307. Schultz, J.R., et al., *Role of LXRs in control of lipogenesis*. Genes & development, 2000. **14**(22): p. 2831-2838.
308. Uyeda, K. and J.J. Repa, *Carbohydrate response element binding protein, ChREBP, a transcription factor coupling hepatic glucose utilization and lipid synthesis*. Cell Metabolism, 2006. **4**(2): p. 107-110.
309. Horton, J.D., et al., *Activation of cholesterol synthesis in preference to fatty acid synthesis in liver and adipose tissue of transgenic mice overproducing sterol regulatory element-binding protein-2*. Journal of Clinical Investigation, 1998. **101**(11): p. 2331.
310. Walisser, J.A., et al., *Gestational exposure of Ahr and Arnt hypomorphs to dioxin rescues vascular development*. Proceedings of the National Academy of Sciences of the United States of America, 2004. **101**(47): p. 16677-16682.

311. Bunger, M.K., et al., *Resistance to 2, 3, 7, 8-tetrachlorodibenzo-p-dioxin toxicity and abnormal liver development in mice carrying a mutation in the nuclear localization sequence of the aryl hydrocarbon receptor*. Journal of Biological Chemistry, 2003. **278**(20): p. 17767-17774.
312. Nguyen, L.P. and C.A. Bradfield, *The search for endogenous activators of the aryl hydrocarbon receptor*. Chemical research in toxicology, 2007. **21**(1): p. 102-116.
313. Quintana, F.J., et al., *Control of Treg and TH17 cell differentiation by the aryl hydrocarbon receptor*. Nature, 2008. **453**(7191): p. 65-71.
314. Veldhoen, M., et al., *The aryl hydrocarbon receptor links TH17-cell-mediated autoimmunity to environmental toxins*. Nature, 2008. **453**(7191): p. 106-109.
315. Mezrich, J.D., et al., *An interaction between kynurenine and the aryl hydrocarbon receptor can generate regulatory T cells*. The Journal of Immunology, 2010. **185**(6): p. 3190-3198.
316. Moennikes, O., et al., *A constitutively active dioxin/aryl hydrocarbon receptor promotes hepatocarcinogenesis in mice*. Cancer research, 2004. **64**(14): p. 4707-4710.
317. Fan, Y., et al., *The aryl hydrocarbon receptor functions as a tumor suppressor of liver carcinogenesis*. Cancer research, 2010. **70**(1): p. 212-220.
318. Pirkle, J.L., et al., *Estimates of the half-life of 2, 3, 7, 8-tetrachlorodibenzo-p-dioxin in Vietnam veterans of Operation Ranch Hand*. Journal of Toxicology and Environmental Health, Part A Current Issues, 1989. **27**(2): p. 165-171.
319. Stohs, S.J., *Oxidative stress induced by 2, 3, 7, 8-tetrachlorodibenzo-p-dioxin (TCDD)*. Free Radical Biology and Medicine, 1990. **9**(1): p. 79-90.
320. Nault, R., et al., *Lipidomic evaluation of aryl hydrocarbon receptor-mediated hepatic steatosis in male and female mice elicited by 2, 3, 7, 8-tetrachlorodibenzo-p-dioxin*. Chemical Research in Toxicology, 2017. **30**(4): p. 1060-1075.
321. Wincent, E., et al., *Inhibition of cytochrome P4501-dependent clearance of the endogenous agonist FICZ as a mechanism for activation of the aryl hydrocarbon receptor*. Proceedings of the National Academy of Sciences, 2012. **109**(12): p. 4479-4484.
322. Esser, C. and A. Rannug, *The aryl hydrocarbon receptor in barrier organ physiology, immunology, and toxicology*. Pharmacological reviews, 2015. **67**(2): p. 259-279.
323. Schiering, C., et al., *Feedback control of AHR signalling regulates intestinal immunity*. Nature, 2017. **542**(7640): p. 242-245.
324. Kurzawski, M., et al., *Expression of genes involved in xenobiotic metabolism and transport in end-stage liver disease: up-regulation of ABCC4 and CYP1B1*. Pharmacological Reports, 2012. **64**(4): p. 927-939.